

Development of Cell-penetrating Peptides Targeting Nuclear and Extra-nuclear  
Signaling Pathways in Cancer Cells



A Dissertation Submitted in Partial Fulfillment of the Requirements  
for the Degree of Doctor of Philosophy in Clinical Biochemistry and Molecular Medicine  
Department of Clinical Chemistry  
FACULTY OF ALLIED HEALTH SCIENCES  
Chulalongkorn University  
Academic Year 2019  
Copyright of Chulalongkorn University

การพัฒนาเปปไทด์ที่มีความสามารถในการแทรกผ่านเซลล์เพื่อยับยั้งการส่งสัญญาณผ่านทาง  
นิวเคลียสและภายนอกนิวเคลียสในเซลล์มะเร็ง



วิทยานิพนธ์นี้เป็นส่วนหนึ่งของการศึกษาตามหลักสูตรปริญญาวิทยาศาสตรดุษฎีบัณฑิต  
สาขาวิชาชีวเคมีคลินิกและอนุทางการแพทย์ ภาควิชาเคมีคลินิก  
คณะสหเวชศาสตร์ จุฬาลงกรณ์มหาวิทยาลัย  
ปีการศึกษา 2562  
ลิขสิทธิ์ของจุฬาลงกรณ์มหาวิทยาลัย



ปณิธิตา แก้วจันทร์ทอง : การพัฒนาเปปไทด์ที่มีความสามารถในการแทรกผ่านเซลล์เพื่อยับยั้งการส่งสัญญาณผ่านทางนิวเคลียสและภายนอกนิวเคลียสในเซลล์มะเร็ง. ( Development of Cell-penetrating Peptides Targeting Nuclear and Extra-nuclear Signaling Pathways in Cancer Cells) อ.ที่ปรึกษาหลัก : ผศ. ดร.วิโรจน์ บุญรัตนกรกิจ, อ.ที่ปรึกษาร่วม : ผศ. ดร.ศรินทร์พสุกใส

โกรทแฟคเตอร์และฮอร์โมนส่งผลทางชีวภาพผ่านการจับกันระหว่างโปรตีน ทั้งที่ทำให้เกิดการส่งสัญญาณบริเวณไซโตพลาสซึมหรือ transcription factors ภายในนิวเคลียส การรบกวนการจับกันระหว่างโปรตีนช่วยลดผลทางชีวภาพและลดการเจริญเติบโตที่เป็นผลจากโกรทแฟคเตอร์และฮอร์โมนได้ การศึกษาก่อนหน้านี้พบว่า progesterone receptor (PR) ประกอบด้วย polyproline domain (PPD) ซึ่งสามารถจับได้โดยตรงกับโมเลกุลที่มี Src homology 3 (SH3) domain และการแสดงออกของ PR-PPD ลดการเจริญเติบโตของเซลล์มะเร็งปอดชนิดไม่ใช้เซลล์เล็กที่เกิดจากการส่งสัญญาณผ่าน epidermal growth factor receptor (EGFR) ได้ งานวิจัยนี้ได้ทำการศึกษาพบว่าการนำ PR-PPD เข้าสู่เซลล์ด้วยเปปไทด์ที่มีความสามารถในการแทรกผ่านเซลล์สามารถลดการเจริญเติบโตของเซลล์มะเร็งปอดที่ถูกกระตุ้นด้วย EGF ได้ โดย PR-PPD ถูกนำมาต่อกับ Buforin2 (BR2) ซึ่งเป็นเปปไทด์ที่มีความจำเพาะต่อเซลล์มะเร็ง ผลการศึกษาพบว่า BR2-2xPPD ซึ่งประกอบด้วย PR-PPD สองตำแหน่งมีประสิทธิภาพในการลดการเจริญเติบโตของเซลล์มะเร็งปอดที่มากกว่าหนึ่งตำแหน่งและสามารถลดการเกิด phosphorylation ของโปรตีน Erk1/2 ได้อย่างมีนัยสำคัญ BR2-2xPPD สามารถยับยั้งวัฏจักรของเซลล์โดยลดการแสดงออกของยีน cyclin D1 และ CDK2 ในเซลล์มะเร็งปอดชนิดที่ไม่มีการกลายพันธุ์ของ EGFR การใช้ Tyrosine kinase inhibitors (EGFR-TKIs) ร่วมกับเปปไทด์ BR2-2xPPD สามารถลดการเจริญเติบโตของเซลล์มะเร็งปอดชนิดที่มีการกลายพันธุ์ของ EGFR ได้มากกว่าการใช้ EGFR-TKIs เพียงอย่างเดียว ยิ่งไปกว่านั้น BR2-2xPPD ยังสามารถลดการเจริญเติบโตของเซลล์มะเร็งปอดที่มีการกลายพันธุ์ของ EGFR และมีการดื้อต่อยา Gefitinib และ Erlotinib นอกจากนี้ PR-PPD แล้วการศึกษาก่อนหน้านี้พบว่าเปปไทด์ที่ประกอบด้วย LXXLL motifs นั้นสามารถยับยั้งการจับกันระหว่างตัวรับฮอร์โมนและ coactivators ได้ ผู้วิจัยจึงได้ออกแบบเปปไทด์ BR2-LXXLL ซึ่งประกอบด้วยลำดับของ LXXLL ที่มาจากโปรตีน GRIP-1 ซึ่งมีประสิทธิภาพในการยับยั้งกระบวนการถอดรหัสของ estrogen receptor (ER) ได้ โดยเปปไทด์จะมีลำดับของ SV40 ซึ่งเป็นตัวช่วยนำเปปไทด์เข้าสู่นิวเคลียสได้ ผลการศึกษาพบว่าเปปไทด์ BR2-LXXLL สามารถลดกระบวนการถอดรหัสของ PR ในเซลล์มะเร็งเต้านมชนิด T47DC42 ที่มีการแสดงออกของ PR-B ได้ ในขณะที่เปปไทด์ที่มีการสลัดตำแหน่งภายใน LXXLL motifs นั้นไม่มีผลต่อการยับยั้งนี้ ทั้งนี้ BR2-LXXLL และ BR2-2xPPD สามารถลดการเจริญเติบโตของเซลล์มะเร็งเต้านมที่ถูกกระตุ้นโดย estradiol ในเซลล์มะเร็งเต้านมชนิด MCF-7 ที่มีการแสดงออกของ ER ได้ และยังสามารถลดการเจริญเติบโตของเซลล์มะเร็งเต้านมชนิดที่ไม่มีการแสดงออกของตัวรับฮอร์โมน (triple-negative breast cancer) ได้อีกด้วย จากผลการศึกษาทั้งหมดแสดงให้เห็นถึงความจำเพาะต่อเซลล์มะเร็งและความสามารถในการยับยั้งการเจริญเติบโตของเซลล์มะเร็งของเปปไทด์ PR-PPD และ LXXLL ซึ่งสามารถนำไปพัฒนาเพื่อใช้รักษาโรคมะเร็งในอนาคตได้

สาขาวิชา	ชีวเคมีคลินิกและอนุทางการแพทย์	ลายมือชื่อนิสิต .....
ปีการศึกษา	2562	ลายมือชื่อ อ.ที่ปรึกษาหลัก .....
		ลายมือชื่อ อ.ที่ปรึกษาร่วม .....

# # 5776952037 : MAJOR CLINICAL BIOCHEMISTRY AND MOLECULAR MEDICINE

KEYWORD: Cell-penetrating peptide Buforin lung cancer EGFR polyproline domain SH3 domain

Panthita Kaewjanthong : Development of Cell-penetrating Peptides Targeting Nuclear and Extracellular Signaling Pathways in Cancer Cells. Advisor: Asst. Prof. VIROJ BOONYARATANAKORNKIT, Ph.D. Co-advisor: Asst. Prof. SARINTIP SOOKSAI, Ph.D.

Growth factors and hormones often mediate their biological effects through series of protein-protein interaction between cytoplasmic signaling molecules or transcription factors. Interfering of these protein-protein interactions has been shown to reduce or inhibit biological and growth responses to various growth factors and hormones. We previously demonstrated that progesterone receptor (PR) contains a polyproline domain (PPD) which directly interact to Src homology 3 (SH3) domain-containing molecules and expression of PR-PPD inhibits EGFR-mediated NSCLC cell proliferation. In this study, we investigated that the introduction of PR-PPD by cell-penetrating peptide could inhibit EGF-induced NSCLC cell proliferation. PR-PPD was attached to a cancer-specific CPP, Buforin2 (BR2), to help deliver the PR-PPD into NSCLC cells. Addition of BR2-2xPPD peptide containing two PR-PPD repeats was more effective in inhibiting NSCLC proliferation and significantly reduced EGF-induced phosphorylation of Erk1/2. BR2-2xPPD treatment could induce cell cycle arrest by inhibiting the expression of cyclin D1 and CDK2 gene in EGFR-wild type A549 cells. The combination treatment of EGFR-TKIs with BR2-2xPPD peptide was more effectively suppressed growth of NSCLC PC9 cells harboring EGFR mutation as compared to EGFR-TKIs treatment alone. Additionally, BR2-2xPPD peptide could mediate growth inhibition in acquired gefitinib- and erlotinib- resistance lung adenocarcinoma cells. In addition to PR-PPD, previous studies had demonstrated that peptide containing LXXLL motifs inhibited interactions between steroid hormone receptor and its coactivator. In this study, BR2-LXXLL peptide was designed from GRIP-1 protein which had high potential to inhibit ER transcription. The nuclear localization of SV40 was also added into peptide in order to facilitate access to nucleus. Our results demonstrated that BR2-LXXLL peptide could effectively inhibit the transcriptional activity of PR in T47DC42 breast cancer cell expressing PR-B isoform while the scramble peptide abolished this inhibition. BR2-LXXLL and BR2-2xPPD treatments dose-dependently decreased Estrogen-induced cell proliferation in ER-positive MCF-7 breast cancer cell lines. Moreover, BR2-LXXLL and BR2-2xPPD peptides also significantly reduced triple-negative breast cancer cell growth which lack of targeted therapy. Altogether, our data suggested that the cancer cell specific peptide of PR-PPD and LXXLL motifs could be used to further develop as novel anticancer treatment in the near future.

Field of Study:	Clinical Biochemistry and Molecular Medicine	Student's Signature .....
Academic Year:	2019	Advisor's Signature .....
		Co-advisor's Signature .....

## ACKNOWLEDGEMENTS

I would like to express my sincere thanks to my advisor Assistant Professor Dr. Viroj Boonyaratanakornkit as well as my co-advisor Assistant Professor Dr. Sarintip Sooksai for an intensive support and expert advice which help me success in this difficult project. I learned a lot of things from them and I feel so proud to be their student.

My appreciation is also to Professor. Gyorgy Hutvagner and Dr.Eileen McGowan , Faculty of Engineering and Information Technology, University of Technology Sydney for giving a good opportunity to do research internship in Australia. I would like to thank Professor. Hironobu Sasano for providing cell lines to my research. Thank to Clinical Biochemistry and Molecular Medicine Program, Department of Clinical Biochemistry, Faculty of Allied Health Sciences and also The Institute of Biotechnology and Genetic Engineering, Chulalongkorn University, for providing a good collaboration and all facilities which required for my research.

I would like to thank all financial support from The 100th Anniversary Chulalongkorn University for Doctoral Scholarship, The 90th Anniversary Chulalongkorn University Fund and The Overseas Research Experience Scholarship for Graduate Students from Chulalongkorn University

I would like to thank my parents and friends who always encourage me. Thank are also expressed to all members of Molecular Endocrinology VB Lab and CBMM family for their friendships and many suggestions in the lab.

Panthita Kaewjanthong

## TABLE OF CONTENTS

	Page
.....	iii
ABSTRACT (THAI).....	iii
.....	iv
ABSTRACT (ENGLISH).....	iv
ACKNOWLEDGEMENTS.....	v
TABLE OF CONTENTS.....	vi
LIST OF TABLES.....	ix
LIST OF FIGURES.....	x
CHAPTER I.....	1
INTRODUCTION.....	1
CHAPTER II.....	4
LITERATURE REVIEW.....	4
2.1 Steroid hormone receptors (SHRs) and signaling pathways.....	4
2.1.1 Genomic signaling pathways of NRs.....	5
2.1.2 Extranuclear signaling pathways of NRs.....	6
2.2 Lung cancer.....	8
2.3 Epidermal Growth Factor Receptor (EGFR).....	8
2.4 Role of EGFR in NSCLC.....	9
2.5 Role of progesterone receptor in NSCLC.....	11
2.6 Role of Steroid receptor coactivator-1 (SRC-1) in breast cancer.....	12
2.7 Cell-penetrating peptides (CPPs).....	14

2.8 <i>Pichia pastoris</i> expression system .....	16
CHAPTER III .....	18
MATERIALS AND METHODS .....	18
3.1 Reagents .....	18
3.2 Materials and Equipment .....	21
3.3 Microorganisms .....	22
3.4 Cell lines and Growth Conditions .....	22
3.5 Peptide designs and plasmid constructions .....	26
3.6 DNA cloning and transformation .....	28
3.7 Isolation of plasmid DNA .....	29
3.8 Yeast transformation and Genomic extraction .....	31
3.9 Peptide expression and purification .....	32
3.10 Detection of Small Peptide by SDS-PAGE .....	33
3.11 Detection of peptide localization .....	34
3.13 Western blot Analysis .....	35
3.14 RNA isolation and Real-Time PCR .....	36
3.15 Cell cycle analysis .....	37
3.16 Detection of Cell Apoptosis .....	38
3.17 Wound Healing Scratched Assay .....	38
3.18 Estradiol-induced breast cancer cell proliferation .....	38
3.19 Luciferase Assay .....	39
3.20 Statistical Analysis .....	39
CHAPTER IV .....	40
RESULTS .....	40

4.1 Peptide Construction and Characterization.....	40
4.2 Effect of the cancer-specific BR2 containing PR-PPD peptides on EGF-mediated NSCLC cell growth.....	52
4.3 Effect of BR2-2xPPD treatment on EGF-induced activation of Erk1/2 in NSCLC	55
4.4 BR2-2xPPD is a novel growth-inhibitory peptide for NSCLC expressing wild-type EGFR.....	58
4.5 Effect of the cancer-specific peptides on EGFR-mutant NSCLC cell proliferation .....	64
4.6 Effect of the cancer-specific BR2 peptide containing LXXLL motif or PR-PPD on Esradiol-induced cell proloferation of breast cancer cells.....	69
4.7 Effect of BR2 containing PR-PPD and LXXLL peptides on Triple-negative breast cancer cell proliferation.....	73
CHAPTER V .....	75
DISCUSSION AND CONCLUSION .....	75
APPENDIX A.....	81
APPENDIX B .....	85
REFERENCES.....	91
VITA.....	108

## LIST OF TABLES

	Page
Table 1 Cell viability of EGF and peptide treatments.....	81
Table 2 pMAPK and total MAPK activation.....	81
Table 3 Cell viability of EGFR-TKIs treatments.....	82
Table 4 Cell cycle distributions.....	82
Table 5 Cell viability of EGFR-TKIs treatment in EGFR mutant cells .....	83
Table 6 Percent apoptotic cells.....	83
Table 7 Percent wound area .....	84
Table 8 Relative luciferase assay.....	84

## LIST OF FIGURES

	Page
Figure 1 A schematic of Nuclear Receptors (NRs).....	4
Figure 2 Classical Nuclear and Extra-Nuclear signaling pathways .....	7
Figure 3 EGFR signaling pathways. ....	11
Figure 4 A schematic of human progesterone receptor (PR) domains. ....	12
Figure 5 The basic SRC structural domains.....	14
Figure 6 The route of Cell-penetrating peptide (CPPs) entry.....	16
Figure 7 A549 cell morphology .....	22
Figure 8 HaCaT cell morphology.....	23
Figure 9 MCF-7 cell morphology.....	24
Figure 10 T47DC42 cell morphology.....	24
Figure 11 MDA-MB-231 cell morphology.....	25
Figure 12 A schematic of BR2 containing PR-PPD peptides.....	27
Figure 13 Plasmid map of modified pPICZ $\alpha$ A containing CPP. ....	28
Figure 14 AKTA start process.....	33
Figure 15 Restriction enzyme digestion of pUC19-CPPs.....	41
Figure 16 Restriction enzyme digestion of pPICZ $\alpha$ A expression vector. ....	42
Figure 17 Cloning of the recombinant pPICZ $\alpha$ A-CPP expression vectors. ....	43
Figure 18 Linearization of the recombinant pPICZ $\alpha$ A-CPPs.....	45
Figure 19 PCR amplifying of yeast genomic DNA.....	46
Figure 20 Chromatogram and SDS-PAGE analysis of BR2 containing PR-PPD peptides. .....	47

Figure 21 Chromatogram and SDS-PAGE analysis of BR2 containing LXXLL motifs peptides.....	48
Figure 22 Western Blot Analysis of Histidine-tagged peptides.....	49
Figure 23 Intracellular localization of cell-penetrating peptides in HaCaT and A549.50	
Figure 24 Intracellular localization of cell-penetrating peptides in MCF-7.....	51
Figure 25 The effect of EGF on A549 cell proliferation.....	52
Figure 26 Effect of BR2-PR-PPD peptides on EGF-induced cell proliferation in A549. ....	54
Figure 27 Effect of BR2-PR-PPD peptides on EGF-induced cell proliferation in HaCat.....	55
Figure 28 Effect of BR2-PR-PPD peptides on EGF-induced Erk1/2 activation. ....	56
Figure 29 Effect of BR2-2x $\Delta$ PPD peptides on EGF-induced Erk1/2 activation.....	57
Figure 30 Effect of BR2-2xPPD and BR2-2x $\Delta$ PPD peptide on EGFR wild-type A549 cell proliferation. ....	58
Figure 31 Cell cycle distribution assessed by flow cytometry.....	59
Figure 32 Relative Cyclin D1 mRNA expression.....	60
Figure 33 Relative CDK2 mRNA expression.....	61
Figure 34 Effect of BR2-2xPPD and BR2-2x $\Delta$ PPD peptide on cell apoptosis.....	62
Figure 35 Effect of BR2-2xPPD and BR2-2x $\Delta$ PPD peptide on cell migration.....	63
Figure 36 Effect of EGFR-TKIs treatment on EGFR-mutant PC9 NSCLC cells .....	65
Figure 37 Effects of EGFR-TKIs and BR2-PRPPD peptide combination treatment TKIs-sensitive PC9 cell lines.....	66
Figure 38 Effects of EGFR-TKIs and BR2-PRPPD peptide combination treatment in TKIs-resistant PC9 cell lines. ....	68
Figure 39 Estradiol-induced MCF-7 breast cancer cell proliferation.....	70
Figure 40 Effect of BR2 coupled with PR-PPD or LXXLL motifs on E2-stimulated breast cancer cell proliferation. ....	71

Figure 41 Effect of LXXLL peptide on PR-dependent transcription. .... 73

Figure 42 Effect of BR2 containing PR-PPD and LXXLL peptides on Triple-negative breast cancer cell proliferation. .... 74



## CHAPTER I

### INTRODUCTION

Growth hormones and steroid hormones are known to influence the development and growth of many human cancers. Epidermal growth factor receptor (EGFR) is a tyrosine kinase receptor protein in ERBB family. EGFR expression has been shown to play a role in the development and progression of several cancer types (1). EGFR overexpression is frequently found in lung cancer, especially in NSCLC (2). Previous study demonstrated that high EGFR expression was correlated with poor prognosis of NSCLC patient (2, 3). Therefore, targeting EGFR signaling could help inhibit lung cancer growth. The ligand-induced EGFR sequentially lead to EGFR dimerization, autophosphorylation, and stimulating of downstream signaling pathways (4, 5). The tyrosine-residue phosphorylation results in the recruitment of growth factor receptor-bound protein 2 (Grb2) and human son of sevenless (hSOS) protein (6, 7). Grb2 contains Src homology 3 (SH3) domain which preferentially interacts with PXXPXR motif or polyproline domain (PPD) of other signaling molecules including hSOS (8, 9). The binding of Grb2-SH3 and hSOS-PPD mediate activation of several downstream signaling pathways such as ERK/MAPK, PI3K/ AKT, and JAK/ STAT pathways, leading to an increase in tumor cell proliferation and decrease apoptosis (10). We previously showed that progesterone receptor (PR) contains a PPD at the N-terminal region that directly interacts with the SH3 domain-containing molecules, including c-Src tyrosine kinases. PR-SH3 domains interaction mediated rapid progestin-dependent activation of c-Src and its downstream signaling in mammalian cells (8, 11).

We recently showed in an *in vitro* NSCLC model that PR expression inhibited EGF-mediated signaling and cell proliferation. Mutation in the PR-PPD, which blocked PPD-SH3 interaction, abolished PR-mediated inhibition of EGFR signaling (12). In this study, we extended our analysis to determine whether the PR-PPD alone is sufficient in mediating the PR growth inhibitory properties by adding cell-penetrating peptides or CPP sequence to the PR-PPD. CPPs are short peptides that can cross the plasma

membrane without a specific receptor. It was widely used in drug delivery (13). However, it has been shown that several CPPs also affect normal cell viability. A CPP called Buforin 2 (BR2) has been shown to have a strong penetrating ability and able to discriminate between normal cells and cancer cell lines (14). BR2 can internalize into the target cell by electrostatic interaction. Herein, we designed the cancer-specific peptides BR2-PRPPD targeting EGFR-dependent growth signaling.

Moreover, we also designed the cancer cell specific peptide to target the nuclear signaling. The activation of steroid hormones and steroid hormone receptors are known to promote cancer cells growth and cell survival. Previous studies established that the transcriptional activation of nuclear receptors (NRs) are required an essential factor known as steroid receptor coactivators (SRCs), which are the member of p160 steroid receptor coactivators family. SRCs contain three LXXLL motifs at the central region domain. This LXXLL motifs are served as the interaction domain for the ligand-binding domain (LBD) of NRs and recruitment of basal transcriptional protein complexes result in transcription machinery of hormone responsive element (15). In this study, BR2-LXXLL peptide was designed from GRIP-1 and F6 peptide sequence and the nuclear localization of SV40 was also added into peptide disrupt the NR/coactivator interaction in nucleus result in cancer cell growth inhibition. Peptides were expressed in yeast *Pichia pastoris* expression system. Our results demonstrate the specificity and ability of BR2-PRPPD and BR2-LXXLL peptides to inhibit the extra-nuclear and nuclear signaling pathways in NSCLC and breast cancer cell lines which provide a promising anticancer peptide for cancer therapy development.

### 1.1 Research questions

- Can the introduction of PR-PPD and LXXLL motifs peptides inhibit cancer cell proliferation via EGFR-dependent and coactivator-dependent signaling pathways?

### 1.2 Objectives

- To produce and characterize the cancer cell specific-CPPs in yeast (*Pichia pastoris*)

- To investigate whether the cancer cell specific-CPPs coupled with PR-PPD can inhibit EGFR-dependent signaling in cancer cell lines

- To investigate whether the cancer cell specific-CPPs coupled with LXXLL motifs can inhibit coactivator-dependent signaling in cancer cell lines

### 1.3 Hypothesis

The presence of PR-PPD or LXXLL by BR2 can disrupt protein-protein interactions in EGFR-dependent and coactivator-dependent signaling pathways leading to the inhibition of cancer cell proliferation.

### 1.4 Expected usefulness of study

Our data established a proof of concept that a cancer cell-specific CPP containing PR-PPD or LXXLL could serve as a novel therapeutic treatment to inhibit cancer cell proliferation.

## CHAPTER II

### LITERATURE REVIEW

#### 2.1 Steroid hormone receptors (SHRs) and signaling pathways

Steroid hormone receptors (SHRs) are the member of nuclear receptor class I (NRs) which serve as the receptor for glucocorticoid (GR), estrogen (ER), progesterone (PR), androgen (AR) and mineralocorticoid (MR) (16). The structure of NRs consists of functionally distinct domains (**Figure 1**). The N-terminal domain (A/B) is unique to each SHR and has different in sequence and length. It contains an autonomous transcriptional activation known as AF-1. The DNA binding domain (C) is highly conserve region which provide a specific site for receptor dimerization and bind to hormone response elements (HREs) on DNA target. The hinge (D) domain allows NR to dimerize with others nuclear receptors and link between DBD and LBD. The C-terminal domain comprise of ligand binding domain (LBD) responsible for ligand or hormone binding. NRs contain two activation function domains, which can activate the transcription, called as AF-1 and AF-2. AF-1 is a domain for phosphorylation even in ligand-independent manner. AF-2 allows ligand-dependent transcriptional activation and work synergistically with AF-1. In addition, AF-2 also interact with various coactivators and corepressors result in activation or inhibition of chromatin remodeling and the transcriptional activation machinery (17).

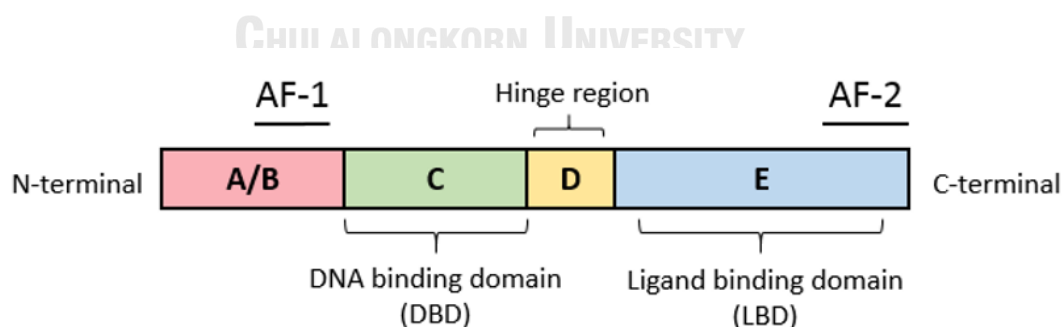


**Figure 1** A schematic of Nuclear Receptors (NRs)

Structure of nuclear receptor consist of DNA-binding domain (c), Hinge region (D) and Ligand-binding domain (E). At the N- and C- terminal contain the activation function domain including AF-1 and AF-2. This figure was adapted from (18).

### 2.1.1 Genomic signaling pathways of NRs

Steroid hormones exert various effects on cell growth, development, differentiation, and cell survival and act via the regulation of transcriptional processes. In the absence of hormone, NRs bind the chaperone protein such as heat shock protein (Hsp) in the cytoplasm lead to inactive form of NRs. In contrast, when ligand bind to LBD of NR in the cytoplasm, the high affinity of ligand-receptor binding result in dissociation of NR from Hsp, dimerization, translocate into the nucleus by nuclear localization sequences (NLS) and bind to HRE on target gene (19, 20). Binding of hormone to its NRs can activate transcription in nucleus (**Figure 2**). However, it has been reported that NR could not activate transcription by itself but it needs the essential factors known as coactivators (21).

Coactivators are non-DNA binding protein, which unable to bind directly to DNA, and function as the bridge which connect NRs to the basal transcriptional proteins lead to transcriptional activation. The first coactivator was identified in 1995 known as p160 steroid receptor coactivators (SRCs) family (22). This family composed of three members including SRC-1, -2 and -3. The SRC proteins are 160 kDa and share overall 50-55% sequence similarity. All of SRCs contain different functional domains which can distinctly interact to other proteins (**Figure 5**). The N-terminal domain is the most conserved region and contains a basic helix-loop-helix-Per/ Ah receptor nuclear translocation/ Sim (bHLH/ PAS) motif. The (bHLH/ PAS) motif involve in protein-protein interaction and recruit coactivator complexes such as SWI/SNF chromatin remodeling complex which bind to SRCs within activation domain 3 (AD3) (23, 24). The C-terminal domain contains two transactivation domains. AD1 is required for the interaction domain of other coactivators such as cAMP response element binding protein (CREB)-binding protein (CBP), the histone acetyltransferase enzyme p300 and p/CAF. Moreover, AD1 can recruit RNA helicase A (RHA) to bind the SRC-CBP/p300 protein complex and interact with RNA polymerase II (25). AD2 domain can recruit the histone methyl transferases (HMTs) such as coactivator-associated arginine methyltransferase I (CARM1) and protein arginine N-methyltransferase 1 (PRMT1) which is a histone H3 and H4 specific arginine, respectively. CARM1 can activate transcription only in the presence of SRC. CARM1 and PRMT1 can also

enhance transcription (26). The central region contains the three  $\alpha$ -helical LXXLL motifs which responsible for the nuclear receptor interaction (L, leucine; X, any amino acid) (27, 28). The variation of flanking sequences of LXXLL motifs display distinctive binding affinity for each NR (29). Secondary structure studies shown that an amphipathic  $\alpha$ -helix of LXXLL motifs bind to a hydrophobic cleft in the LBD of NRs after ligand-binding result in stabilization of SRC and NR protein complex (30). It has been found that single mutation of LXXLL motifs by alanine substitutions decreased the ability to bind to the LBD of the mouse ER fused to glutathione S-transferase (GST-AF2). Moreover, the nine LXXLL motifs present in RIP-140 also shown a strong ligand-dependent interaction with LBD of estrogen receptor (27, 28). These results suggested that LXXLL motifs is unique sequences which essential for SRCs and NRs interaction and facilitate the downstream transcriptional activation of the receptor by change chromatin remodeling and recruit RNA polymerase II (Pol II). In addition to direct interaction with hormone response element (HRE), NRs can regulate transcription by without directly bind to DNA. For example, in ER positive breast cancer ER associate with specific transcription factors, such as AP-1, Sp-1 and NF- $\kappa$ B, are formed transcriptional complex and bind to DNA target. The transcription via AP-1, Sp-1 and NF- $\kappa$ B result in expression of gene targets which involve in cell cycle, including insulin-like growth factor 1, *MYC* and cyclin D1, respectively. The expression of *MYC* and cyclin D1 promote cell cycle progression in MCF-7 breast cancer cells (31).

### 2.1.2 Extranuclear signaling pathways of NRs

More recently, the rapid signaling which mediated by the activation of various protein kinase cascade has been found. Estradiol-ER $\alpha$  complex and many growth factor receptors on the cell membrane, such as epidermal growth factor receptor (EGFR), nerve growth factor receptor (NGFR), platelet-derived growth factor receptor (PDGFR), and insulin-like growth factor receptor (IGFR), rapidly activate MAPK through Shc-Grb2-SOS pathway (32-35) (**Figure 2**). In this pathway, Shc acts as adapter protein. Shc consist of two domains are the phosphotyrosine binding (PTB) domain at

the N-terminal region and the Src homology 2 (SH2) domain at the C-terminal region. Shc can directly bind to the tyrosine kinase residues of receptors and activates the autophosphorylation on tyrosine residues. The phosphorylated tyrosine residues recruit the docking sites for the binding of the SH2 domain of Grb2 (Growth factor receptor-bound protein-2). Grb2 has a modular structure with one SH2 domain flanked by two Src homology 3 (SH3) domains. The Grb2-SH3 domains are necessary for the protein-protein interaction between Grb2 and other signaling molecules. It has been shown that SH3 domain has high affinity binding to PXXPXR motif, which also present within the guanine nucleotide exchange protein hSOS (36-39). The binding of Grb2-SH3 domain and SOS-PXXPXR motifs is the critical step for activation of MAPK leading to phosphorylation of nuclear proteins involved in transcriptional control which affect to cancer cell proliferation and survival (36-39).

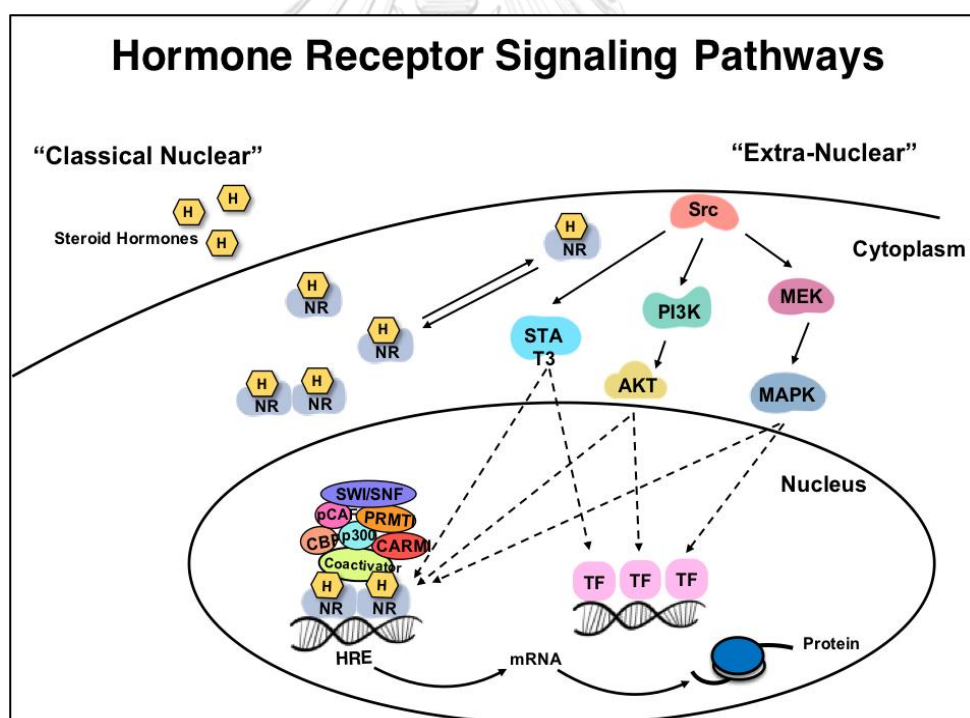


Figure 2 Classical Nuclear and Extra-Nuclear signaling pathways of Steroid Hormone Receptors.

Binding of hormone receptor with its ligand induce the conformational change and dissociates from chaperone protein in cytoplasm. The receptor then

dimerizes, translocate into the nucleus and binds to specific HREs on DNA target. The DNA-bound PR recruits coactivators leading to transcriptional effects. Hormone receptor can also activate the cytoplasmic signaling pathways, such as c-Src/Ras/MAPK and PI3K/Akt and STAT3 pathways. This figure was modified from (40).

## 2.2 Lung cancer

Cancer is a major problem which causes a high rate of global mortality. The estimated new cases of lung cancer are 228,150 and 142,670 patients died from lung cancer in both of male and female in 2019 (41). Lung cancer is a heterogeneous disease which differs in various subtypes in pathology and clinical manifestations. By immunohistochemistry, lung cancer is classified into two major types including small-cell lung cancer (SCLC) and non-small cell lung cancer (NSCLC) (42). SCLC is often found in patients who continued smoking and contribute to approximately 10-15 percent of lung cancer cases. NSCLC is the predominant type of lung cancer which 85-90 percent of patients were diagnosed as NSCLC. For NSCLC, it can be divided into 3 groups: Adenocarcinoma (38%), Squamous cell carcinoma (20%), and Large-cell lung carcinoma (3%). Treatment of lung cancer includes surgery, radiation, and chemotherapy. The alteration in molecular targets, such as BRAF, ALK, PIK3CA, HER2 and EGFR, are also related to disease progression. Abnormality of these genes emerged the development of novel targeted therapy which can prolong patient survival rate more than using the conventional treatments alone.

## 2.3 Epidermal Growth Factor Receptor (EGFR)

The epidermal growth factor receptor or EGFR is a transmembrane protein which belongs to the ERBB family of receptor tyrosine kinase. EGFR consists of 3 domains: the extracellular ligand-binding domain, transmembrane domain, and intracellular tyrosine kinase domain (43). EGFR plays a crucial role in several biological activities including cell proliferation, cell survival and cell apoptosis (44). EGFR activation can be induced by its cognate ligands such as epidermal growth factor (EGF), transforming growth factor  $\alpha$  (TNF- $\alpha$ ) and amphiregulin (AR) (43). These ligands specifically bind to the extracellular domain and consequently induce the dimerization among the

ERBB members as heterodimer or homodimer. The ligand binding of EGFR activates phosphorylation at Thy 992, 1045, 1068, 1148 and 1173 of intracellular kinase domain. The autophosphorylation lead to the recruitment of the binding site for adaptor protein containing the specific Src homology 2 or SH2 domain and induce signal transduction of MAPK, PI3/AKT and STAT pathways (45) (**Figure 3**).

#### 2.4 Role of EGFR in NSCLC

Dysregulation of EGFR occurs in various type of malignant cells including NSCLC. The EGFR gene is frequently found to be upregulated or amplified in 40-80% of NSCLC cases (46). The overexpression of EGFR is associated with poor prognosis and reduce survival in NSCLC patients (47). Hyperactivation of EGFR kinase domain by its overexpression increase cancer cell proliferation, invasion, angiogenesis and decrease cancer cell apoptosis (47). Therefore, EGFR is often targeted for treatment of NSCLC. The first generation of tyrosine kinase inhibitors (EGFR-TKIs) have been developed to inhibit ligand-induced phosphorylation of kinase domain (48). Gefitinib and Erlotinib competitively bind to ATP-binding pocket with ATP by reversible binding lead to decreasing of signal transductions (49). However, the most patients who achieved to EGFR-TKIs treatment were found as NSCLC bearing the mutation of EGFR (50). Thus, EGFR mutation status is commonly estimated in NSCLC patients for the proper treatment.

Ligand-independent activation of EGFR is mainly caused by mutation in tyrosine kinase domain of EGFR. The two most common mutations of the EGFR genes have been identified. The in-frame deletion in exon 19 was eliminated the amino acids sequence from leucine-747 to glutamic-749 residue and a single nucleotide substitution from arginine to leucine in exon 21 (L858R) (51-53). These two types represent 85-90% of EGFR mutations and are defined as the classical activating EGFR mutations (54). In NSCLC patients with exon 19 deletion exhibit high sensitivity to Gefitinib (55). The evidence showed that mutation in kinase domain of EGFR disrupt the binding of ATP to its binding pocket and allow Gefitinib to block phosphorylation of the receptors. However, there are some types of EGFR mutation fail to EGFR-TKIs treatment such as the insertion in exon 20 which become an

acquired resistance to TKIs (56). Acquired resistance to EGFR-TKI is mediated through 3 pathways. In approximately 50% of patients with advance stage NSCLC have been diagnosed to develop the secondary mutation after EGFR-TKIs treatment for a long-time. The substitution of methionine for threonine at position 790 (T790M) occurs in the ATP binding site result in higher affinity to ATP than the TKI molecules (57). Afatinib, Aacomtinib, Rociletinib and Osimertinib are the second and third generation of EGFR-TKIs which display irreversible and covalent binding to the pocket. These EGFR inhibitors are suitable for both wild-type and mutant EGFR, particularly Osimertinib is a selective inhibitor for T790M-EGFR (58). In recent years, the tertiary mutation in kinase domain of EGFR has been reported. A substitution of C797S mutation confers the resistance to Osimertinib (59). Thus, it is an urgent need to develop a novel drug to target these EGFR mutations.

In addition to the secondary mutation, a variety of others receptor kinase tyrosine are also activated in acquired resistant cells. MET is receptor for the hepatocyte growth factor (HGF) which is the most common bypass pathway and important to cell proliferation, apoptosis and migration. MET amplification and mutation have been found to relate with EGFR-mutant NSCLC (60). Using of MET inhibitors could improve survival and response in patients with EGFR-TKIs resistance. The upregulation of HER2, IGFR1 and BRAF were also identified in EGFR-mutant NSCLC (61, 62). These proteins are a part of RAS/MAPK, PI3K and STAT3 signaling pathways. The altered expression of survival or apoptosis-related genes such as Bcl2, BIM, p53 and NF-KB also confer to TKI resistance (63, 64).

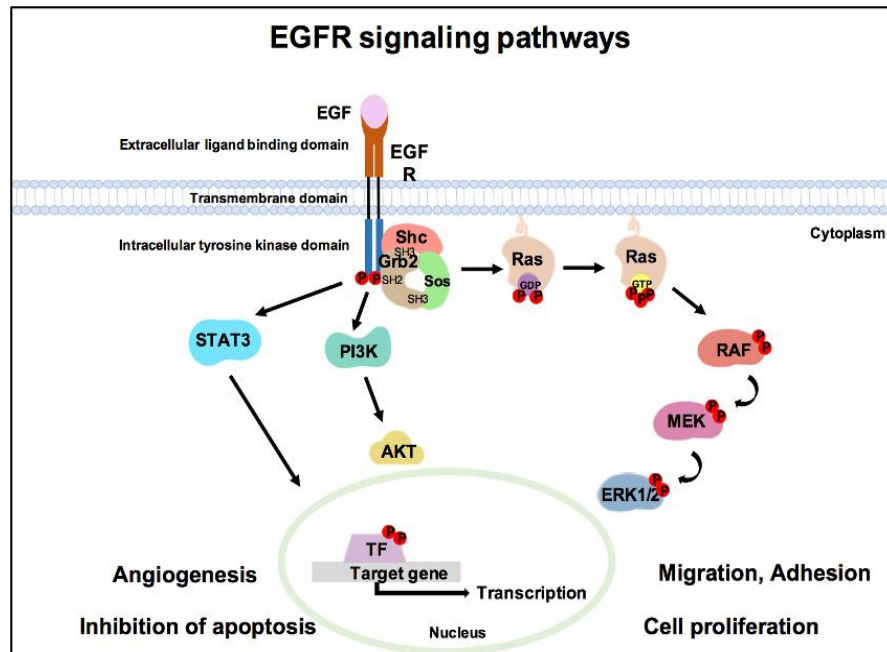


Figure 3 EGFR signaling pathways.

The binding of EGF to EGFR can induce the dimerization and autophosphorylation of the receptor lead to the recruitment of binding site for various adaptor protein. Grb2 protein structure consists of one Src homology 2 (SH2) domain flanked by two Src homology 3 (SH3) domains. These SH3 domain has high affinity binding to polyproline domain (PPD) of others signaling molecules including Sos protein. The interaction between Sh3 and PPD can mediate several downstream cascades including (MAPK), PI3K/AKT, and STAT pathways which are involved in cell proliferation, survival, and inhibition of apoptosis. This figure was adapted from (65).

## 2.5 Role of progesterone receptor in NSCLC

It is well known that sex steroid hormones play a crucial role in various human tissues and in hormone-related cancers. Previous studies have been revealed the role of ER which its expression contributed the increasing of NSCLC cell growth and progression (66). While PR is used as a prognostic marker in hormone therapy, but its responsibility in NSCLC is remain unclear (67). Expression of PR has been reported in adenocarcinoma tissues. PR localize in both the nuclear and extranuclear

compartments observing by immunohistochemistry (10, 68). High level of PR expression was mainly detected in female and associated with better clinical outcome in NSCLC patients (69). Both of PR-A and PR-B isoforms also expressed in NSCLC cell lines such as H23, H1975, HCC827, H3255 and A549 (70). Administration of progesterone significantly inhibited PR-positive NSCLC cell proliferation compared to PR-negative cells. While this inhibition effect was reversed by PR antagonist. *In vivo* studies have been shown the reduction of tumor volume after mice were treated with progesterone. We previously demonstrated the decreasing of cancer cell growth in NSCLC expressing PR-B isoform (71). The results shown the significant of polyproline SH3 recognition motif or PXXPXR motif of PR which effectively inhibit NSCLC cell proliferation. PR-PXXPXR motif can directly bind to c-Src and various SH3-containing molecules which has been described as an extranuclear actions of PR (Figure 4) (8, 71).

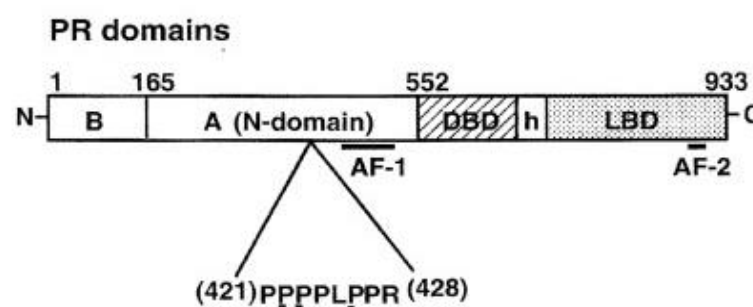


**Figure 4** A schematic of human progesterone receptor (PR) domains.

Human PR protein consists of four distinct domains: the DNA binding domain (DBD), a small hinge region, and the C-terminal ligand-binding domain (LBD) and the N-terminal transactivation domain (NTD) which contain polyproline domain (PPD) at position 421-428 (8).

## 2.6 Role of Steroid receptor coactivator-1 (SRC-1) in breast cancer

Among all members of SRC, many studies interested in SRC-1 because it largely expressed in various tissues such as testis, brain, lung, kidney, prostate, uterus, bone, adipose and tissue. SRC-1 can coactivate NRs including glucocorticoid receptor

(GR), estrogen receptor  $\alpha$  (ER $\alpha$ ), thyroid receptor (TR), retinoid X receptor (RXR), hepatocyte nuclear factor 4 (HNF4 $\alpha$ ) and peroxisome proliferator-activated receptor  $\gamma$  (PPAR $\gamma$ ) (22, 72). SRC-1 is required for the development of normal mammary gland which normally has low expression of SRC-1. In the absence of SRC-1, ductal density, alveoli number and size were reduced resulting in lower milk production in the null mice. SRC-1 also interacts with androgen receptor (AR) and thyroid hormone receptor (TR). SRC-1 knockout mice exhibited reduced weight of prostate, urethra and body growth compared with wild-type mice (73, 74). In addition to normal tissues, SRC-1 is also expressed in several cancers such as endometrial cancer, thyroid cancer, cutaneous melanoma and breast cancer. In the case of breast cancer, SRC-1 was expressed in 19–34% of human breast cancers. High expression of SRC-1 correlated with large tumor size, high tumor grade and decreased disease-free survival. In the presence of E2, overexpression of SRC-1 in transfected-MCF-7 cells significantly increased cell growth and pS2 levels, which is the E2-responsive gene. Furthermore, SRC-1 can increase breast cancer cell survival via suppression of tumor necrosis factor alpha (TNF- $\alpha$ ) (75-77). The role of SRC-1 in metastasis has been investigated. Mouse mammary tumor virus-polyoma middle T (*MMTV-PyMT*) transgenic mice were knocked out of SRC-1. The mammary tumor cells in the blood circulation of *MMTV-PyMT* mice were higher than SRC-1  $-/-$ ; *MMTV-PyMT* mice and the intravasation of tumor cells also reduced lung metastasis (78). Tamoxifen is a selective estrogen receptor modulator (SERM) which is the most widely used as antiestrogen therapy in ER positive breast cancers. Unfortunately, many patients experience recurrence in a few years after treatment. It has been demonstrated that the upregulation of SRC-1 and ER $\alpha$  was increased after tamoxifen treatment (79). These data show the correlation between SRC-1 and breast cancer cell development and survival. Therefore, SRC-1 may represent as a therapeutic target for breast cancer.

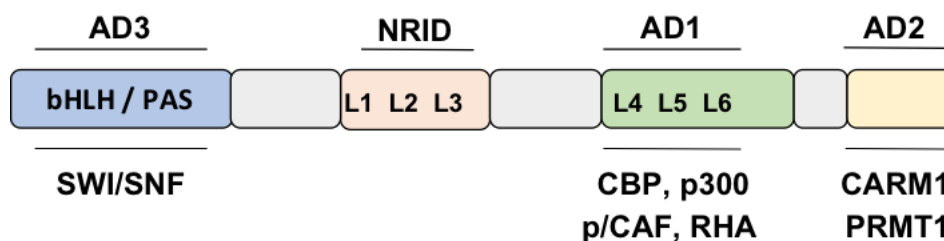


**Figure 5** The basic SRC structural domains

SRCs contain three major domains. The amino-terminal basic helix–loop–helix–Per/ARNT/Sim (bHLH–PAS) domain can interact with several transcription factors. The central region contains the three  $\alpha$ -helical LXXLL motifs which are responsible for the nuclear receptor interaction (L, leucine; X, any amino acid). At C-terminal, AD1 is required for the interaction domain of other coactivators such as cAMP response element binding protein (CREB)-binding protein (CBP), the histone acetyltransferase enzyme p300 and p/CAF. Moreover, AD1 can recruit RNA helicase A (RHA) to bind the SRC-CBP/p300 protein complex and interact with RNA polymerase II (25). AD2 domain can recruit the histone methyl transferases (HMTs) such as coactivator-associated arginine methyltransferase I (CARM1) and protein arginine N-methyltransferase 1 (PRMT1) which is a histone H3 and H4 specific arginine, respectively (80).

## 2.7 Cell-penetrating peptides (CPPs)

Cell membrane, consist of lipid bilayer with embedded protein, is selectively permeable to molecules which essential to the cell survival and prevent cell from the disguised molecules. Many therapeutic drug targets are mainly localized intracellular compartment. So, many studies were performed to improve the ability of molecules to transport across the cell membrane lead to effectively treatment such as carbon nanotubes, liposomal drugs or nanoparticles. Among the new approaches, cell-penetrating peptides (CPPs) is one the most frequently developed for intracellular delivery of various molecules (81, 82).

Cell-penetrating peptides or CPPs are short peptide normally contain 5-30 amino acids which can cross the plasma membrane without specific receptor (83). CPPs can transport various types of molecules including small molecules, peptides,

proteins, enzyme, nanoparticles, small interfering RNA (siRNA) and liposomes. The trans-activator of transcription (TAT) protein of the human Immunodeficiency Virus (HIV) was identified as the first CPP. The researcher found that the TAT purified protein can be uptake and localize in nucleus of cells (84). The following studies found the third helix of the DNA binding domain of *Drosophila antennapedia* (pAntp) are necessary for translocation into the cells (85). After discovering of these two CPPs, the several CPPs were discovered successively. CPPs were divided into 3 major groups. First, CPPs derive from natural protein including viral proteins, RNA-binding proteins, homeoproteins and antimicrobial peptides. Second, the fusion of two natural peptides or chimeric peptides such as Pep1 and MPG which is the fusion of tryptophan-rich domain or HIV glycoprotein 41 with the nuclear localization signal (NLS) of SV40, respectively. The last is synthetic CPPs which are designed based on structure-activity studies such as polyarginine (83). Rely on the physical and chemical properties, CPPs can separated into three groups (**Figure 6**). Since the cell membrane contain the negative charge from polysaccharides and phospholipids on the cell surface. The electrostatic can be induced by the interaction between the cationic CPPs, which contain highly positive net charges, and the negative charge of cell membrane lead to CPPs internalizations. The second one is hydrophobic CPPs. These CPPs contain nonpolar residues and hydrophobic amino acid which important for cell uptake. The last is amphipathic CPPs contain polar and nonpolar residues (86).

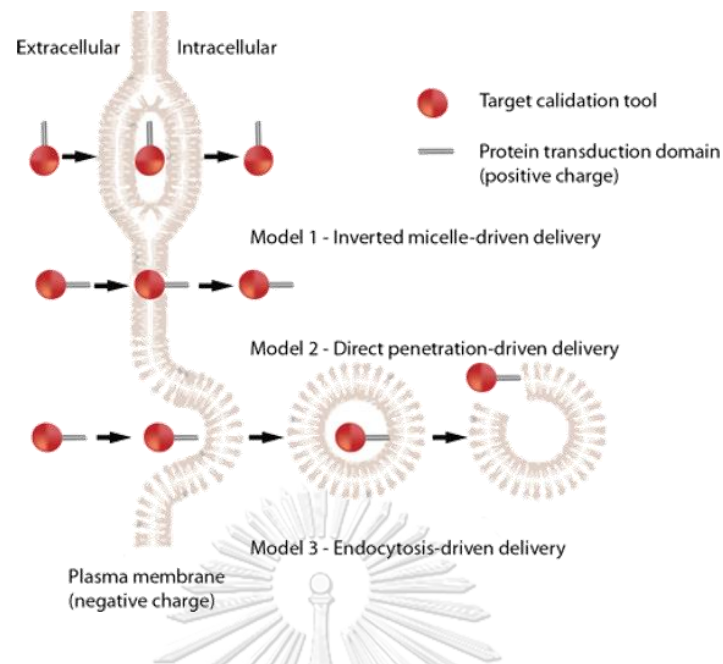


**Figure 6** The route of Cell-penetrating peptide (CPPs) entry

Buforin IIb (BRIIb), a histone H2A-derived peptide, has been shown a strong permeability and anticancer activity in various cancers. BRIIb displayed selective cytotoxicity in 62 cancer cells by specific to cancer cells surface ganglioside (87). However, it still has been affected the viability of normal cells at high concentration. Buforin2 or BR2 has been found as a novel cancer-specific and nontoxic to the normal cells (88). BR2 is antimicrobial peptide or AMP which has ability to kill bacterium cells. It contains a proline hinge within C-terminal domain. It has been reported that BR2 effectively internalization into various cancers such as human cervical cancer cell line Hela, mouse melanoma cell lines B16/F10 and human colon cancer cell lines HCT116 but not affected to normal cell lines such as HaCaT and NIH3T3 (89).

### 2.8 *Pichia pastoris* expression system

In the past, prokaryote cells were acted as protein expression system. *Escherichia coli* or *E. coli* is one of microorganism which was widely used to generate the recombinant proteins. This expression system is simple to manipulate and cost-effective. Although, these recombinant proteins were successful and can be used in

many researches, it also has some limitations. Proteins which derives from prokaryote genome lack of the posttranslational modification steps lead to miss-fold inclusion bodies and insoluble proteins. Thus, many studies need to increase refolding and solubilization steps to obtain the functional proteins. Moreover, *E. coli* expressed proteins are non-stable and can cause immune response. Therefore, the production of recombinant protein was developed from *E.coli* to yeast system (90).

*Pichia pastoris* is methylotrophic yeast which can metabolize the carbon source from methanol. The first step in methanol metabolism is alcohol oxidase (AOD) which oxidize methanol to generate formaldehyde and hydrogen peroxide. The toxic of hydrogen peroxide is broken down to oxygen and water by enzyme catalase (CAT). Next, formaldehyde is oxidized by two pathways, assimilation and dissimilation. Formaldehyde is fixed by dihydroxyacetone synthase (DAS) to form dihydroxyacetone (DHA) and glyceraldehyde 3-phosphat (GAP) which assimilate into the cytosol. These reactions are occurred in special organelle, called peroxisome. The alcohol oxidase promoter is used to drive the recombinant protein expression from *P. pastoris*. *AOX1* and *AOX2* are two genes which serve for alcohol oxidase. *AOX1* gene regulates the high levels of the methanol utilization and can growth in medium containing methanol. *Mut*<sup>+</sup> is defined for the wild-type methanol utilization phenotype strains such as SMD1168 and GS115. The KM71H strain is *Mut*<sup>s</sup> phenotype containing the *AOX2* gene which exhibit lower expression and can growth on methanol slower than *AOX1* strain (90). *P. pastoris* has been used extensively and successfully to produce the recombinant protein because it able to express the heterologous eukaryotic proteins. This expression system can effectively produce the soluble proteins and can modify the target protein by posttranslational processes, such as glycosylation, phosphorylation and lipidation, which are the limitations of *E. coli* system. The target protein can be secreted into culture medium by the secretion signal which contain in the expression vector. Therefore, the supernatant can be directly purified without harvesting yeast cells (91-93).

## CHAPTER III

### MATERIALS AND METHODS

#### 3.1 Reagents

##### 3.1.1 Reagents for bacteria and yeasts cloning

Tryptone	Bio-Basic, Canada
Peptone	Oxiod, U.K
Yeast extract	Oxiod, U.K
Glycerol	Vivantis, Malaysia
Yeast Nirogen Base w/o amino acids and Ammonium Sulphate	Himedia, India
pPICZ $\alpha$ A expression vector	Invitrogen, U.S.A
Zeocin	Invitrogen, U.S.A
Ampicilin	Applichem, Germany
NaCl	Merck Millipore, Germany
Methanol	Merck Millipore, Germany
Agar A	Bio-Basic, Canada
HEPES, free acid	Bio-Basic, Canada
DTT	Sigma Aldrich, U.S.A
EDTA	Bio-Basic, Canada D-
Sorbitol	Bio-Basic, Canada
Dextrose	Sigma Aldrich, U.S.A
Biotin	Fluka, Germany
Isopropanol	Merck Millipore, Germany
SYBR <sup>TM</sup> Safe DNA Gel Stain	Invitrogen, U.S.A
DNA ladder 100 bps and 1 kb	Gene direx, U.S.A
Agarose	Apsalagen, U.S.A
<i>EcoRI</i>	Thermo scientific, U.S.A
<i>PstI</i>	Thermo scientific, U.S.A
<i>SacI</i>	Thermo scientific, U.S.A
Alkaline Phosphatase	Thermo scientific, U.S.A



### 3.1.2 Kits

QIAprep Spin miniprep kit	Qiagen, Germany
QIAquick Gel extraction kit	Qiagen, Germany
QIAGEN Plasmid Maxi kit	Qiagen, Germany
YeaStar Genomic DNA kit	Zymo Research, U.S.A
FITC Annexin V Apoptosis Detection Kit with PI	BioLegend, U.S.A
Muse® Cell Cycle Assay Kit	Merck Millipore, Germany

### 3.1.3 Reagents for peptide purification

Imidazole	Sigma Aldrich, U.S.A
Ethanol	Merck Millipore, Germany
<i>di</i> -Potassium hydrogen phosphate	Sigma Aldrich, U.S.A
<i>di</i> -Sodium hydrogen phosphate	Sigma Aldrich, U.S.A
Sodium phosphate, monobasic	Bio-Basic, Canada
Sodium phosphate, dibasic	Bio-Basic, Canada
EDTA	Sigma Aldrich, U.S.A
NI <sub>SO</sub> <sub>4</sub>	Sigma Aldrich, U.S.A

### 3.1.4 Reagents for cell cultures

DMEM phenol red free, powder	Sigma Aldrich, U.S.A
Fetal bovine serum (FBS)	Merck Millipore, Germany
Charcoal Stripped Fetal Bovine Serum	Sigma Aldrich, U.S.A
Penicillin Streptomycin	HycloneLaboratorie, U.S.A
EDTA-Trypsin 0.25 (1x)	HycloneLaboratorie, U.S.A
AntiBiotic-Antimycotic (100x)	Life Technologies, U.S.A
Phosphate Buffered Saline (PBS)	HycloneLaboratorie, U.S.A
MTT	Invitrogen, U.S.A
SDS	Merck Millipore, Germany
Muse Cell Cycle Kit	Merck Millipore, Germany
Epidermal Growth Factor (EGF)	Merck Millipore, Germany
Gefitinib	Sigma Aldrich, U.S.A

Erlotinib	Sigma Aldrich, U.S.A
DMSO	Sigma Aldrich, U.S.A
Trypan blue stain	Thermo scientific, U.S.A

### 3.1.5 Reagents for protein SDS-PAGE and western blotting

RIPA lysis buffer	Merck Millipore, U.S.A
Proteinase inhibitor cocktail	Roche, Germany
Bovine serum albumin	Merck Millipore, U.S.A
Bradford dye reagent	Bio-Rad, U.S.A
Precision Plus Protein All Blue Standard	Bio-Rad, U.S.A
PageRuler Unstained Low Range Protein Ladder	Invitrogen, U.S.A
Blotting-Grade Blocker	Bio-Rad, U.S.A
TEMED	Bio-Rad, U.S.A
Ammonium Persulfate	Bio-Rad, U.S.A
Tricine	Sigma Aldrich, U.S.A
Tris	Vivantis, Malaysia
Glycine	Vivantis, Malaysia
SimplyBlue SafeStain	Thermo scientific, U.S.A
Phospho-p44/42 MAPK (Erk1/2) antibody	Cell Signal Technology, U.S.A
p44/42 MAPK (Erk1/2) antibody	Cell Signal Technology, U.S.A
Anti-rabbit IgG HRP-linked antibody	Cell Signal Technology, U.S.A
Pierce ECL Western Blotting Substrate	Thermo scientific, U.S.A

### 3.1.6 Reagents for immunofluorescence staining

Hoechst 33342 solution	Thermo scientific, U.S.A
Anti-6X His tag antibody [HIS.H8]	Abcam, Cambridge, U.K.
Goat Anti-mouse IgG&L (Alexa Fluor 568)	Abcam, Cambridge, U.K.
Prolong Gold Antifade Mountant	Thermo scientific, U.S.A

### 3.2 Materials and Equipment

HisTrap FF column 5 ml	GE healthcare, U.K.
Glass microfiber filter Grade GF/C diameter 47 mm	GE healthcare, U.K.
Gene Pulser/Micro Pulser Electroporation Cuvettes	Bio-Rad, U.S.A
Electroporator	Thermo scientific, U.S.A
SnakeSkin™ Dialysis Tubing 3.5 MWCO	Thermo scientific, U.S.A
SnakeSkin™ Dialysis Clips	Thermo scientific, U.S.A
Syringe Filter 0.22 and 0.45 $\mu\text{M}$	Sigma Aldrich, U.S.A
Baffled Flasks 500 ml and 1000 ml	DURAN, U.K.
Erlenmeyer Flasks	Pyrex, U.S.A
Akta start	GE healthcare, U.K.
Refrigerated Centrifuge	Thermo scientific, U.S.A
Wet Tank Blotting system	Bio-Rad, U.S.A
Gel Electrophoresis chamber	ATTO, JAPAN
96-well TC-treated Microplate	Corning Life Sciences, U.S.A
6-well Clear TC-treated Multiple well plates	Corning Life Sciences, U.S.A
Easy Flask 25 cm <sup>2</sup> Filter	NUNC, DENMARK
Autopipette 0.5-1000 $\mu\text{l}$	Gilson, France
Pipette Filler	Thermo scientific, U.S.A
Pipette tips	Gilson, France
Nalgene PPCO Centrifuge Bottle 250 ml	Thermo scientific, U.S.A
Nalgene Hi-speed Centrifuge Tube	Thermo scientific, U.S.A
Centrifuge Tube	NEST, U.S.A
Microcentrifuge tube 1.5 ml	NEST, U.S.A
Cryotube cryogenic vial	NUNC, DENMARK
Freezer -20	SANYO electric, Japan
Refrigerator 4	SHARP, Japan
Biosafety cabinet	Haier, China

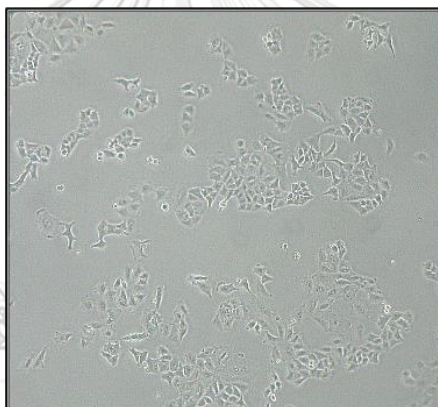
Autoclave	HIRAYAMA, Japan
Millipore Milli Q	Merck Millipore, U.S.A
Exicycler 96 Real-Time PCR	Bioneer, Korea
EnSpier Multimode Plate Reader	PerKinElmer, U.S.A

### 3.3 Microorganisms

Competent <i>E. coli</i> Dh5 $\alpha$ strain	New England Biolabs, UK
Competent <i>P.pastoris</i> KM17H strain	Invitrogen, U.S.A

### 3.4 Cell lines and Growth Conditions

#### 3.4.1 A549 (Human Lung Adenocarcinoma Cells)



จุฬาลงกรณ์มหาวิทยาลัย  
**Figure 7 A549 cell morphology**

The NSCLC A549, is a human non- small cell lung carcinoma cell line, has wild-type EGFR expression. A549 was gifted from Diana C.Marquez-Garban, Department of Medicine in Hematology/Oncology, David Geffen School of Medicine, U.S.A. A549 was cultured in Roswell Park Memorial Institute medium (RPMI) supplemented with 10% fetal bovine serum (FBS) and 1% Penicillin Streptomycin (PenStrep). Cells were cultivated in a humidified tissue culture incubator at 37°C with 5% CO<sub>2</sub>.

### 3.4.2 PC9 (Human Lung Adenocarcinoma Cell Line)

EGFR- mutant PC9 cells were gifted from Prof.Hironobu Sasano (Department of Pathology, Tohoku University Graduate School of Medicine, Sendai, Japan). PC9 cells were cultured with increasing concentrations of gefitinib or erlotinib; 10 nM (2 months), 1  $\mu$ M (2 months) and 5  $\mu$ M (2 months) to obtain gefitinib- or erlotinib-resistant cell lines (PC9-GR and PC9-ER, respectively). The parent PC9-6M cells were also cultured in culture medium without EGFR-TKIs for 6 months to keep the same cultural conditions as previously described. PC9-6M, PC9-GR and PC9-ER were also examined for EGFR mutation status as followed: PC96M and PC9-GR; exon 19 deletion, PC9-ER; exon 19 deletion, L858R and T790M mutations (94). Cells were maintained in 10%FBS-RPMI plus 1% PenStrep.

### 3.4.3 HaCaT (Human Normal Keratinocyte Cell Line)

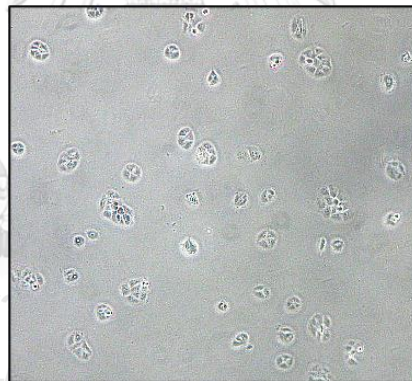


**Figure 8 HaCaT cell morphology**

Spontaneously Transformed Human Keratinocyte Cell Culture (HaCaT) were obtained from the American Type Culture Collection (ATCC). HaCaT cells were cultured in Dulbecco's Modified Eagle Medium (DMEM) plus with 10% FBS and 1% PenStrep.

#### 3.4.4 MCF7 (Human Breast Cancer cell line, ER+/PR+/HER2+)

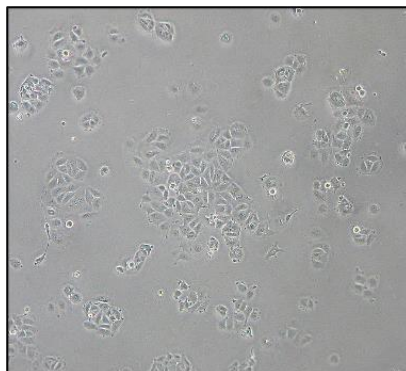


**Figure 9** MCF-7 cell morphology

MCF-7 is a human epithelial breast cancer cell line with positive for estrogen receptor, progesterone receptor and HER2. Cells were cultured in DMEM with high glucose medium plus 10% FBS and 1% PenStrep. For cell proliferation assay, cells were plated in phenol-red free DMEM supplemented with 5%DCC (Charcoal-stripped serum) for 3 days before initial the treatment.

#### 3.4.5 T47DC42 (Human Breast Cancer cell lines, ER-/PR-/HER2+)

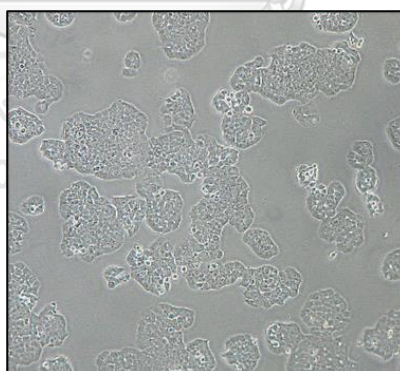


**Figure 10** T47DC42 cell morphology

T47DC42 is PR negative breast cancer cells which were gifted from V. Craig Jordan. T47DC42 was originated from T47D (the ER- and PR-positive cell) breast cancer cell which cultured for long term in estrogen-deprived medium. Cells were maintained in DMEM with high glucose supplemented with 5% FBS and 1% PenStrep.

### 3.4.6 MDA-MB-231 (Human Triple-Negative Breast Cancer Cell line, ER-/PR-/HER2-)

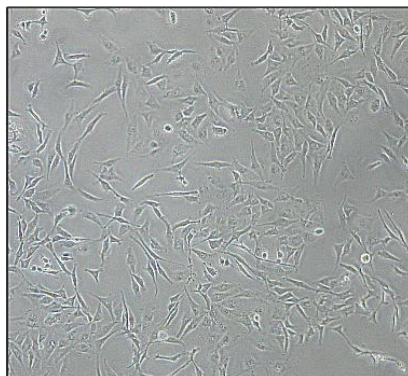


**Figure 11 MDA-MB-231 cell morphology**

MDA-MB-231 is a human triple-negative breast cancer (TNBC) cell line which lack of estrogen receptor, progesterone receptor and HER2 expression. Cells were grown in DMEM with high glucose medium supplemented with 10% FBS and 1% PenStrep. The cells were maintained at 37°C with 5% CO<sub>2</sub>.



### 3.5 Peptide designs and plasmid constructions

The consensus PPPPLPPR is defined as a class II SH3 ligand (PXXPXR) which locates at the N-terminal domain of human PR, including both the PR-A and PR-B isoforms. We previously established that this proline-rich motif interacts with SH3-domain-containing proteins and sequentially exert progestin activation of nongenomic signaling pathways in mammalian cells (8). Binding of SH3-PPD domains is essential for several growth factor signal transduction pathways, such as EGFR (95). Expression of PR-B containing the PPD inhibited NSCLC cell proliferation in both progestin dependent and independent manners, suggesting that the PR-PPD expression suppressed cytoplasmic/ membrane signaling through inhibiting the activation of the EGFR pathway (12). To determine if the PR-PPD is the minimal domain required to mediate the growth inhibitory effect, a cancer-specific cell-penetrating peptide PR-PDD peptides were expressed and constructed. A cancer-specific CPP, buforin-2 (BR2), was added to the N-terminus of PR-PPD (BR2-PPD) to aid the delivery of PR-PPD inside the cells. In addition, BR2-2xPPD was constructed to carry two repeats of PR-PPD separated by an intervening sequence similar to a sequence that separates two PPD sequences in hSOS (NP\_001369324.1) to mimic endogenous Grb2-SOS interaction. A mutant BR2-2x $\Delta$ PPD peptide was also constructed to determine the specificity of the PR-PPD interaction by replacing key prolines with alanines.

For the cancer cell-specific peptide targeting nuclear signaling pathways, steroid receptor coactivators or SRCs have been shown to their ability to interact and coactivate several nuclear receptors, especially SRC-1 (96). SRC-1 contains three alpha-helical LXXLL motifs at the C-terminus which serve as nuclear receptor binding domain. LXXLL-peptide was designed for interfering nuclear receptor/coactivator interaction. Expression of glucocorticoid receptor interacting protein 1 or GRIP-1 was able to decrease the ER transcription activity. The recombinant protein containing two repeats of the F6 peptide separating by GRIP-1 was more effective to inhibit ER function (97). Therefore, NRx2 peptide was constructed from two LXXLL motifs of peptide F6 linked by GRIP-1 amino acid sequence (BR2-LXXLL). Moreover, NRx2 was

further combine to the SV40 nuclear localization sequence to access the nucleus. A scramble or control peptide was generated by the permutation in NRx2 amino acids of the original peptide (BR2-LXXLLscramble).

All peptides were added a polyhistidine tag which consist of six histidine (His) residues at the C-terminal to be used for peptide purification. The enzyme restriction sites for DNA cloning including *EcoRI* (G'AATTC) and *PstI* (CTGCA'G) were added to the N-terminal and C-terminal, respectively. Pichia codon optimization was used to design each nucleotide sequences. The nucleotide sequences were synthesized as double-stranded DNA into pUC19 plasmid by GeneArt/Thermo scientific, U.S.A. Peptides sequences were shown in **Figure 12**.



- A. **BR2 sequence:** RAGLQFPVGRLLRLLR  
 B. **PR-PPD sequence:** FPLGPPPPLPPRATPSRPG  
 C. **1xPPD sequence:** FPLGPPPPLPPRATPSRPG  
 D. **2xPPD sequence:** FPLGPPPPLPPRATPSRPGAESSPSKIMSFLPGPPPPLPPRATPSRPG  
 E. **Sos sequence:** DEVVPPPPVPPRRRPESAPAESSPSKIMSKHLDSPPAIPRQPTSKAY  
 F. **ΔPPD sequence:** FPLGPPAALAARATPSRPGAESSPSKIMSFLGPPAALAARATPSRPG  
 G. **GRIP-1 sequence:** LKEKHKILHRLLDSSSPVDLAKLTAEATGKELSQESSSTAPGSEVTVKQEPASPKKENALLRYLLDKDDTKD  
 H. **F6 peptide:** GHEPLTLLERLLMDDKQAV  
 I. **NRx2 sequence:** GHEPLTLLERLLMDDKQAVDLAKLTAEATGKELSQESSSTAPGSEVTVKQEPASPGHEPLTLLERLLMDDKQAV  
 J. **SV40NLS sequence:** PPKKKRKV

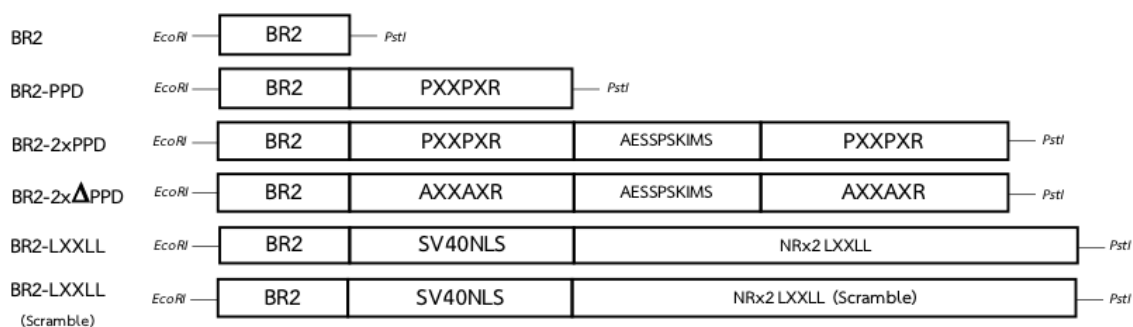


Figure 12 A schematic of BR2 containing PR-PPD peptides.

### 3.6 DNA cloning and transformation

pPICZ $\alpha$ A expression vector was previously modified by inserting the *Pst*I restriction site, polyhistidine sequence and stop codon, respectively (constructed by Asst. Prof. Sarintip Sooksai, Ph.D.) (**Figure 13**). pUC19 plasmid containing the recombinant peptide sequences and pPICZ $\alpha$ A vector were digested with *Eco*RI and *Pst*I and analyzed by gel electrophoresis to obtain the individual recombinant peptide DNA fragments. The expected bands were cut and purified by gel extraction kit. pPICZ $\alpha$ A vector was dephosphorylated by alkaline phosphatase at 37°C for 1 h followed by product purification. Then, the sticky ends of recombinant peptide and pPICZ $\alpha$ A were ligated. The reaction included 40 ng of pPICZ $\alpha$ A, 10 ng of recombinant peptide DNA, 1  $\mu$ l of T4 DNA ligase and 1  $\mu$ l of 5xT4 ligation buffer. Adjusted total volume to 10  $\mu$ l and incubated at 25°C. The following day, the ligation mixture was transformed into *E. coli* by heat shock. The competent *E. coli* DH5 $\alpha$  cells were thawed on ice. Then, gently mixed 5  $\mu$ l of ligated-plasmid DNA with 50  $\mu$ l of competent cells, placed on ice for 30 mins and immediately heat shock at 42°C for 30 sec and then placed on ice for 5 mins. Growth the competent cells by shaking with 300  $\mu$ l of SOC medium at 37°C, 225 rpm for 60 mins. Spread 50-100  $\mu$ l on low salt Luria-Bertani (LSLB) agar containing 25  $\mu$ g/ml zeocin and incubated at 37°C overnight. Plasmid DNA was extracted from transformant *E. coli* and then confirmed by sequencing analysis.

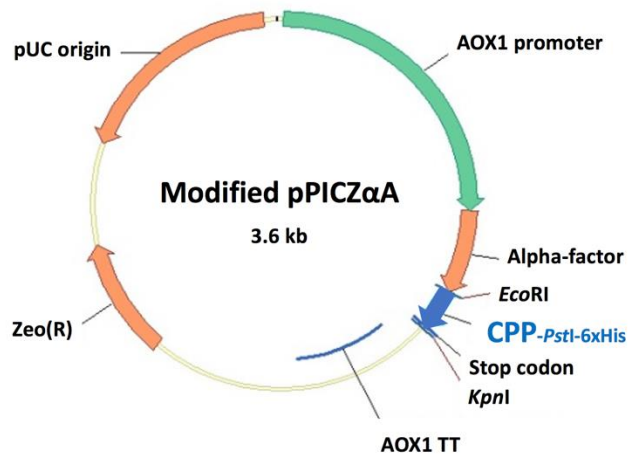


Figure 13 Plasmid map of modified pPICZ $\alpha$ A containing CPP.

### 3.7 Isolation of plasmid DNA

#### 3.7.1 Alkaline lysis

The transformant *E. coli* were subcultured. Fresh single colony was grown in LSLB broth with 25 µg/ml zeocin by shaking at 37°C, 225 rpm overnight. Pellet 3 ml of bacterial culture by centrifugation at 13,000 rpm for 1 min at room temperature. The supernatant was removed, and cells were resuspended in 330 µl buffer P1 (50 mM Tris-HCl, pH 8.0; 10 mM EDTA; 100 mg/mL RNase A). Added 380 µl buffer P2 (0.2 M NaOH; 10% w/v SDS), gently mixed by inverting and incubated at room temperature for 5 mins. Added 380 µl buffer P3 (3M Potassium acetate, pH 5.5), gently mixed by inverting and incubated at -20°C for 15 mins. Collected the supernatant after centrifugation at 13,000 rpm for 10 mins. To precipitate DNA 1 volume of cold-isopropanol was added, mixed and incubated at -20°C for 30 mins. Centrifuged all samples at 13,000 rpm for 10 mins and then carefully removed the supernatant from DNA pellet. Washed pellet with 70% ethanol and dried by SpeedVac. Resuspended pellet with 30 µl of DEPC treated water and incubated at C for 15 mins to dissolve DNA. Total DNA was quantified by spectrophotometer (OD 260/280 ratio).

#### 3.7.2 QIAGEN® Plasmid Mini kit

After growth the transformant cells in LSLB medium overnight, pellet cells 3 ml by centrifugation at 10,000 rpm for 1 min. Resuspended pellet with 250 µl buffer P1 and gently mixed with 250 µl buffer P2 by inverting until the mixture become blue. Added 350 250 µl buffer N3 and mixed until the mixture turned into colorless. Centrifuged sample at 13,000 rpm for 10 mins and transfer 800 µl of the supernatant to the QIAprep spin column. Centrifuged column and discarded the flow-through. Washed column by 500 µl buffer PB, centrifuged 13,000 rpm for 1 min and discarded the flow-through. Washed column again by adding 750 µl buffer PE, then centrifuged and discarded the flow-through. Centrifuged again to remove the excess buffer and placed column in a new microcentrifuge tube. Added prewarmed DEPC (65°C) to the middle of column, incubated at 65°C for 15 mins and collected the elution by centrifugation at 13,000 rpm for 1 min.

### 3.7.3 QIAGEN® Plasmid Maxi kit

Grew the starter culture of bacteria in 3 ml LSLB broth with shaking at 37°C, 225 rpm overnight. Following day, poured the starter culture into 250 ml LSLB and grew it overnight. Cells were harvested by centrifugation at 6,000xg for 15 mins at 4°C. The supernatant was discarded, resuspended pellet in 10 ml buffer P1 and transferred into hi speed centrifuge tube. Buffer P2 10 ml was added and gently mixed by inverting and incubated at room temperature for 5 mins. Next, added 10 ml buffer P3 and incubated on ice for 20 mins. Centrifugation at 18,000xg for 10 mins at 4°C and re-centrifuged again. After equilibrated a QIAGEN tip with 10 ml buffer QBT, the supernatant was transferred to the QIAGEN tip and allowed it flow by gravity. Then, washed the QIAGEN tip with 30 ml buffer QC 2 times. DNA was eluted by 15 ml buffer QF into a new hi speed centrifuge tube and 10.5 ml Isopropanol was added to precipitate DNA. Then, centrifuged at 15,000xg for 30 min at 4°C. the supernatant was carefully removed, then washed the pellet by 5 ml of 70% ethanol and centrifuged 15,000xg for 10 min. Air-dried the pellet and dissolved DNA by prewarmed DEPC 350 µl.

### 3.7.4 QIAquick® Gel extraction kit

After enzyme digestion and gel electrophoresis, the expected bands were cut by scalpel. Gel was mixed with 3 volumes buffer QG to 1 volume gel and melted on heat block at 50°C for 10 mins. Precipitated DNA by adding 1 gel volume isopropanol to the solution, mixed, transferred to QIAquick column and centrifuged at 13,000 rpm for 1 min. Removed the flow-through and washed column by 750 µl buffer PE and centrifuged for 1 min. Placed the column in a new microcentrifuge tube and eluted DNA in 30 µl DEPC.

### 3.8 Yeast transformation and Genomic extraction

#### 3.8.1 Preparation of competent yeast

Fresh *Pichia pastoris* strain KM71H single colony was inoculated in 10 ml YPD broth and cultured with shaking at 30°C, 250 rpm overnight. After 24 h, pipetted 4 ml from yeast cultured to 200 ml YPD ( $OD_{600} \sim 0.1$ ) and growth with shaking for 3 h until reach an  $OD_{600}$  to  $\sim 1$ . Yeast cells were transferred to 50 ml conical tubes and harvested by centrifugation at 2000xg for 5 mins at 4°C. Resuspended yeast pellet in 10 ml YPD broth and 2 ml 1M HEPES buffer pH.8. Gently mixed the cells with 250  $\mu$ l fresh 1M DTT and incubated at 30°C for 15 mins and then placed the cells in ice-cold water for 5 mins. Harvested cells by centrifugation at 2000xg for 5 mins at 4°C, washed 2 times with 25 ml cold sterile water and centrifuged. Washed cells in 10 ml of cold 1M D-sorbitol 2 times and resuspended yeast pellet in 50  $\mu$ l of cold 1M D-sorbitol (total volume 100  $\mu$ l). Cells were used immediately or stored at -80°C.

#### 3.8.2 Yeast transformation

Total plasmid DNA 15  $\mu$ g were digested with *SacI* and a complete linearization was analyzed by gel electrophoresis compared to undigested plasmid. The digested DNA was purified using QIAquick® Gel/PCR extraction kit and eluted in 15  $\mu$ l DEPC. Total DNA was measured by Nanodrop. Purified 5-10  $\mu$ g plasmid DNA in 10  $\mu$ l was mixed to 40  $\mu$ l of competent yeast and transferred into prechilled 2-mm gap cuvette on ice. Pulsed cells with high voltage (2.8 kV) and immediately added 500  $\mu$ l of cold 1M D-sorbitol. Transferred the solution to a microcentrifuge tube and incubated at 30°C for 1 h. Added 500  $\mu$ l YPD broth and incubated with shaking at 30°C, 200 rpm for 1 h. Spread 300  $\mu$ l on YPD plate containing 100 mg/ml zeocin and incubated at 30°C at least 2 days.

#### 3.8.3 Yeast Genomic extraction and PCR analysis

To determine the recombinant gene has integrated into *P. pastoris* KM71H, genomic DNA was isolated from *Pichia* clone using YeaStar Genomic DNA kit. After colonies formed on YPD plate, 3-5 colonies were streaked for single colony at 30°C for 3 days. Cells were growth in YPD medium with shaking at 30°C, 250 rpm

overnight. Yeast culture 1-1.5 ml were harvested by centrifugation at 500xg for 2 mins and pellet were resuspended in 120  $\mu$ l of YD digestion buffer and 5  $\mu$ l of R-Zymolase (Rnase A+Zymolase) by vortexing and incubated at 37°C for 1 h. Added 120  $\mu$ l of YD lysis buffer and mixed by vortexing for 10 sec. Then, chloroform 250  $\mu$ l was added and mixed for 1 min. The supernatant was separated by centrifugation at 13,000 rpm for 2 mins, then transferred to Zymo-spin III column and centrifuged for 1 min. Added 300  $\mu$ l of DNA wash buffer and centrifuged for 1 min 2 times. Placed Zymo-spin III column to a new microcentrifuge tube and eluted DNA in 30  $\mu$ l of DEPC. Total DNA was measured by Nanodrop. Genomic DNA 50 ng/ $\mu$ l, Forward primer 5'AOX1 (5'-GACTGGTTCCAATTGACAAGC-3'), 0.4 pmole and Reverse primer 3'AOX1 (5'-GCAAATGGCATTCTGACATCC-3') 0.4 pmole were added into Green mastermix (2x) and run the following steps. The plasmid without insert was used as a negative control. PCR products were analyzed by gel electrophoresis.

### **3.9 Peptide expression and purification**

#### **3.9.1 Peptide expression**

Fresh single colony of transformant *P. pastoris* was picked and growth in 10 ml Buffer Glycerol-complex Medium (BMGY) with shaking at 30°C, 280 rpm overnight. Inoculated 1 ml of starter culture in 100 ml BMGY medium and incubated with shaking at 30°C, 280 rpm overnight. After the OD<sub>600</sub> of an overnight cultured reached to 2-6, cells were harvested by centrifugation at 5,000xg for 5 min at room temperature. The supernatant was discarded. The pellet was resuspended in 10 ml of Buffer Methanol-complex Medium (BMMY) containing 0.5% final concentration of methanol to induce protein expression. Cells were continuously incubated with shaking at 30°C, 280 rpm for 24 h. The cultured medium was collected by centrifugation at 8,000xg, 4°C for 20 mins and stored at -80°C.

#### **3.9.2 Peptide purification and dialysis**

The cancer-specific peptides were expressed as histidine-tagged peptide which could be purified by nickel affinity chromatography. The supernatant was thawed on ice overnight and sterilized by filtration with 0.45  $\mu$ M membrane. To prepare purification system, the HisTrap column was cleaned with sterile deionized

water and equilibrated with binding buffer (20 mM Sodium Phosphate buffer pH 7.4, 0.5 M NaCl and 5 mM imidazole). Filtered supernatant was mixed with binding buffer in 1:2 ratio and loaded into column by pump injection. After sample loading, the HisTrap column was loaded with binding buffer for 5 column volumes to wash the unbound proteins. Histidine-tagged peptide was eluted by elution buffer (20 mM Sodium Phosphate buffer pH 7.4, 0.5 M NaCl and 500 mM imidazole). Peptide was collected by fraction collector. The expected fractions were pooled and then dialyzed to remove the excess salt. Peptide solution was transferred to 3.5 MWCO dialysis tubing, two ends of tubing were closed by dialysis clips. Dialysis tubing was placed in 0.01M PBS pH 7.4 buffer with stirring on magnetic stirrer plate at 4°C.

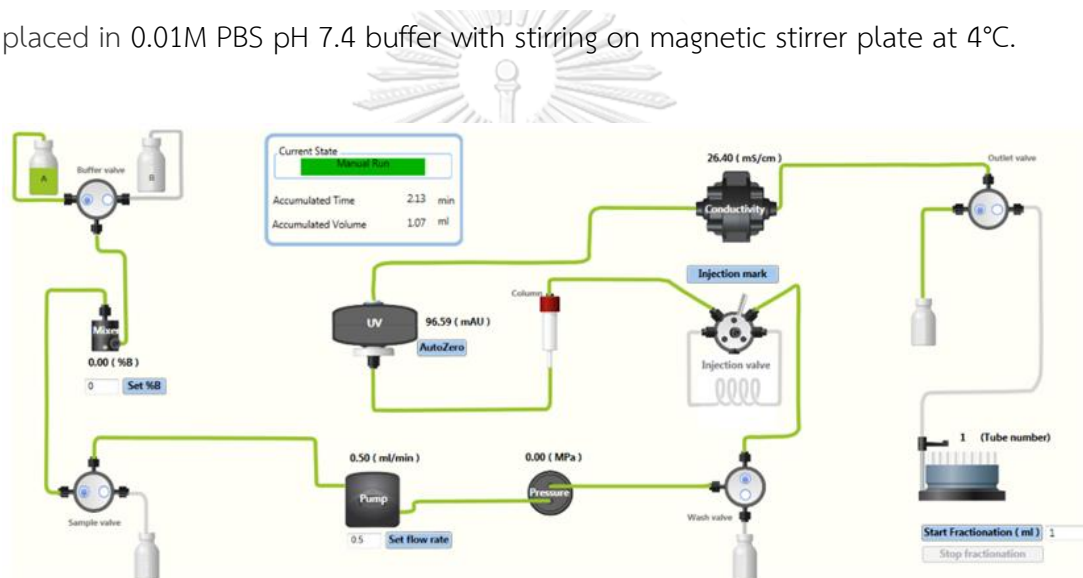


Figure 14 AKTA start process.

The flow path of AKTA start consists of valves, buffer mixer, pump, pressure detector, column, UV monitor, and conductivity monitor and fraction collection.

### 3.10 Detection of Small Peptide by SDS-PAGE

The purified peptide was measured concentration by Bradford Protein Assay. Diluted bovine serum albumin (BSA) at concentration 0, 0.03, 0.06 0.125, 0.25, 0.5 and 1 mg/ml were used as standard protein. Ten microliters of each standard and peptide was pipetted into 96-well plate. Bradford reagent was diluted to 1x final concentration and then 200  $\mu$ l of dye was thoroughly mixed in each well and incubated at room temperature for 5 mins. Absorbance was measured by

spectrophotometer at 595 nm. Peptide concentration was determined by reference to standard curve.

To detect size and purification, peptide was further analyzed by SDS-PAGE and immunoblotting. For SDS-PAGE, one hundred nanograms of supernatant, flow-through, wash fraction and the eluted peptide were mixed with loading buffer and denatured at 95°C for 10 mins. The solution was loaded into 16% Tris-Tricine gel and separated with constant voltage 125 volts for 90 mins. Gel was fixed with fixing solution (50% Methanol and 10% Acetic acid) for 1 h, washed 3 times with deionized water and then stained with Coomassie Blue. Molecular weight of peptide was compared to low-range molecular weight protein marker. For immunoblotting, one microgram of the eluted peptide was separated by 4-20% precast polyacrylamide gel with constant 120 volts for 60 mins and then transferred to PVDF membrane with constant 150 mA for 45 mins. Membrane was blocked in 5% non-fat dry milk in 1xTBST for 1 h. Histidine tagged peptides were recognized by His-monoclonal antibody (1:1000 v/v in 5%BSA-TBST) overnight, at 4°C. Next, blots were incubated with anti-mouse secondary antibody (1:5000 v/v in 5%BSA-TBST) for 1 h at room temperature and virtualized on X-ray film by chemiluminescence using Pierce® ECL Immunoblotting Substrate.

### 3.11 Detection of peptide localization

A549 and HaCaT  $2 \times 10^5$  cells were cultured on sterile cover glass in 6 wells plate in 2% DCC-RPMI medium. After 24 h, cells were treated with 2.5  $\mu$ M BR2-2xPPD in serum-free-RPMI medium for 1 h. Cells were washed and fixed with 4% Paraformaldehyde (PFA) for 20 min. Wash the cells by 1xPBS 3 times and incubated with 0.5% Triton x-100 for 10 min. After washing, cells were blocked with 1%FBS-PBS for 1 h. Then, cells were incubated with mouse monoclonal 6xHis tag antibody [HIS.H8] (1:200 v/v) at 4°C, overnight. The following day, cells were incubated with Goat anti-Mouse IgG (H+L) Secondary Antibody, Alexa Fluor 568 (1:2500 v/v in 1% BSA-PBS) for 1 h at room temperature in the dark. Wash the cells by 1xPBS 3 times. Incubated cells with Hoechst (DNA stain) for 10 min and washed with PBS. Mounted

the coverslip with a drop of Prolong Antifade mounting medium, sealed with nail polish and visualized under confocal microscopy.

### 3.12 Cell viability assay (MTT)

A549 cells were plated in RPMI supplemented with 1% DCC-FBS and 1% PenStrep at 6,000 cells per well in a 96-well culture plate and incubated for 24 h to achieve 80% confluence. For HaCaT, cells were plated at 8,000 cells per well in 10%FBS-DMEM. The following day, the cultured medium was removed. To activate EGF-induced cell growth, cells were treated with EGF 50 ng/ml compare to the combination of EGF and increasing dose of peptides (0, 0.625, 1.25 and 2.5  $\mu$ M). Cells were incubated at 37°C with 5% CO<sub>2</sub> for 24 h. MTT solution (5 mg/ml) was added to the cells and incubated for 4 h. The insoluble formazan was dissolved by 10% SDS. Then, absorbance was measured at 570 nm by a microplate spectrophotometer.

To determine the effect of EGFR-TKIs and peptides on EGFR-mutant NSCLC cell proliferations, PC9-6M, PC9-GR and PC9-ER were plated at 8,000 cells per well in 10% FBS-RPMI for 24 h. Then, cells were treated with gefitinib or erlotinib alone compared to the combination with peptides (0-2.5  $\mu$ M) for 72 h and analyzed cell viability by MTT.

### 3.13 Western blot Analysis

#### 3.13.1 Preparation of cell lysate from cell culture

A549  $2 \times 10^5$  cells were cultured in 2% DCC-RPMI medium for 24 h. Cells were washed with 1xPBS and then pretreated with BR2-2xPPD or BR2-2x $\Delta$ PPD 2.5  $\mu$ M in serum-free medium for 4 h. To induce MAPK signaling, cells were treated with EGF 20 ng/ml for 5, 10 and 30 mins. Culture medium was discarded, and cells were washed with cold 1xPBS 2 times. Adherent cells were lysed with 70  $\mu$ l ice-cold 1xRIPA lysis buffer (5 mM NaF, 2 mM Na<sub>3</sub>VO<sub>4</sub>, 1xproteinase inhibitor). Cells were incubated with lysis buffer for 5 mins on ice and then scraped cells and transferred the lysate to a new microcentrifuge tube. Placed the sample tubes on ice and mixed by vortex every 5 mins for 15 mins for completely lysed cells. Centrifuged the lysate

at 12,000 rpm, 4°C for 10 mins. Carefully transferred the supernatant to a new 1.5 ml tube. Cell lysate was diluted in lysis buffer with a 1:15 ratio and protein concentration was determined by Bradford assay as previously described.

### 3.13.2 SDS-PAGE and Western blotting

The SDS-PAGE was divided into 4% stacking gel and 8% separating gel to separate the target proteins (42 and 44 KD). Two glass plates were clamped on gel casting apparatus. Mixed solution of separating gel was firstly loaded into the gap between glass plates and poured some water on acrylamide gel. Allowed the gel to polymerized for 20 mins and discarded the overlaid water. Loaded the solution of stacking gel, immediately put the comb and allowed the gel to set for 30 mins. Placed the gel in running tank and filled the tank with 1xrunning buffer. Ten micrograms of cell lysate were mixed with 4xLaemli loading buffer and denatured at 95°C for 10 mins. Loaded the solution to each lane of acrylamide gel. Run the stacking gel with constant 70 volts for 30 mins followed by running of separating gel with constant 120 volts for 60 mins. Proteins were transferred onto PVDF membrane with constant 150 mA for 1 h and was then incubated with 5% non-fat dry milk blocking solution for 1 h. Membranes were washed with 1xTBST and probed with primary antibody recognizing phospho-p44/42 MAPK (1:1000 v/v, Cell Signaling Technology, USA) and total MAPK antibody (1:1000 v/v, Cell Signaling Technology, USA) overnight at 4°C. Next, blots were incubated with anti-rabbit secondary antibody (1:5000 v/v in 5%BSA-TBST) for 1 h at room temperature and virtualized on X-ray film by chemiluminescence using Pierce® ECL Immunoblotting Substrate. Images were analyzed by ImageJ software.

### 3.14 RNA isolation and Real-Time PCR

A549  $2 \times 10^5$  cells were plated in 10%FBS-RPMI medium for 24 h in 6 well culture plate. Then, cells were treated with BR2-2xPPD or BR2-2x $\Delta$ PPD 2.5  $\mu$ M for 0, 8, 12 and 24 h. Cells were wash with cold-PBS. Total RNA was extracted using 1 ml of GENEzol reagent and incubated at room temperature for 5 mins. Pipetted the solution up and down and transferred to a new microcentrifuge tube. Added 200  $\mu$ l

chloroform, mixed the sample vigorously for 10 sec and centrifuged at 14,000xg, 4°C for 15 mins. RNA was separated in the colorless upper aqueous phase. Carefully transferred the aqueous to a new tube. One volume of isopropanol was added to the sample, mixed by inverting several times and incubated at room temperature for 10 mins. Centrifuged at 14,000xg, 4°C for 10 mins. Washed the RNA pellet with 70% Ethanol and centrifuged 14,000xg, 4°C for 5 mins. Discarded the supernatant and washed the pellet 2 times. Discarded the supernatant and dried the pellet at room temperature for 2 to 3 h. Dissolved the pellet with prewarmed DEPC and incubated at 65°C for 15 mins. Total RNA was determined by Nanodrop at the OD 260/280. cDNA was synthesized by adding 1 µg RNA and DEPC water up to 20 µl in Maxime™ RT Premix tube. Performed cDNA synthesis reaction at 45°C for 60 mins followed by RTase inactivation at 95°C for 5 mins. To perform real-time PCR, the master mix containing 1xRealMOD™ Green 2xqPCR mix, 10 µM forward primer and 10 µM reverse primer were prepared. cDNA 1 µl was pipetted to each sample tube and DEPC water was added to adjust the final volume of each reaction to 20 µl. Real-time PCR with specific primers for cyclin D1 and CDK2 were performed. GAPDH was used as an internal control.

### 3.15 Cell cycle analysis

A549 were seeded in 6 cm dish at  $2 \times 10^5$  cells in 10%FBS-RPMI medium. After 24 h, cells were treated with BR2-2xPPD or BR2-2x $\Delta$ PPD 2.5 µM for 8, 12 and 24 h. A549 cells were collected by trypsinization and washed with cold 1xPBS. Slowly added 200 µl of ice-cold 70% ethanol to fix the cells and kept at -20°C at least 3 h before performing cell cycle analysis. The fixed cells were washed by 1xPBS. Centrifuged the cell at 300xg for 5 mins and resuspended the pellet in 200 µl of Muse™ Cell Cycle Reagent (Merck Millipore, Germany) in the dark and incubated for 30 mins at room temperature. One-thousand cells of each samples were analyzed by flow cytometry (BD Biosciences, U.S.A).

### 3.16 Detection of Cell Apoptosis

A549 were seeded in 6 cm dish at  $2 \times 10^5$  cells in 10%FBS-RPMI medium. The following day, cells were treated with increasing dose of BR2-2xPPD or BR2-2x $\Delta$ PPD (0-2.5  $\mu$ M) for 24 h. Cells were harvested by trypsinization and washed with cold 1xPBS. Discarded the washing buffer and resuspended the pellet in 100  $\mu$ l of Annexin V Binding Buffer at a concentration of  $0.25-1.0 \times 10^7$  cells/ml. Cell were mixed until separated as single cell. Transferred the cell suspension to 5 ml flow cytometry tube. Added 5  $\mu$ l of FITC Annexin V and mixed by vortex, incubated in the dark at room temperature for 15 mins. Added 3  $\mu$ l of propidium iodide (PI), gently vortexed and incubated for 15 mins at room temperature in the dark. Added the Annexin V Binding Buffer 300  $\mu$ l and gently mixed by vortex. Then, analyzed by flow cytometry (BD Biosciences, U.S.A).

### 3.17 Wound Healing Scratched Assay

A549  $3 \times 10^5$  cells were seeded in 12-well plate in 10%FBS-RPMI medium. After 24 h, the confluence of cell culture was 90-100% and then cells were starved with 2%DCC-RPMI. Before peptide treatment, the monolayer of cells was subjected to a mechanical scratch wound using 10  $\mu$ l pipette tips and gently washed with 1xPBS for 2-3 times to remove the floating cells. Cells were treated with BR2-2xPPD or BR2-2x $\Delta$ PPD peptides at concentration 2.5  $\mu$ M in 2%DCC-RPMI medium and incubated for additional 24 and 48 h. The wounded cells were visualized under microscopic at 0, 24 and 48 h after scratching. The percentage of wound area was measured by ImageJ software.

### 3.18 Estradiol-induced breast cancer cell proliferation

MCF-7 3,000 cells were cultured in 96 well plate in 5%DCC-DMEM. After 72 h, cells were treated with increasing concentration of  $17\beta$ -Estradiol (0-100 nM) in 5%DCC-DMEM. Cell viability assays were performed at 0 to 96 h after treatment compared to vehicle (ethanol).

### 3.19 Luciferase Assay

To examine whether BR2 containing LXXLL motif can inhibit the transcriptional activity of steroid hormone receptor, T47DC42 expressing PRB (T47DC42-PRB) cells were plated in 96 well plate at 5,000 cells/well in DMEM supplemented with 5% DCC-FBS (Charcoal stripped fetal bovine serum) for 24 h. Cells were transfected with 20 ng pRL-CMV Luciferase control (Renilla) and 180 ng of PRE<sub>2</sub>-TK-Luciferase reporter plasmid and Lipofectamine3000 reagent was used to perform the transient transfection. The following day, the cultured medium was discarded and changed to the medium containing Doxycycline at concentration 1,000 ng/ $\mu$ l for 6-8 h to induce PRB expression. Then, cells were treated with 10 nM R5020 (a Synthetic Progestin) or ethanol (vehicle) in the absence or presence of BR2-LXXLL or BR2-LXXLL (scramble) peptide from 0 to 7.5  $\mu$ M and incubated for 24 h.

For Luciferase assay, the Dual-Glo<sup>®</sup> Luciferase Assay Reagent was thawed at room temperature and mixed well. Changed the cultured medium in 96 wells plate to the total 75  $\mu$ l of fresh medium. Added 75  $\mu$ l of Dual-Glo<sup>®</sup> reagent to each well, mixed by pipette and incubated for 10 mins at room temperature for completely cell lysis. Then, the firefly luminescence was measured by the luminometer. Added the Dual-Glo<sup>®</sup> Stop & Glo<sup>®</sup> Reagent 75  $\mu$ l to each well and incubated for 10 mins followed by Renilla luminescence measurement. The ratio of luminescence from the firefly reporter to luminescence from the Renilla control reporter was calculated.

### 3.20 Statistical Analysis

The statistical analysis was determined by employing a paired *t*-test and a two-way ANOVA with Bonferroni correction using GraphPad Prism 8.0 (GraphPad Software, CA, USA). All data were represented as mean  $\pm$  SEM and *P* values of < 0.05 were considered significant in all studies. \**p*  $\leq$  0.05; \*\**p*  $\leq$  0.01; \*\*\**p*  $\leq$  0.001; \*\*\*\**p*  $\leq$  0.0001.

## CHAPTER IV

### RESULTS

#### 4.1 Peptide Construction and Characterization

##### 4.1.1 Plasmid design and gene synthesis

After the nucleotide sequences were synthesized by the company, the lyophilized plasmids were dissolved in 50  $\mu\text{l}$  of sterile TE buffer to make the final concentration at 100  $\text{ng}/\mu\text{l}$ . All recombinant genes were previously added the enzyme restriction site at the N- and C-terminus. To determine whether pUC19 contain the sequence of target recombinant gene, the plasmid DNA was digested with *EcoRI* and *PstI*. Gel electrophoresis was performed with 1.5% agarose gel, 100 volts for 40 mins. Size of target gene was compared to undigested plasmid. As shown in **Figure 15A and 15B**, the expected size of BR2-PPD, BR2-PPDscramble, BR2-2xPPD, BR2-LXXLL, BR2-LXXLLscramble and BR2-2x $\Delta$ PPD was 120, 120, 207, 309, 309 and 207 base pairs, respectively. For BR2 plasmid construction, BR2 sequence was amplified by PCR from BR2-PPDscramble plasmid. PCR reaction was performed using forward 5'AOX primer and reverse primer. PCR product in size 636 base pairs was shown in **Figure 15C**.



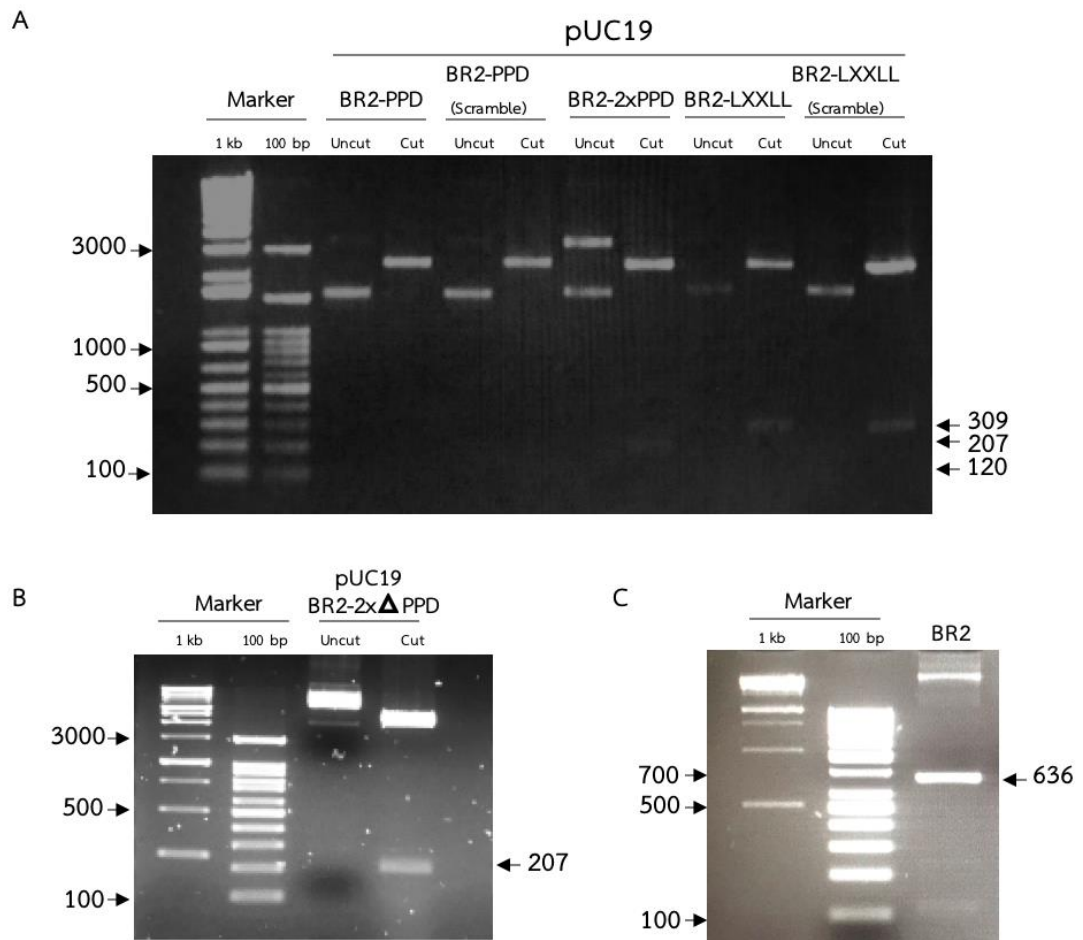


**Figure 15** Restriction enzyme digestion of pUC19-CPPs.

(A) and (B) pUC19-CPP plasmids were digested by *EcoRI* and *PstI* restriction enzymes and 1.5% gel electrophoresis were performed. Digested plasmid was compared to undigested plasmid. (C) BR2 was amplified from pUC19-PPD plasmid and PCR product was analyzed by electrophoresis.

#### 4.1.2 DNA cloning and transformation

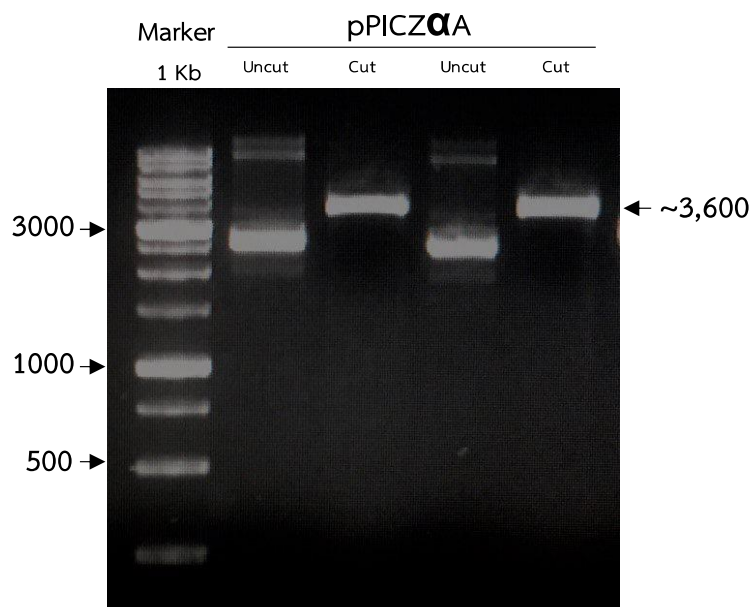


**Figure 16** Restriction enzyme digestion of pPICZ $\alpha$ A expression vector.

pPICZ $\alpha$ A plasmid was digested by *Eco*RI and *Pst*I restriction enzymes and 1% gel electrophoresis were performed. The size of pPICZ $\alpha$ A is approximately 3,600 bp.

To generate the pPICZ $\alpha$ A expression vector containing the recombinant gene, the expected band from enzyme digestion was excised from agarose gel and purified using gel extraction kit (**Figure 16**). After dephosphorylation of pPICZ $\alpha$ A vector, each recombinant gene was ligated into pPICZ $\alpha$ A and transformed to competent *E. coli* by heat shock. The transformant *E. coli* was selected on low salt LB agar containing 25  $\mu$ g/ml Zeocin antibiotic. The positive clones were growth in LSLB medium with shaking at 30°C, 280 rpm overnight. Plasmid DNA was extracted by traditional alkaline lysis to screen the positive clone. After restriction enzyme digestion, gel electrophoresis was performed. The purified recombinant plasmids were further confirmed by sequencing analysis.

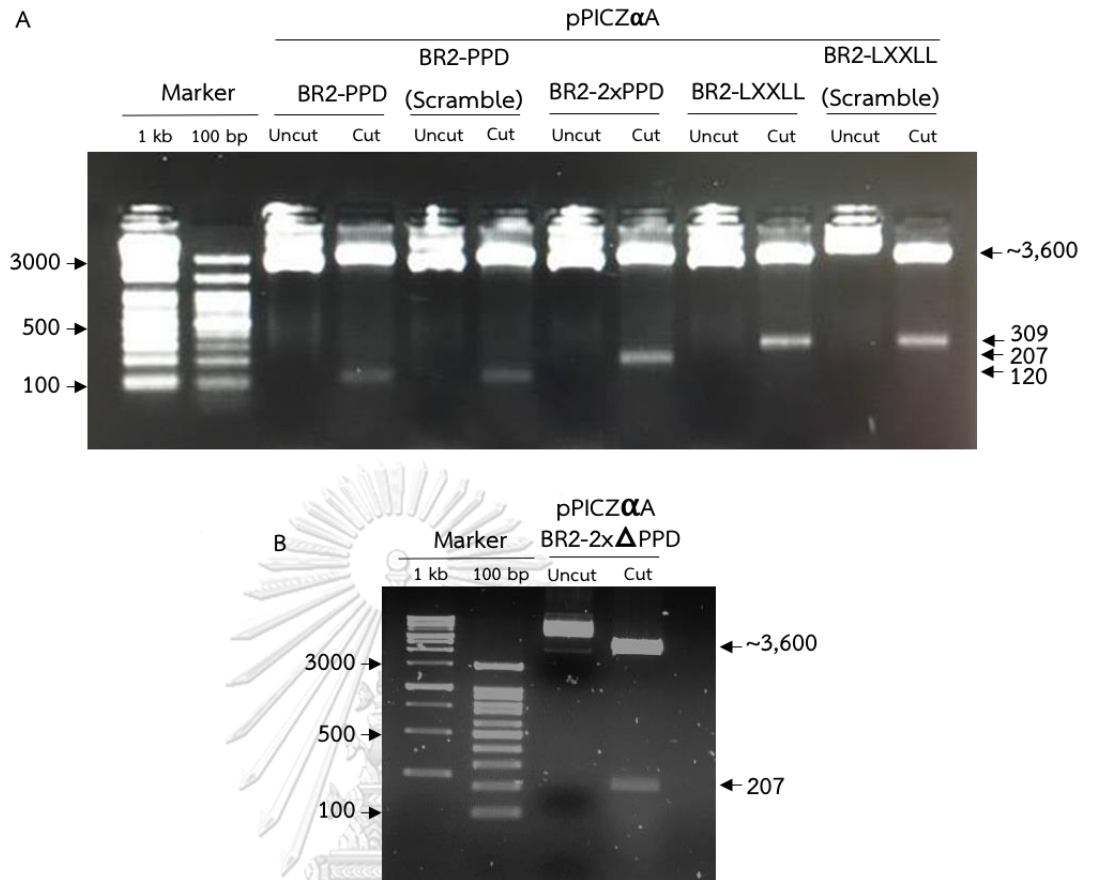


**Figure 17** Cloning of the recombinant pPICZ $\alpha$ A-CPP expression vectors.

(A) and (B) All CPPs and pPICZ $\alpha$ A were previously digested by *Eco*RI and *Pst*I. After gel extractions, the digested CPPs were ligated into pPICZ $\alpha$ A expression vector and transformed into *E. coli*. The recombinant plasmids were extracted by Qiagen mini kits and electrophoresis were performed.

#### 4.1.3 *Pichia pastoris* transformation

Before yeast transformation, the purified plasmid DNA 5-10 µg were digested by *SacI* to cut at the 5'AOX region and linearized the pPICZαA. A small aliquot of each reaction was examined by gel electrophoresis for completely linearization as shown in **Figure 18**. All products were next purified using PCR cleanup kit to remove the residual enzyme and buffer. Total plasmid DNA were eluted in DEPC water and determined the concentration by Nanodrop. Competent *Pichia pastoris* strain KM71H were prepared followed by electroporation at 2.8 kV. The transformant *Pichia* were selected on YPD plate containing 100 µg/ml Zeocin for 2-4 days. The transformant yeasts which express the zeocin resistance gene were formed. To determine whether gene of interest has integrated into the *Pichia* genome, the transformant yeasts were next examined by PCR. Firstly, the positive clones were picked and growth in YPD broth with shaking at 30°C, 280 rpm overnight. Yeast genomic DNA were extracted using YeaStar Genomic DNA extraction kit. Then, the total DNA 50 ng were performed PCR reaction with specific primers including 5'AOX and 3'AOX primer compared to the parent plasmid which lack of gene insertion (**Figure 19**).



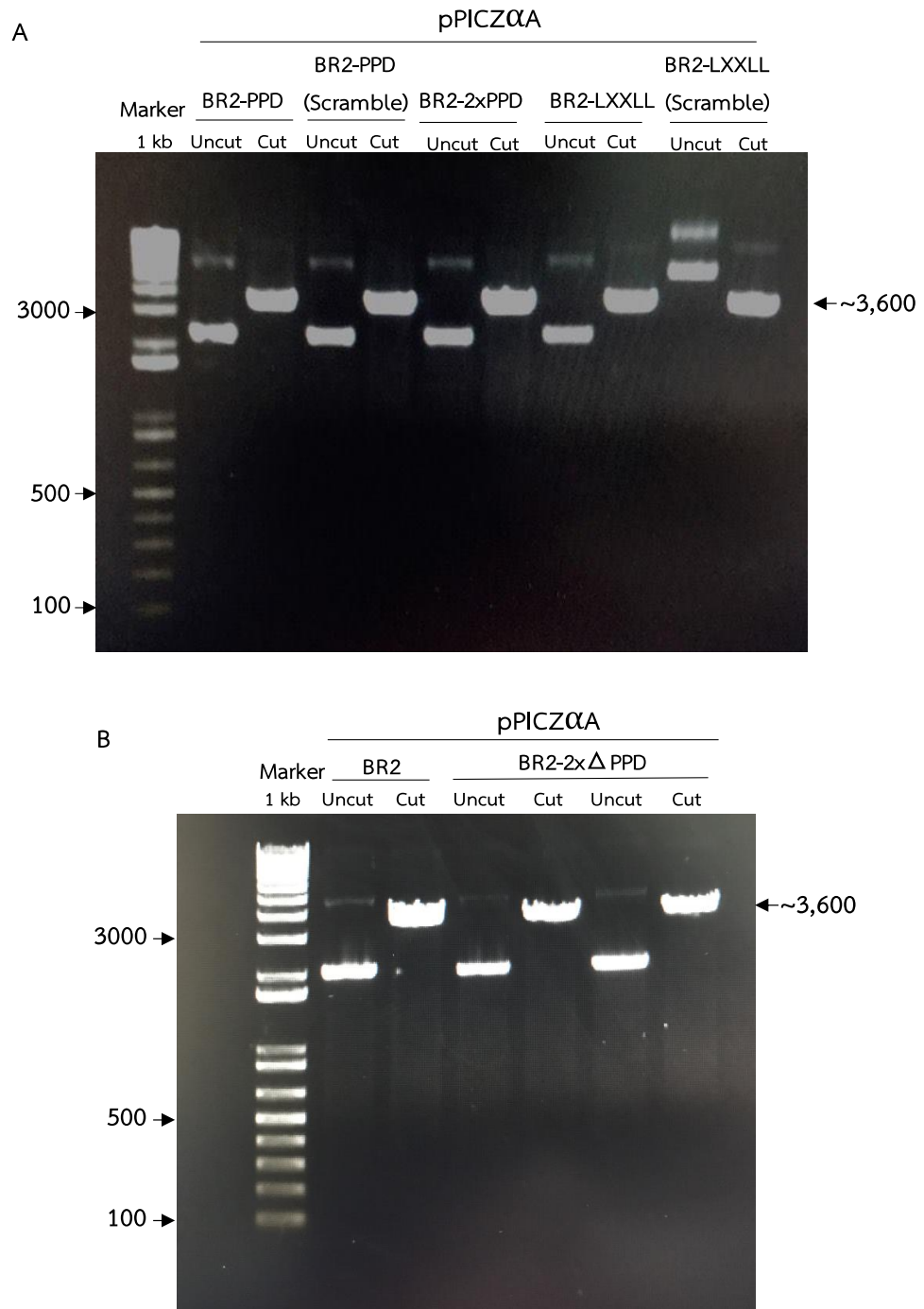


**Figure 18** Linearization of the recombinant pPICZ $\alpha$ A-CPPs.

(A) and (B) Purified pPICZ $\alpha$ A-CPP plasmids were digested by *Sac*I. The aliquots were analyzed by electrophoresis. Size of linearized plasmid was in approximately 3,600 bp compared to undigested plasmid.

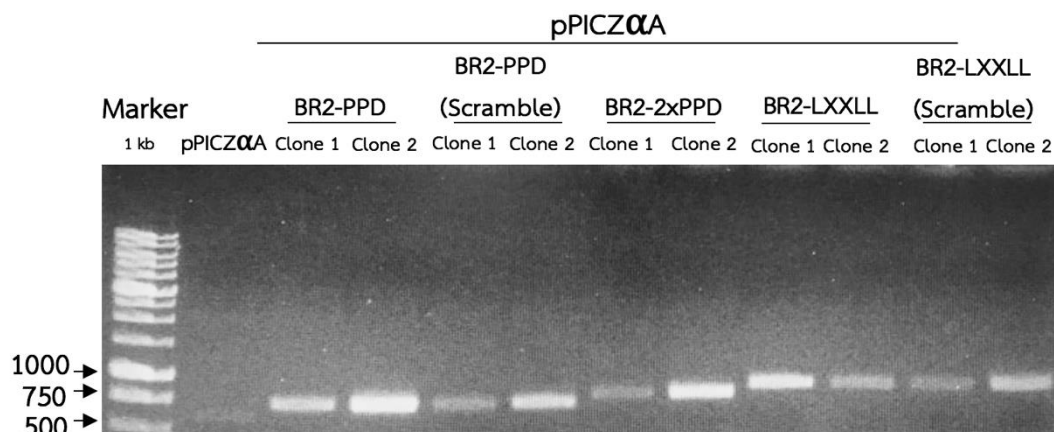


**Figure 19** PCR amplifying of yeast genomic DNA.

The PCR products amplified with a pair of primers 5'AOX and 3'AOX were analyzed by 1% gel electrophoresis. Size of pPICZ $\alpha$ A without gene insertion is 599 base pairs. Size of pPICZ $\alpha$ A-BR2-PPD, pPICZ $\alpha$ A-BR2-2xPPD, pPICZ $\alpha$ A-BR2-2x $\Delta$ PPD, pPICZ $\alpha$ A-BR2-LXXLL and pPICZ $\alpha$ A-BR2-LXXLLscramble were 719, 806, 806, 908 and 908 base pairs, respectively.

#### 4.1.4 Peptide expression and purification

The positive clones from starter culture were growth in BMGY medium with shaking at 30°C, 280 rpm overnight. After the OD<sub>600</sub> was reached to 2-6, cells were harvested by centrifugation and resuspended in BMMY medium containing 0.5% Methanol to induce AOX1 promoter. The supernatant from culture medium was collected after 24 h and purified by nickel fast flow column using AKTA start. As shown in **Figure 20 and 21**, each peptide was eluted as a single peak shown in chromatogram. Peptide purity was analyzed using SDS-PAGE followed by Coomassie blue staining compared with supernatant, flow-through and wash fractions. We successfully produced the highly purified peptides as shown in a single band on SDS-PAGE. Molecular weight of BR2-PPD, BR2-2xPPD, BR2-2x $\Delta$ PPD, BR2-LXXLL and BR2-LXXLLscramble were 5.3, 8.3, 7.3 12.3 and 12.3 KD, respectively. In addition, peptides were also analyzed by His-monoclonal antibody to confirm that these peptides were Histidine-tagged peptides (**Figure 22A and 22B**).

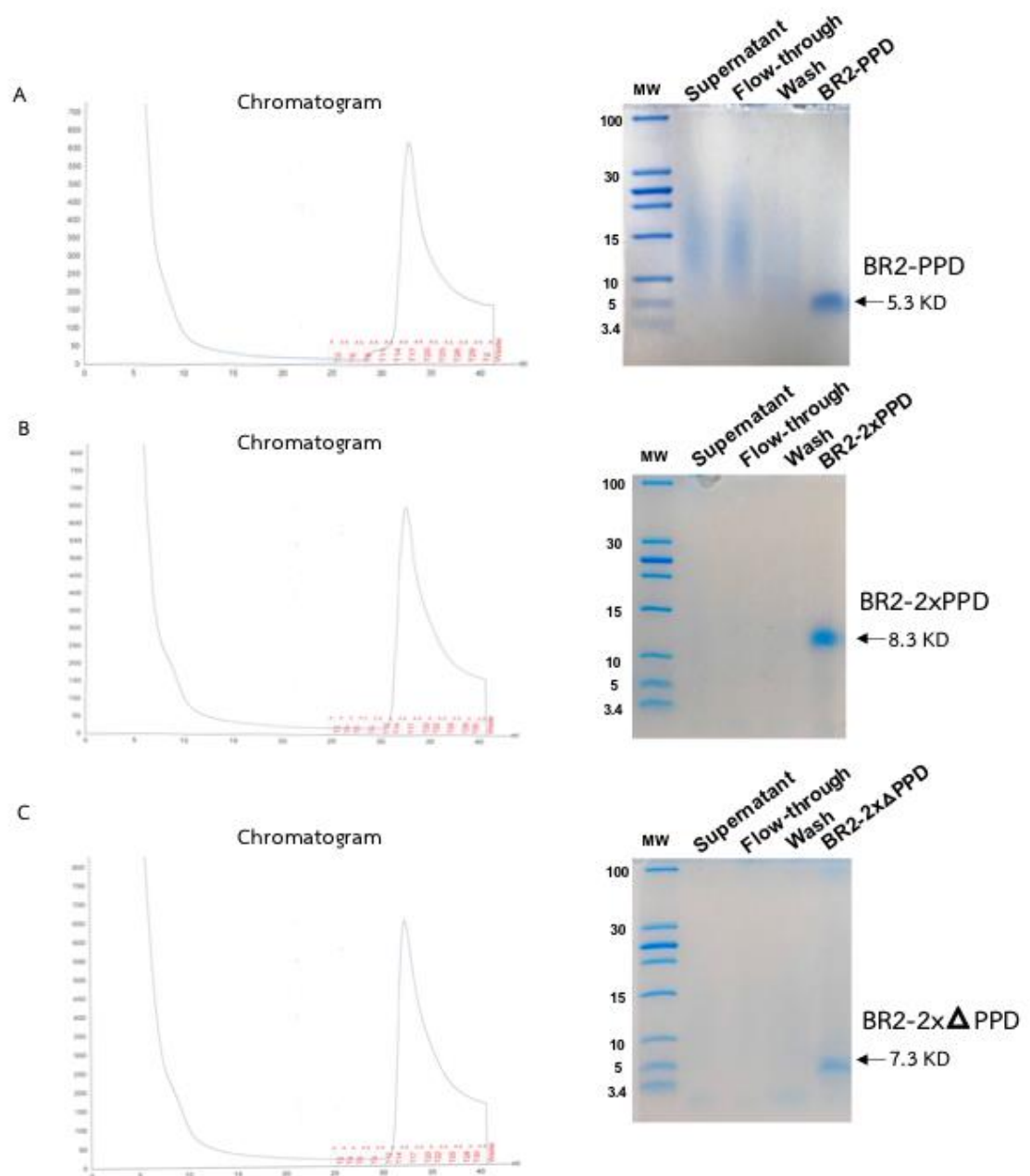


**Figure 20** Chromatogram and SDS-PAGE analysis of BR2 containing PR-PPD peptides.

The supernatant from culture medium was collected after 24 h and purified by nickel fast flow column using AKTA start. Each peptide was eluted as a single peak shown in chromatogram. Peptide purity was analyzed using SDS-PAGE followed by Coomassie blue staining compared with supernatant, flow-through and wash fractions.

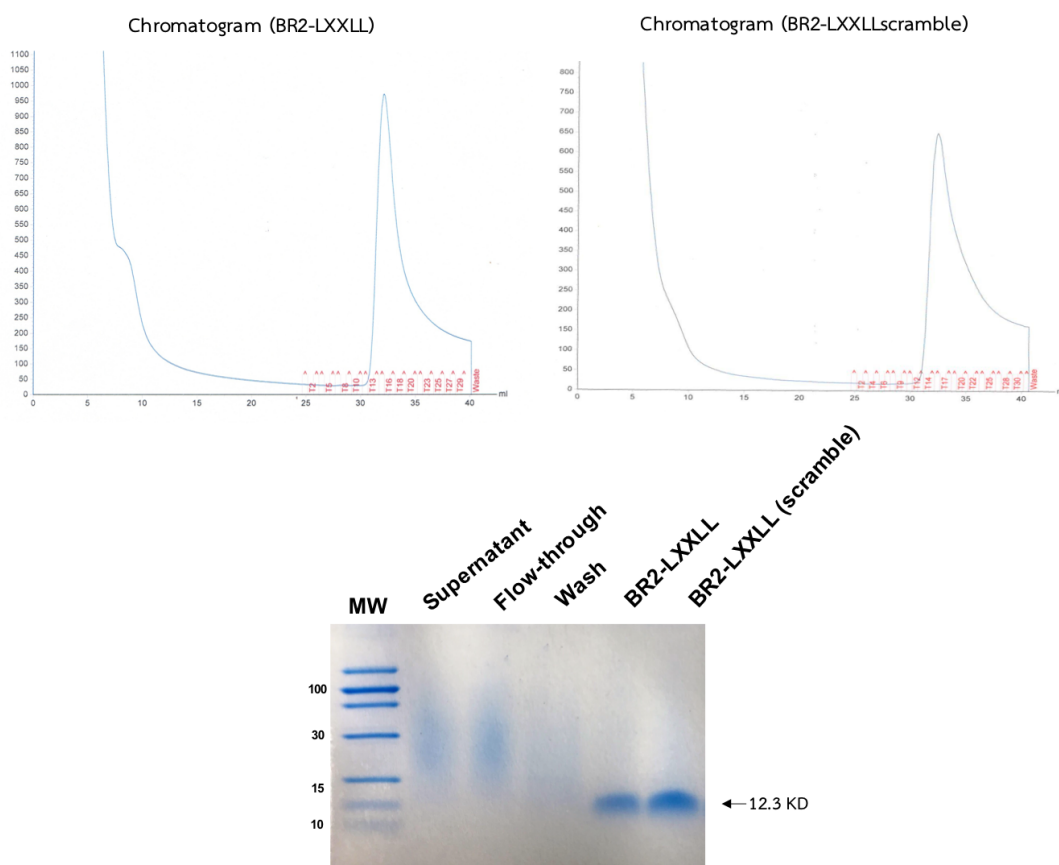
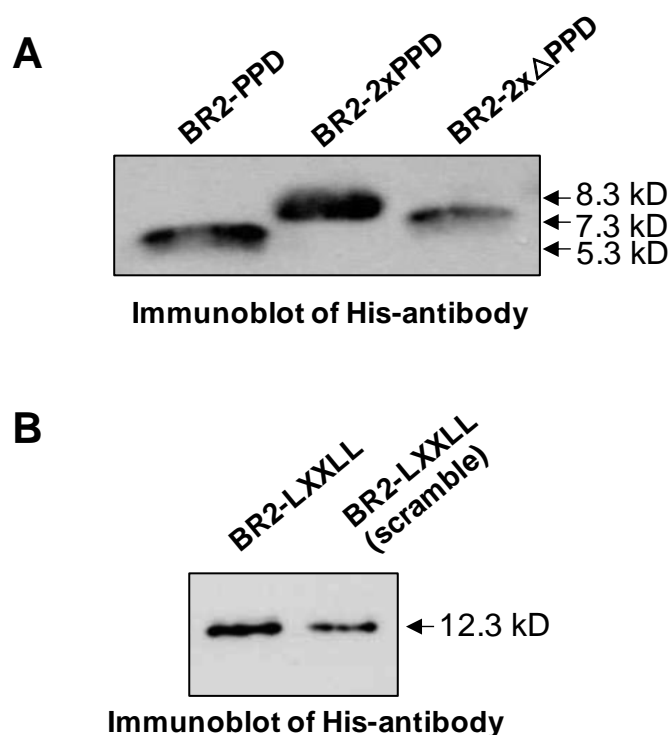


Figure 21 Chromatogram and SDS-PAGE analysis of BR2 containing LXXLL motifs peptides.

The supernatant from culture medium was collected after 24 h and purified by nickel fast flow column using AKTA start. Each peptide was eluted as a single peak shown in chromatogram. Peptide purity was analyzed using SDS-PAGE followed by Coomassie blue staining compared with supernatant, flow-through and wash fractions.



**Figure 22** Western Blot Analysis of Histidine-tagged peptides.

After purification, one microgram of purified peptide was loaded into 4-20% SDS-PAGE. 6xHis-tag antibody was used to recognize his-tagged peptide by immunoblotting.

#### 4.1.5 Peptide specificity and localization

To determine the intracellular localization of peptides. A549 NSCLC cell lines was incubated with 2.5  $\mu$ M of peptides for 1 h. Cells were fixed and stained by immunofluorescence recognize 6-His synthetic peptide. As shown in **Figure 23**, BR2-PPD, BR2-2xPPD and BR2-2x $\Delta$ PPD peptides could penetrate and accumulate in both cytoplasm and nucleus (red color) in A549 compared to untreated cells. However, these peptides could not pass into normal keratinocyte HaCaT cells at equal concentration and time. For MCF7 breast cancer cell lines, cells were treated with BR2-LXXLL, BR2-LXXLL(Scramble), BR2-2xPPD and BR2-2x $\Delta$ PPD peptides at 2.5  $\mu$ M for 1 h. BR2-LXXLL and BR2-LXXLL(Scramble) peptides were mainly localized in nucleus resulting from nuclear localization sequence of SV40 while BR2-2xPPD and BR2-

2x $\Delta$ PPD peptides were located in both cytoplasm and nucleus as shown in **Figure 24**. These data confirmed the cancer-specific penetration activity of BR2 peptide that correlated with previous study (89, 98).

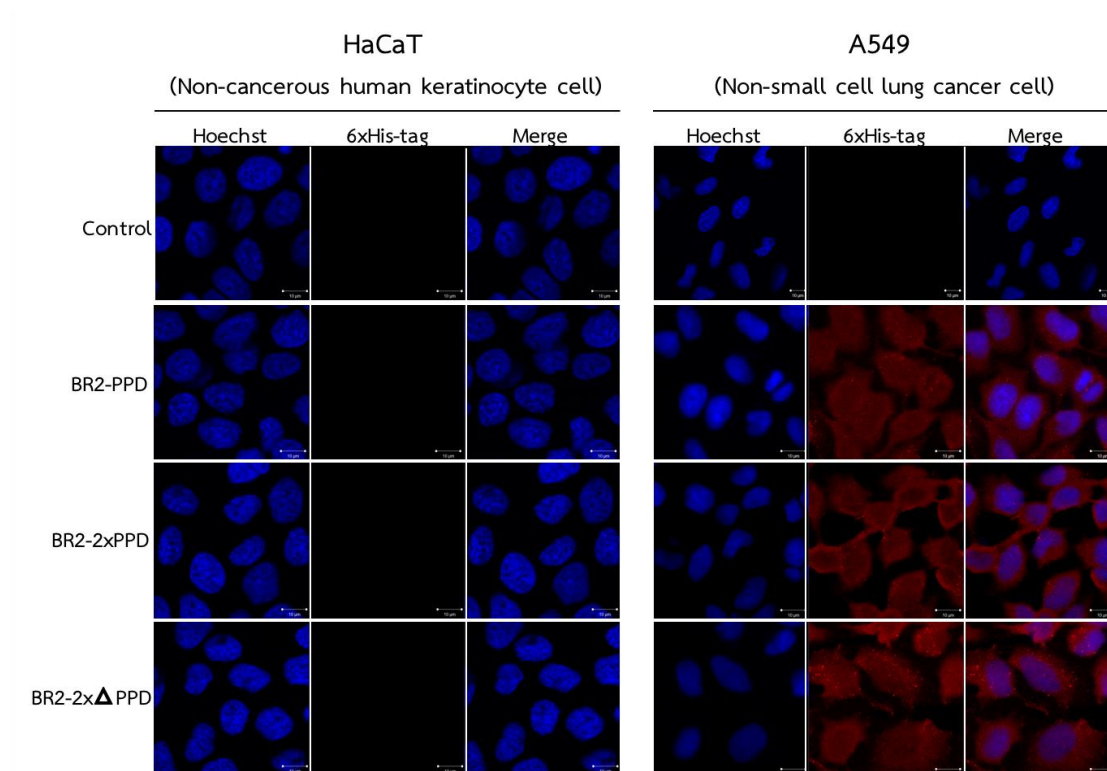


**Figure 23** Intracellular localization of cell-penetrating peptides in HaCaT and A549.

A549 NSCLC cells and normal HaCaT keratinocyte cells were incubated with His-tagged peptides (2.5  $\mu$ M) for 1 h at 37  $^{\circ}$ C and stained with 6-His specific antibody (red). Hoechst was used to stain nucleus (blue). Intracellular distribution of His-tagged peptides was visualized by confocal microscopy.

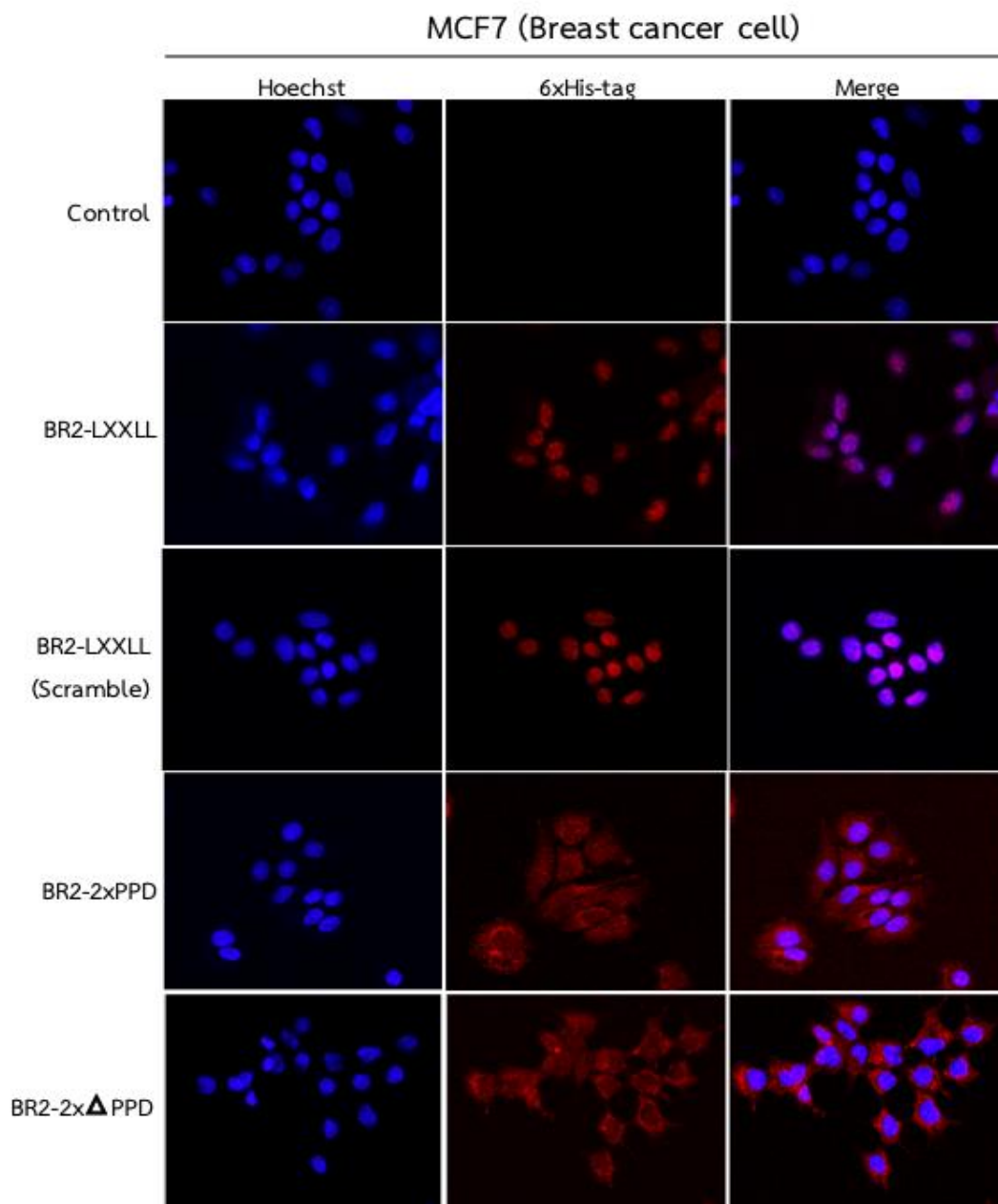


**Figure 24** Intracellular localization of cell-penetrating peptides in MCF-7.

MCF-7 breast cancer cell lines were incubated with His-tagged peptides (2.5  $\mu$ M) for 1 h at 37 °C and stained with 6-His specific antibody (red). Hoechst was used to stain nucleus (blue). Intracellular distribution of His-tagged peptides was visualized by confocal microscopy.

## 4.2 Effect of the cancer-specific BR2 containing PR-PPD peptides on EGF-mediated NSCLC cell growth

### 4.2.1 Optimization of Epidermal Growth Factor (EGF) concentrations.

Transactivation of EGFR by cognate ligands such as epidermal growth factor (EGF) can promote NSCLC cell proliferation through PPD and SH3 domain interaction and eventually induce downstreams cascade such as MAPK signaling. A549 cells were treated with increasing dose of EGF (0-500 ng/ml) in 1%DCC-RPMI medium for 24 h. Then, cell viability test was performed by MTT assays. EGF-treated A549 cells were significantly increased cell viability at all EGF concentrations tested compared to untreated cells (**Figure 25**). Previous study has been shown that PR-PPD expression was more significant to the growth inhibition of EGF-induced A549 cell proliferation at the maximum dose of EGF at 50 ng/ml (12). Therefore, dose of EGF at 50 ng/ml was used in the following experiment.

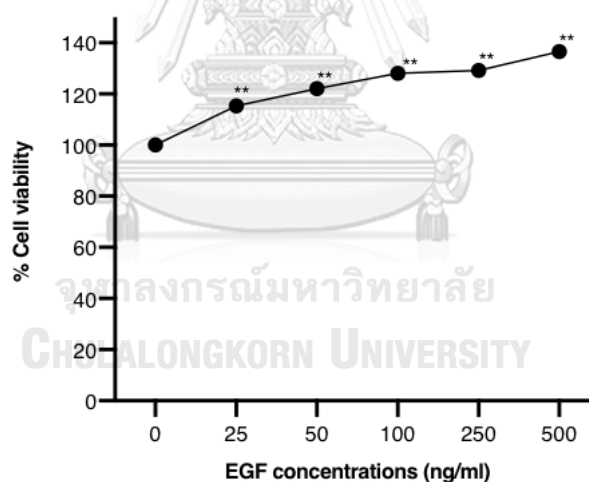
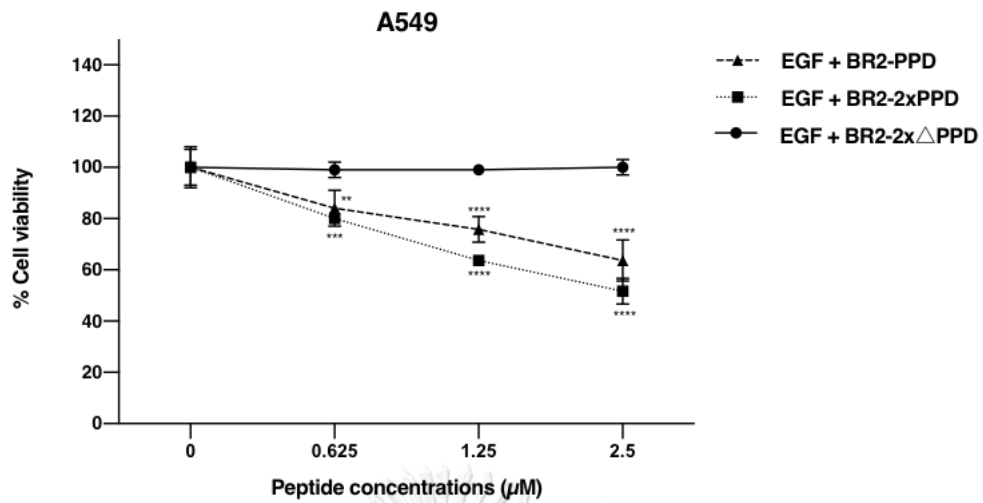


Figure 25 The effect of EGF on A549 cell proliferation.

A549 cells were plated in 1%DCC-RPMI for 24 h. Cells were treated with increasing dose of EGF from 0 to 500 ng/ml in 1%DCC-RPMI medium. After 24 h, cell viability assays were performed by MTT. Percent cell viability in EGF-treated A549 cells was significantly different from untreated cells. Error bars represent the standard errors of the mean (n=3) (\*\* $p \leq 0.01$ ).

#### 4.2.1 BR2 containing PR-PPD peptides mediate the inhibitory effect of EGF-induced cell proliferation

Transactivation of EGFR by cognate ligands such as epidermal growth factor (EGF) promotes NSCLC cell proliferation through PPD and SH3 domain interaction and eventually induce a downstream cascade such as MAPK signaling (8). To determine whether the presence of PR-PPD could inhibit EGF-mediated NSCLC cell growth. A549 NSCLC cells were treated with 50 ng/ml EGF alone or in combination with 0-2.5  $\mu\text{M}$  of BR2-PPD, BR2-2xPPD, or BR2-2x $\Delta$ PPD peptides. As shown in **Figure 26**, BR2-PPD dose-dependently inhibited EGF-induced A549 cell proliferation with maximum growth inhibition of  $36\pm 8\%$  when cells were treated with 2.5  $\mu\text{M}$  of BR2-PPD compared with EGF alone. Interestingly, the addition of BR2-PRPPD peptide containing two PR-PPD repeats (BR2-2xPPD) was more effective in inhibiting NSCLC proliferation and showed a maximum growth inhibition by  $48\pm 5\%$  inhibition. Mutations in the PPD the mutant BR2- $\Delta$ PPD peptide abolished this inhibition. Interestingly, the BR2 containing PR-PPD peptides did not affect the growth of normal keratinocyte HaCaT cells at all concentrations tested (**Figure 27**). These data suggested that PR-PPD is the minimum PR domain required to inhibit NSCLC cell proliferation, and BR2 containing PR-PPD peptides effectively suppressed EGF-induced NSCLC cell, with little to no effect on noncancerous cells.



**Figure 26** Effect of BR2-PPD peptides on EGF-induced cell proliferation in A549.

A549 cells were plated in RPMI supplemented with 1% DCC-FBS and 1% PenStrep at 6,000 cells per well in a 96-well culture plate and incubated for 24 h. The following day, the culture medium was removed. A549 were treated with EGF 50 ng/ml compared to the combination of EGF 50 ng/ml with increasing peptides (0, 0.625, 1.25 and 2.5  $\mu\text{M}$ ) for 24 h. Cell viability was analyzed by MTT assays. Cell viability of A549 treated with BR2-PPD, BR2-2xPPD peptides was significantly decreased than BR2-2x $\Delta$ PPD (control) (\*\* $p \leq 0.01$ ) (\*\*\*) $p \leq 0.001$ ) (\*\*\*\* $p \leq 0.0001$ ). Error bars represent the standard errors of the mean (n=3).

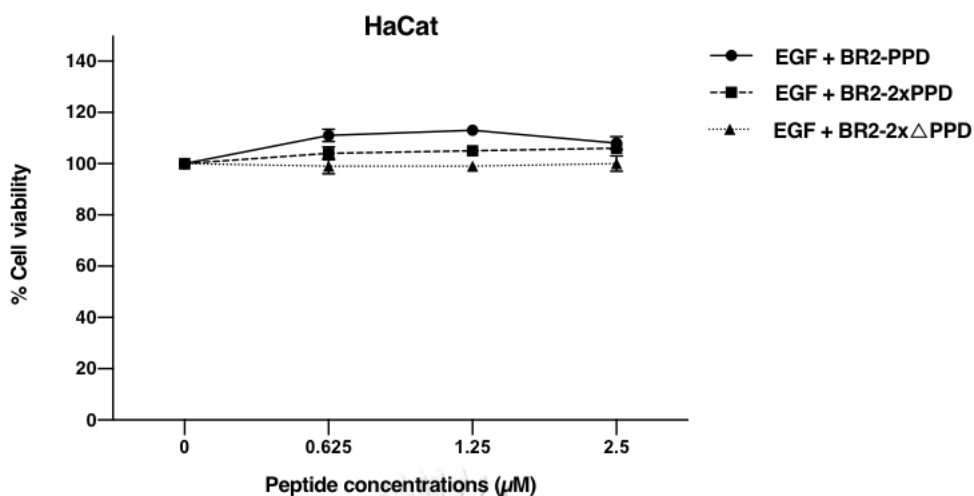


Figure 27 Effect of BR2-PPD peptides on EGF-induced cell proliferation in HaCat.

HaCaT cells were cultured in 1% DCC-RPMI plus 1% PenStrep at 8,000 cells per well and incubated for 24 h. Cells were treated with EGF 50 ng/ml or combined with increasing concentration of peptides (0, 0.625, 1.25 and 2.5 µM) for 24 h. Cell viability was analyzed by MTT assays. Error bars represent the standard errors of the mean (n=3).

#### 4.3 Effect of BR2-2xPPD treatment on EGF-induced activation of Erk1/2 in NSCLC

MAPK or Erk1/2 signaling pathway is involved in cell proliferation, differentiation, cell survival, apoptosis, and metastasis (99). Dysregulation of MAPK is often found in advanced cancer, including NSCLC (100). Previous results demonstrated that BR2-2xPPD peptide effectively inhibited EGF-induced A549 cell proliferation. We next investigated whether BR2-2xPPD peptide treatment could block EGF-mediated Erk1/2 activation. A549 were pretreated with 2.5 µM of BR2-2xPPD peptide for 4 h and followed by EGF treatment at 20 ng/ml for 5, 10, and 30 mins. Phosphorylation of Erk1/2 and total MAPK were determined by immunoblotting compared to EGF treatment alone. As shown in **Figure 28**, the activation of Erk1/2 was significantly increased when cells were treated with EGF 20 ng/ml after 5, 10, and 30 mins compared to untreated cells. In contrast, the

activation of Erk1/2 showed reduced considerably in every time point tested when cells were pretreated with BR2-2xPPD. However, pretreatment with BR2-2x $\Delta$ PPD peptide had little to no effect on EGF-induced MAPK at all time tested (**Figure 29**). These data suggested that the introduction of PR-PPD CPP could inhibit EGF-induced NSCLC cell proliferation by specifically blocking EGF activation of the MAPK signaling pathway, as previously reported (12).

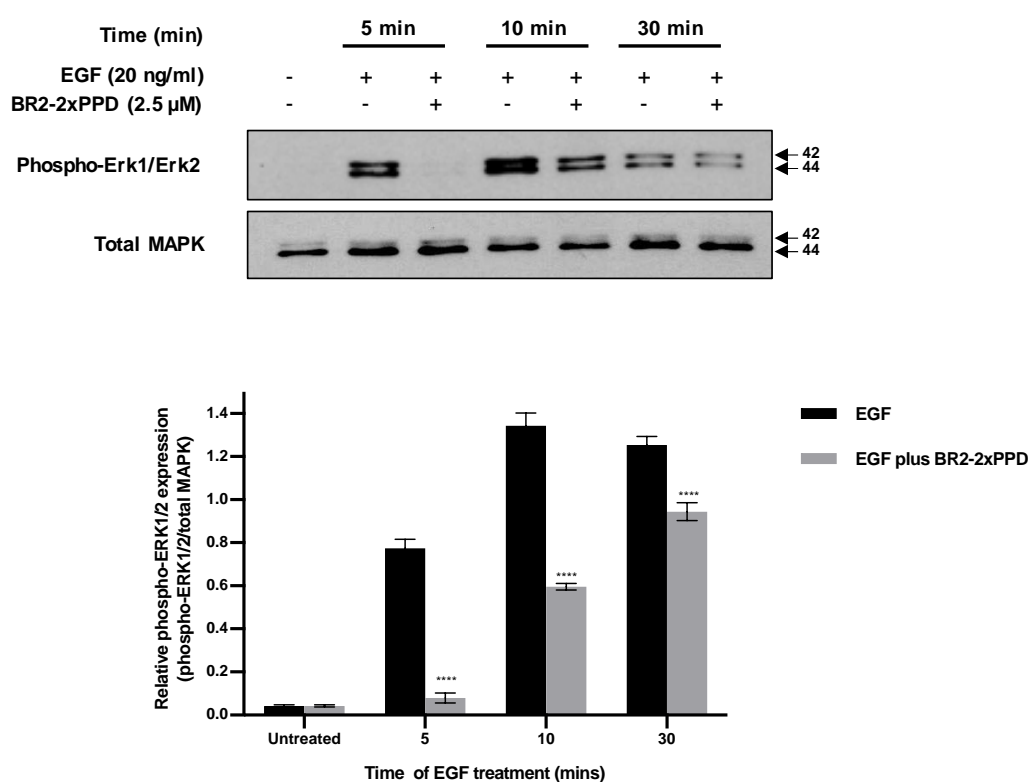


**Figure 28** Effect of BR2-PR-PPD peptides on EGF-induced Erk1/2 activation.

A549  $2 \times 10^5$  cells were cultured in 2% DCC-RPMI medium for 24 h. Cells were pretreated with BR2-2xPPD 2.5  $\mu$ M for 4 h. Then, cells were induced with EGF 20 ng/ml for 5, 10 and 30 min to activate MAPK signaling. Phospho-Erk1/2 and total MAPK were recognized by western blotting compared to untreated cells. Ten micrograms of protein were loaded in each lane. Bar graphs show relative pMAPK activities (pMAPK/totalMAPK) (\*\*\*\* $p \leq 0.0001$ ) and data are shown as means  $\pm$  SEM (n=3).

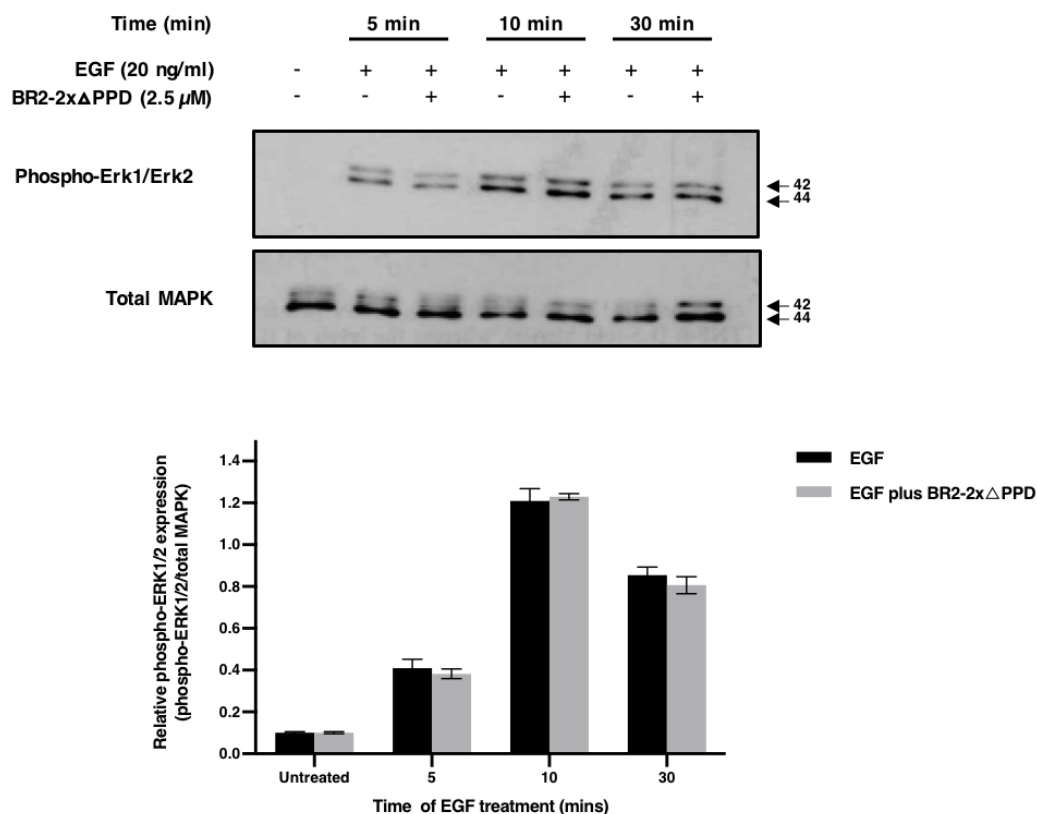


**Figure 29** Effect of BR2-2x $\Delta$ PPD peptides on EGF-induced Erk1/2 activation.

A549  $2 \times 10^5$  cells were cultured in 2% DCC-RPMI medium for 24 h. Cells were pretreated with BR2-2x $\Delta$ PPD 2.5  $\mu$ M for 4 h. Then, cells were induced with EGF 20 ng/ml for 5, 10 and 30 min to activate MAPK signaling. Phospho-Erk1/2 and total MAPK were recognized by western blotting compared to untreated cells. Ten micrograms of protein were loaded in each lane. Bar graphs show relative pMAPK activities (pMAPK/totalMAPK). Data are shown as means  $\pm$  SEM (n=3).

#### 4.4 BR2-2xPPD is a novel growth-inhibitory peptide for NSCLC expressing wild-type EGFR

##### 4.4.1 Effect of BR2 containing PR-PPD peptide on EGFR-wild type NSCLC cell proliferation

Several drugs and chemotherapies are currently available for the treatment of NSCLC, including tyrosine kinase inhibitors (TKIs). However, the first generation of TKIs such as Gefitinib and Erlotinib are quite effective in inhibiting cells expressing mutated EGFR, but much less effective in the cells expressing wild-type EGFR (101). Therefore, a novel alternative approach is needed for patients with NSCLC expressing wild-type EGFR. Our results demonstrated that BR2-2xPPD peptide treatment of NSCLC inhibited EGF-mediated cell proliferation. We next tested the effect of BR2-2xPPD peptide on NSCLC cell proliferation in medium with supplemented with fetal bovine serum (FBS) without additional EGF. NSCLC expressing wild-type EGF, A549, were cultured with the presence of BR2-2xPPD or BR2-2x $\Delta$ PPD peptides at concentrations ranging from 0 to 2.5  $\mu$ M for 24 h. Cell viability was assessed by MTT assay. BR2-2xPPD peptide dose-dependently inhibited A549 cell proliferation with a maximum inhibition at  $62 \pm 5\%$  at the highest dose while the presence of BR2-2x $\Delta$ PPD peptide had little to no effect on A549 cell proliferation (Figure 30).

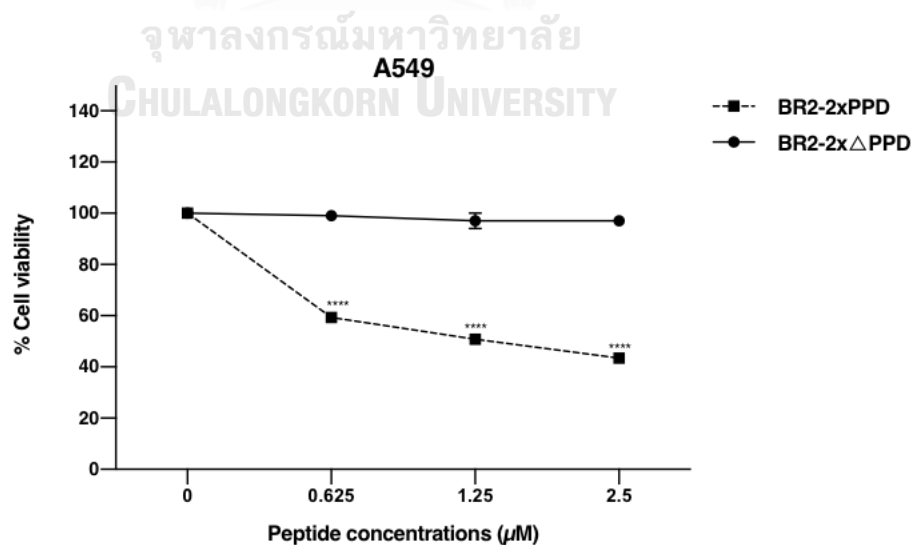
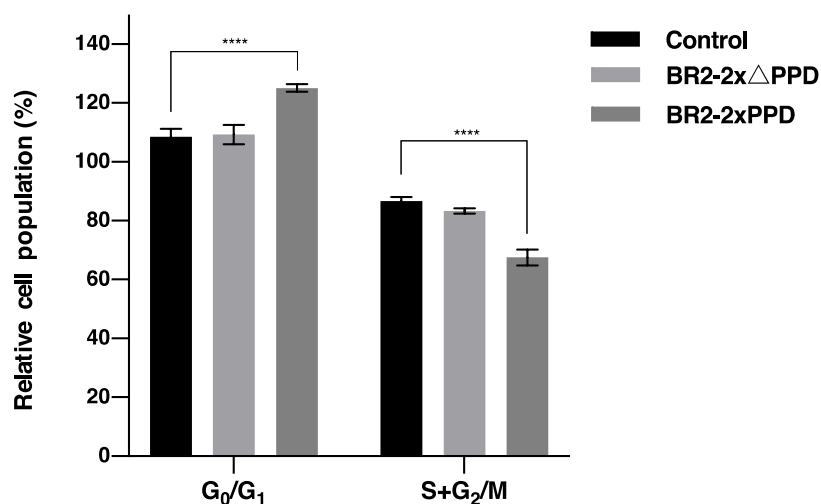


Figure 30 Effect of BR2-2xPPD and BR2-2x $\Delta$ PPD peptide on EGFR wild-type A549 cell proliferation.

A549 cells were cultured in 10% FBS-RPMI plus 1% PenStrep at 3,000 cells/well. After 24 hours, cells were treated with increasing dose of BR2-2xPPD or BR2-2x $\Delta$ PPD (0, 0.625, 1.25 and 2.5  $\mu$ M) for 24 h. Cell viability was performed by MTT assays. Value are represented as means  $\pm$  SEM (n= 3). Percent cell viability of peptide treatments were normalized with DMSO (\*\*\*\* $p \leq 0.0001$ ).

#### 4.4.2 Effect of BR2 containing PR-PPD peptide on cell cycle progression

We next determine whether the presence of BR2-2xPPD affected cell cycle regulation in NSCLC. To assess the distribution of cells in different phases of the cell cycle, A549 were treated with BR2-2xPPD or BR2-2x $\Delta$ PPD for 24 h, and cell cycle were analyzed by flow cytometry. As shown in **Figure 31**, the percentage of G<sub>0</sub>/G<sub>1</sub> phase was significantly increased while S+ G<sub>2</sub>/M populations was significantly decreased in A549 treated with BR2-2xPPD compared to control, suggesting that BR2-2xPPD peptide inhibited NSCLC growth in G<sub>0</sub>/G<sub>1</sub> phase arrest, leading to a decrease in the percentage of proliferative cells. However, a detailed underlying mechanism that mediated cell cycle repression by BR2-2xPPD treatment remains unclear and will need to be examined.



**Figure 31** Cell cycle distribution assessed by flow cytometry.

A549 cells were treated with BR2-2xPPD or BR2-2x $\Delta$ PPD peptide at concentration 2.5  $\mu$ M in 10% FBS-RPMI for 24 h. Cells were collected and analyzed by flow cytometry as described in Materials and Methods. Bar graphs represent

percent relative cell population of cells in  $G_0/G_1$  and  $S+G_2/M$  phase as normalized to untreated cells at 0 h. Results are shown as means  $\pm$  SEM ( $n=4$ ) (\*\*\*\* $p \leq 0.0001$ ).

During cell cycle progression, there are cyclins and cyclin-dependent kinase (CDKs) which act as regulatory molecules. Cyclin D1 and CDK2 are critical cell cycle regulators that involve in  $G_0/G_1$  to S phase transition and serve as therapeutic targets in several types of cancers, including NSCLC (102, 103). Our results suggested that BR2-2xPPD altered cell cycle progression. We next examined how BR2-2xPPD peptide treatment affected cyclin D1 and CDK2 expression. A549 were treated with BR2-2xPPD 2.5  $\mu$ M at various time points. Cyclin D1 and CDK2 mRNA levels were quantitated by real-time PCR, using GAPDH as an internal control. Cell treated with BR2-2xPPD exhibited significant suppression of cyclin D1 and CDK2 gene expression as compared to BR2-2x $\Delta$ PPD peptide treatment at all time points tested (**Figure 32 and 33**). Together, these data indicated that the BR2-2xPPD mediated cell cycle arrest and displayed antiproliferative activity resulting in a significant ( $57 \pm 1\%$ ) inhibition of NSCLC proliferation, suggesting that BR2-2xPPD peptide could be used as an alternative treatment to inhibit NSCLC expressing wild-type EGFR.

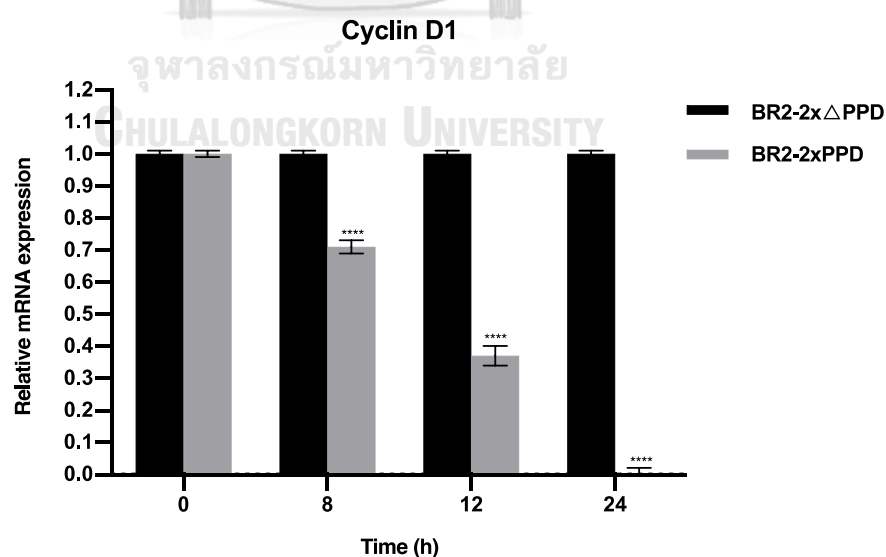


Figure 32 Relative Cyclin D1 mRNA expression.

A549 were cultured with BR2-2xPPD or BR2-2x $\Delta$ PPD peptide at concentration 2.5  $\mu$ M in 10%FBS-RPMI for indicated time points shown in the x-axis. Total RNA was extracted and amplified by RT-PCR. Values represent relative gene expression normalized with GAPDH. All data are reported as means  $\pm$  SEM (n=3) compared with BR2-2x $\Delta$ PPD peptide treatment (\* $p \leq 0.05$ ) (\*\*\*\* $p \leq 0.0001$ ).

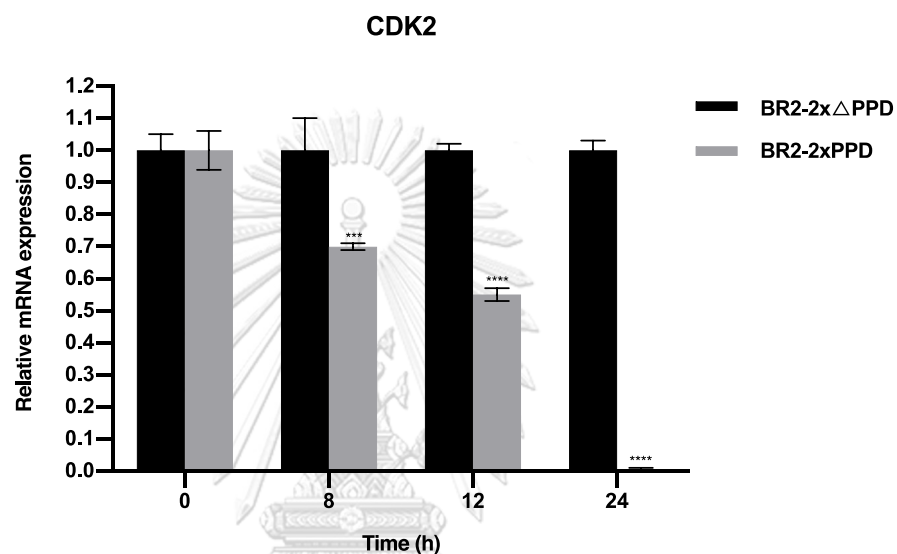


Figure 33 Relative CDK2 mRNA expression.

A549 were cultured with BR2-2xPPD or BR2-2x $\Delta$ PPD peptide at concentration 2.5  $\mu$ M in 10%FBS-RPMI for indicated time points shown in the x-axis. Total RNA was extracted and amplified by qRT-PCR. Values represent relative gene expression normalized with GAPDH. All data are reported as means  $\pm$  SEM (n=3) compared with BR2-2x $\Delta$ PPD peptide treatment (\*\*\*) ( $p \leq 0.001$ ) (\*\*\*\* $p \leq 0.0001$ ).

#### 4.4.3 Effect of BR2 containing PR-PPD peptide on cell apoptosis

To investigate the effect of the cancer-specific BR2-2xPPD peptide on cell apoptosis, A549 cells were treated with BR2-2xPPD or BR2-2x $\Delta$ PPD peptide at 2.5  $\mu$ M for 24, 48 and 72 h. Apoptosis analysis was performed by Annexin V and PI staining followed by flow cytometry. As shown in **Figure 34**, BR2-2xPPD and BR2-2x $\Delta$ PPD had no effect on cell apoptosis at every time points of treatment.

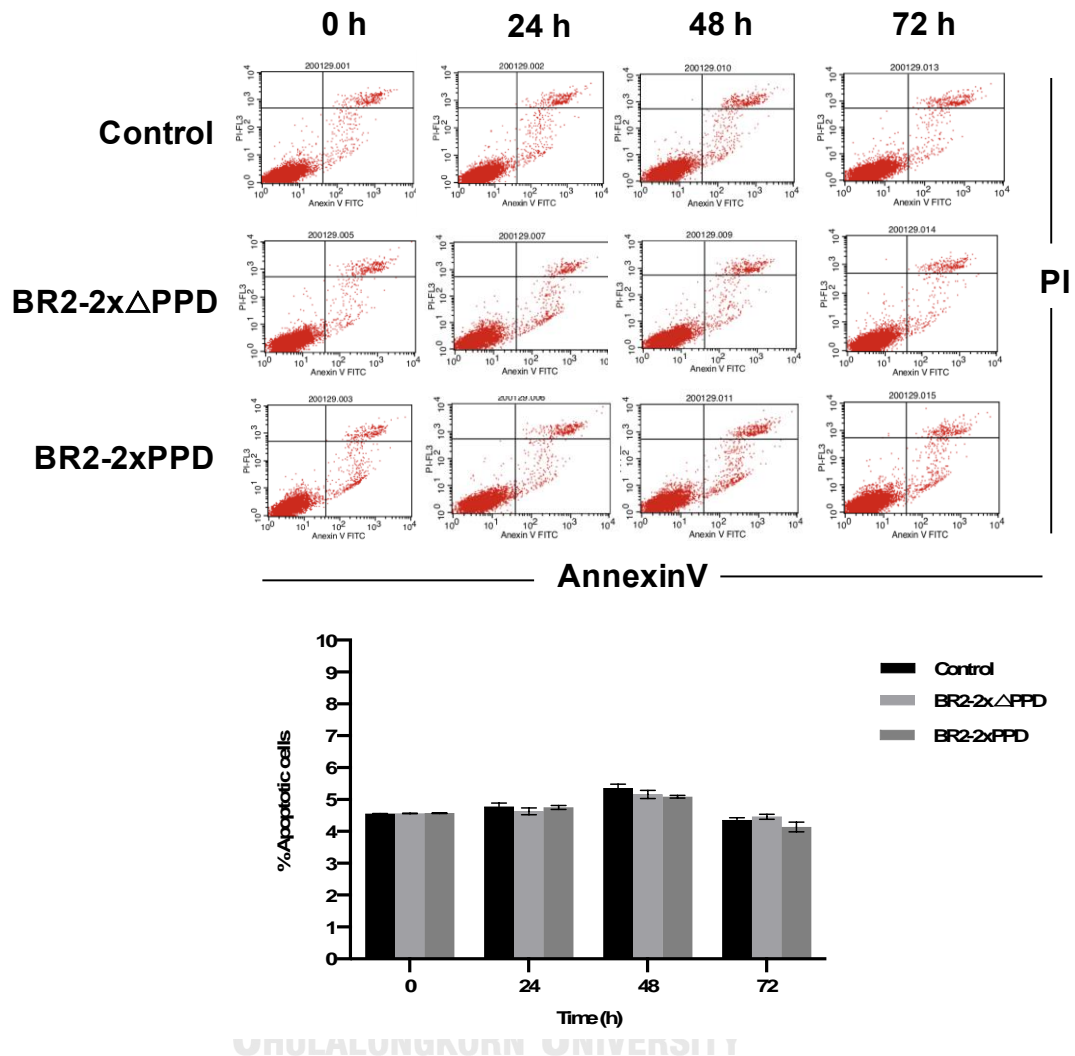


Figure 34 Effect of BR2-2xPPD and BR2-2x $\Delta$ PPD peptide on cell apoptosis.

A549 cells were treated with BR2-2xPPD or BR2-2x $\Delta$ PPD peptide at concentration 2.5  $\mu$ M in 10% FBS-RPMI for 24, 48 and 72 h. Flowcytometric analysis was performed by Annexin V and PI staining. Bar graphs represent percent of apoptotic cells of individual treatment. Value are represented as means  $\pm$  SEM (n=3). There was no significant difference ( $p > 0.05$ ) between each group of treatment compared to untreated group.

#### 4.4.4 Effect of BR2 containing PR-PPD peptide on cell migration

The cancer-specific peptides were next examined their ability to inhibit cancer cell migration by wound healing assay. After cell scratching, A549 were treated with BR2-2xPPD or BR2-2x $\Delta$ PPD peptide at concentration 2.5  $\mu$ M and the wounded cells was imaged at 0, 24 and 48 h. As shown in **Figure 35**, BR2-2xPPD peptide treatment was significantly suppressed A549 cell migration by nearly 19% at 24 h and 37% at 48 h, whereas BR2-2x $\Delta$ PPD peptide had no effect on cell migration inhibition when compared to untreated control cells.

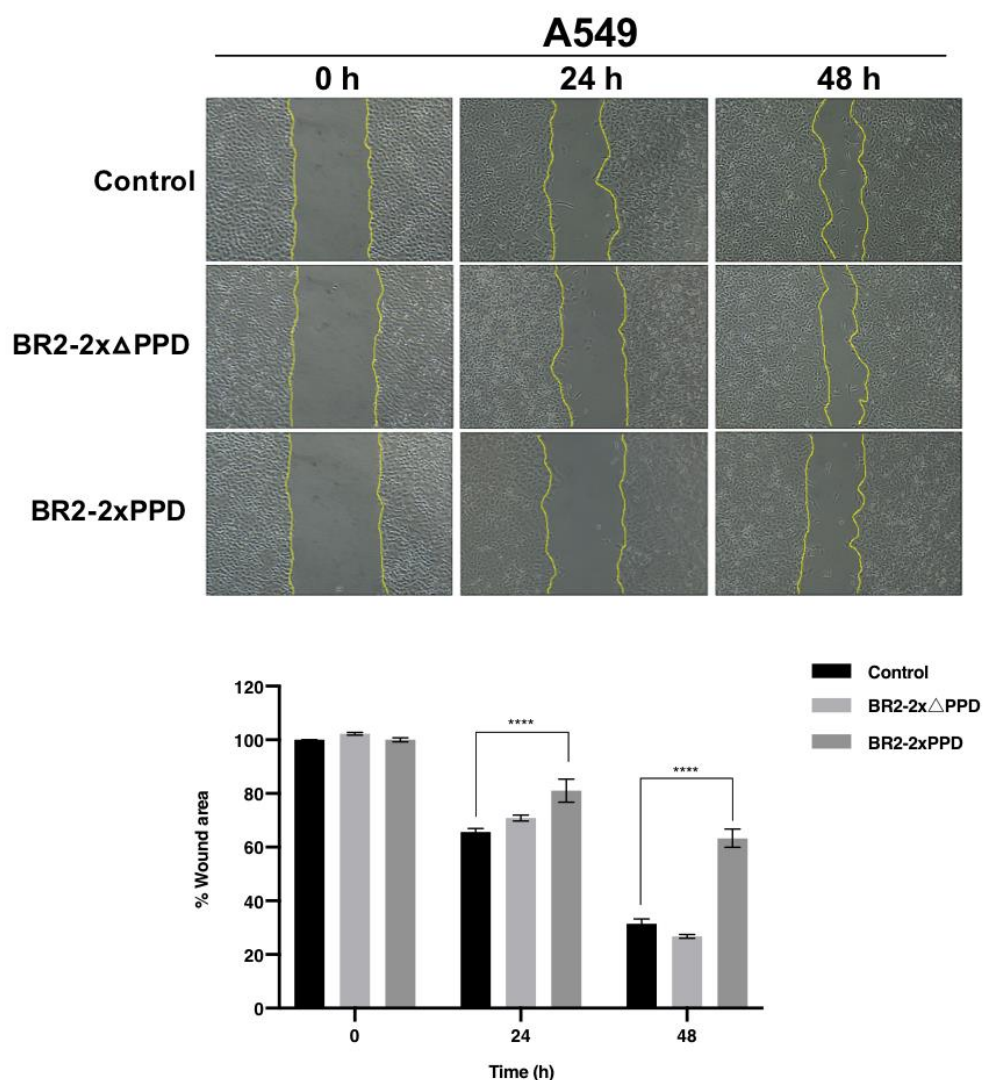


Figure 35 Effect of BR2-2xPPD and BR2-2x $\Delta$ PPD peptide on cell migration.

Wounded A549 cells were treated with BR2-2xPPD or BR2-2x $\Delta$ PPD peptide at concentration 2.5  $\mu$ M in 10%FBS-RPMI. Wound areas were imaged under microscopy at 0, 24 and 48 h after treatment. Wound areas were analyzed by ImageJ software. Bar graphs represent percent of wound areas in triplicated experiment compared to untreated control (\*\*\*\* $p \leq 0.0001$ ).

#### 4.5 Effect of the cancer-specific peptides on EGFR-mutant NSCLC cell proliferation

##### 4.5.1 Characteristics of EGFR-TKIs resistant lung adenocarcinoma cells

The activating mutation of EGFR is frequently found 5-20% in NSCLC patients (104, 105). It has been reported that patients who respond to the first-generation EGFR-TKIs are mostly diagnosed as EGFR mutation. However, the most patients (50-60%) eventually developed the acquired resistance to EGFR-TKIs after 12 months. In this study, we also investigated the effect of BR2 containing PR-PPD peptide treatment in EGFR-mutant NSCLC. PC9 is a non-small cell lung cancer cell lines which harbor the exon 19 deletion mutation in EGFR tyrosine kinase domain. To establish the EGFR-TKIs resistant cell lines, PC9 cells were cultured with increasing concentration of gefitinib and erlotinib for 6 months. The gefitinib-resistant and erlotinib-resistant cells were generated as PC9-GR and PC9-ER, respectively. PC9-6M is the parental PC9 which also cultured for 6 months in the medium without EGFR-TKIs.

To characterize the resistance to TKIs, PC9-6M, PC9-GR and PC9-ER were cultured with increasing dose of gefitinib or erlotinib. After 72 h, cell viability assay was performed by MTT. The  $IC_{50}$  of gefitinib and erlotinib was  $\sim 1 \mu$ M in the EGFR-TKI sensitive PC9-6M cells. While PC9-GR and PC9-ER showed significantly more resistance to gefitinib and erlotinib in approximately 8.5  $\mu$ M as shown in **Figure 36**.

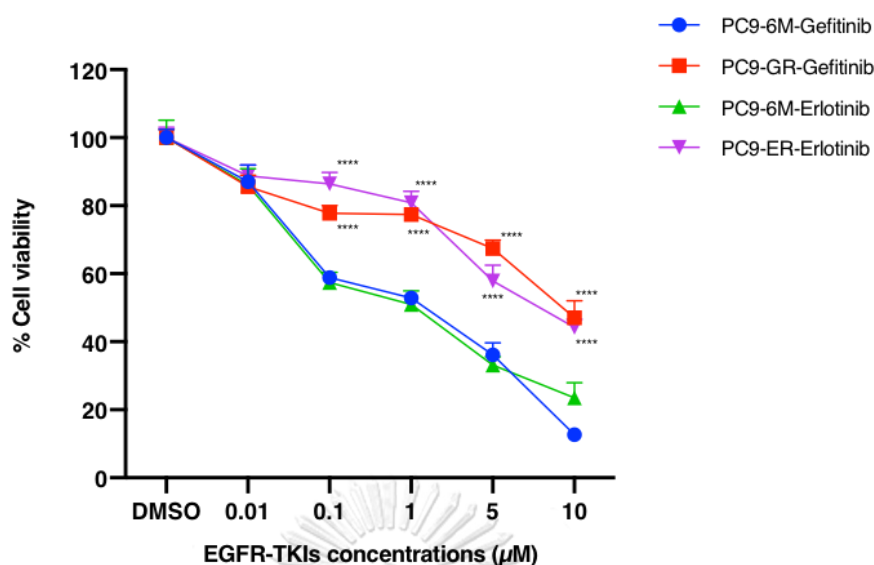


Figure 36 Effect of EGFR-TKIs treatment on EGFR-mutant PC9 NSCLC cells

EGFR-mutant PC9-6M, PC9-GR and PC9-ER cells were treated with increasing dose of Gefitinib or Erlotinib 0-10  $\mu\text{M}$ , incubated for 72 h and analyzed for cell viability. Graphs represent percent cell viability of PC9 cells after indicated treatments normalized to DMSO (control) treated cells. Values are shown as means  $\pm$  SEM in triplicate experiments ( $n=3$ ) and \*\*\*\* denotes  $p \leq 0.0001$ .

#### 4.5.2 The combination of BR2-2xPPD peptide with Tyrosine Kinase Inhibitors (TKIs) enhanced growth inhibitory effects of TKI in NSCLC harboring mutant EGFR

We next tested whether the combination treatment of BR2 containing PR-PPD peptide (BR2-2XPPD) and TKIs could be more effective than TKIs alone in inhibiting NSCLC cell proliferation. EGFR-TKI-sensitive (PC9-6M) lung adenocarcinoma cells were treated with 0.1  $\mu\text{M}$  concentration of Gefitinib or Erlotinib alone compared or in combination with TKIs- with increasing concentration of BR2-2xPPD peptide (0-2.5  $\mu\text{M}$ ) for 72 h. In TKI-sensitive PC9-6M cells, Gefitinib and Erlotinib could reduce cancer cell proliferation by  $41 \pm 2\%$  and  $43 \pm 2\%$  as compared to control no treatment. The combination of BR2-2xPPD and TKIs, Gefitinib or Erlotinib, was more effective in reducing cancer cell proliferation by inhibiting  $85 \pm 1\%$  and  $81 \pm 1\%$  (Figure 37A and

37B), while the presence of mutant PPD peptide, BR2-2x $\Delta$ PPD had little to no effects on PC9-6M cell proliferation.

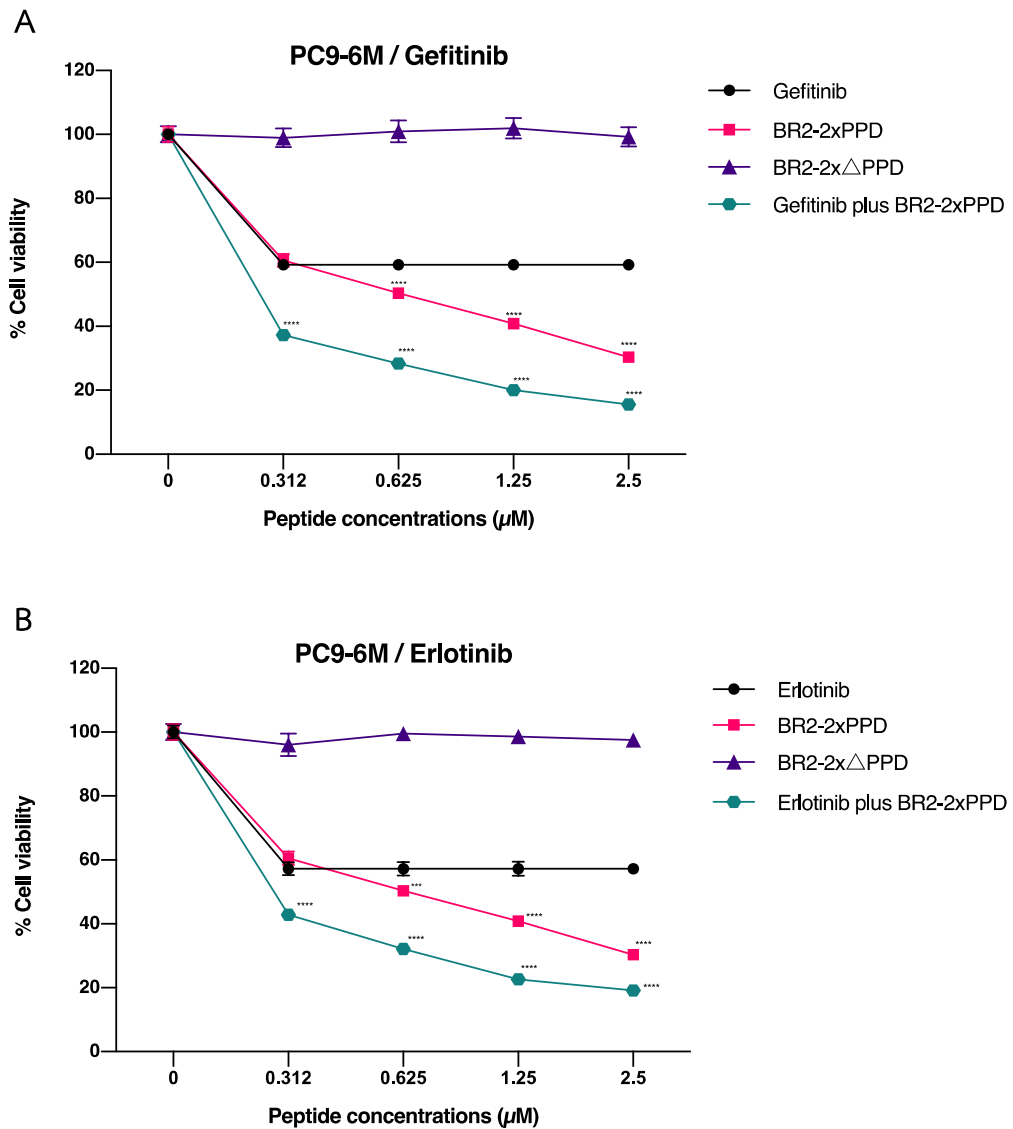
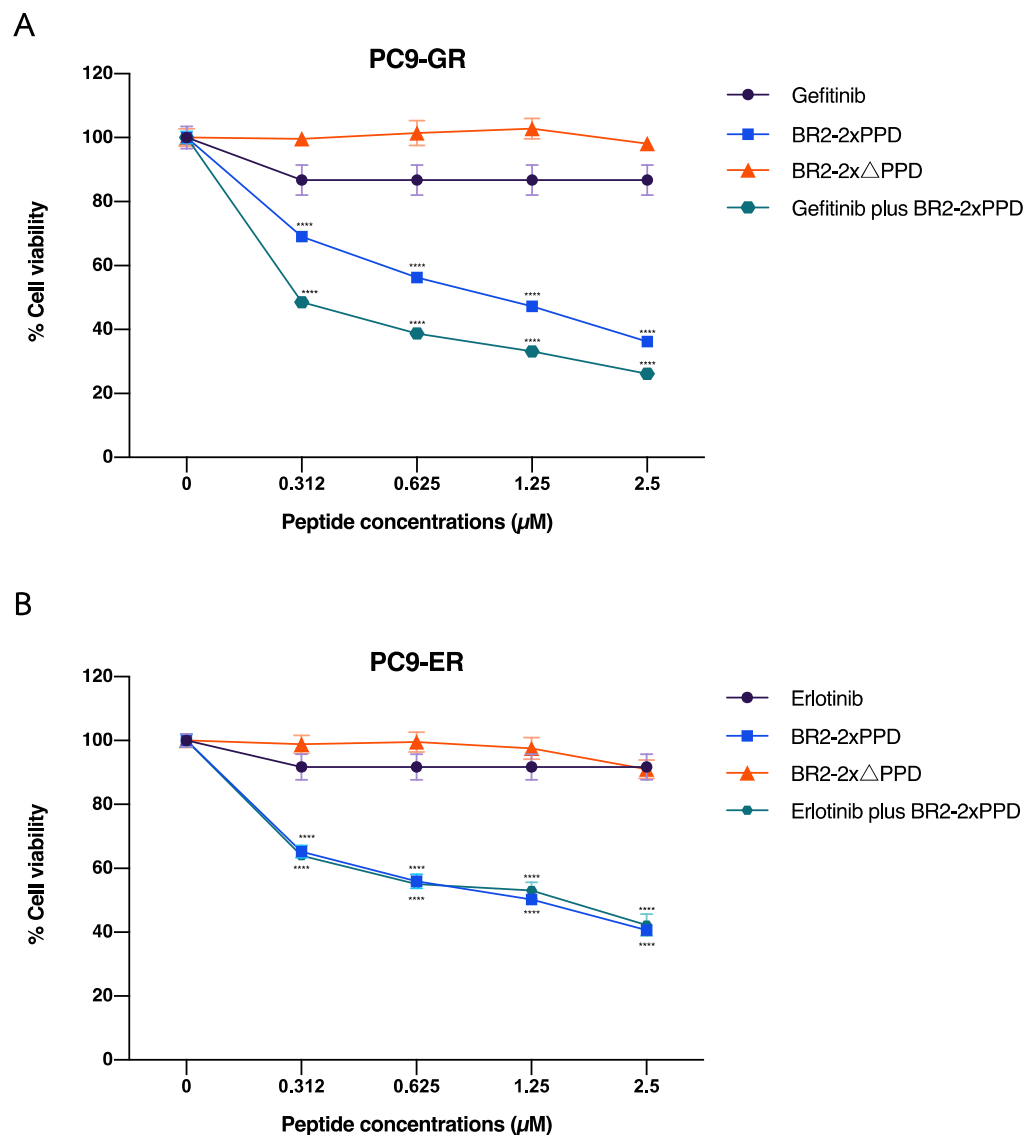


Figure 37 Effects of EGFR-TKIs and BR2-PRPPD peptide combination treatment TKIs-sensitive PC9 cell lines.

EGFR-mutant PC9-6M cells were treated with Gefitinib or Erlotinib 0.1  $\mu\text{M}$  alone or combined with increasing dose of BR2-2xPPD peptide (0-2.5  $\mu\text{M}$ ) for 72 h and analyzed for cell viability. Graphs represent percent cell viability of PC9 cells after indicated treatments normalized to untreated cells. The percent cell viability of

BR2-2xPPD or in combination with EGFR-TKIs (Gefitinib or Erlotinib) treatment of PC9-6M are shown in (A) and (B), respectively. Values are shown as means  $\pm$  SEM in triplicate experiments (n=3) and \*\*\*\* denotes  $p \leq 0.0001$ .

To next test whether BR2-2XPPD could enhance the growth-inhibitory effect of TKIs, EGFR-TKI-resistant variants (PC9-GR and PC9-ER) cell lines. As shown in **Figure 38A and 38B**, Gefitinib or Erlotinib alone weakly inhibited PC9-GR and PC9-ER cell proliferation and inhibited only  $13 \pm 5\%$  and  $8 \pm 4\%$  as compared control untreated cells, respectively. The treatment of BR2-2xPPD peptide in Gefitinib-resistant PC9-GR cells dose-dependently inhibited cell proliferation with a maximum inhibition at  $64 \pm 1\%$  of control untreated cells. Interestingly, the treatment of BR2-2XPPD peptide in combination with Gefitinib enhanced the Gefitinib growth inhibitory effects and showed a maximum inhibition at  $74 \pm 1\%$  as compared to control untreated cells. However, BR2-2x $\Delta$ PPD failed to significantly improve the growth inhibitory effect of Erlotinib. Combination treatment of BR2-2XPPD peptide in combination with Erlotinib showed a maximum inhibition at  $59 \pm 1\%$  as compared to control untreated cells. These data suggested that the BR2 peptide containing PR-PPD could enhance the growth inhibitor effect of TKIs, suggesting that combination treatment of the BR2-2XPR-PPD peptide in combination with Gefitinib may serve as a new perspective in NSCLC treatment.



**Figure 38** Effects of EGFR-TKIs and BR2-PRPPD peptide combination treatment in TKIs-resistant PC9 cell lines.

EGFR-mutant PC9 cells were cultured with increasing concentrations of Gefitinib or Erlotinib to generate Gefitinib or erlotinib-resistant PC9 cell lines (PC9-GR and PC9-ER, respectively) compared to the parental PC9-6M cells. Cells were treated with Gefitinib or Erlotinib 0.1  $\mu\text{M}$  alone or combined with increasing dose of BR2-2xPPD peptide (0-2.5  $\mu\text{M}$ ) for 72 h and analyzed for cell viability. Graphs represent percent cell viability of PC9 cells after indicated treatments normalized to untreated

cells treated cells. The percent cell viability of BR2-2xPPD or in combination with EGFR-TKIs (Gefitinib or Erlotinib) treatment of PC9-GR and PC9-ER are shown in (A) and (B), respectively. Values are shown as means  $\pm$  SEM in triplicate experiments (n=3) and \*\*\*\* denotes  $p \leq 0.0001$ .

#### 4.6 Effect of the cancer-specific BR2 peptide containing LXXLL motif or PR-PPD on Estradiol-induced cell proliferation of breast cancer cells

##### 4.6.1 Optimization of 17 $\beta$ -estradiol (E2) concentrations

The classical mechanism of steroid hormones are involved in the nucleus. In ER-positive breast cancer, binding of estrogen agonist, such as 17 $\beta$ -estradiol or E2, to the ligand binding domain (LBD) at the N-terminus of ER. The conformational change of receptor can recruit the others coactivators to be activated and allowed ER bind to estrogen response element which sequentially express various genes including control of cell proliferation. In this study, MCF-7 cell lines, which were defined as an ER-positive breast cancer cells, were used as a cell model. To induce cancer cell proliferation, MCF-7 cells were treated with increasing dose of E2 (0-100 nM) and cell viability assays were performed after treatment at 0, 24, 48, 72 and 96 h. As shown in **Figure 39**. MCF-7 cells showed a significant increase in cell proliferation at 72 and 96 h after cells were treated with 10 nM E2 compared to vehicle. Previous study has been shown that E2 at concentration 10 nM could induce the estrogen-responsive genes stronger than lower concentration (106). Therefore, the concentration of E2 at 10 nM was used in the following experiments.

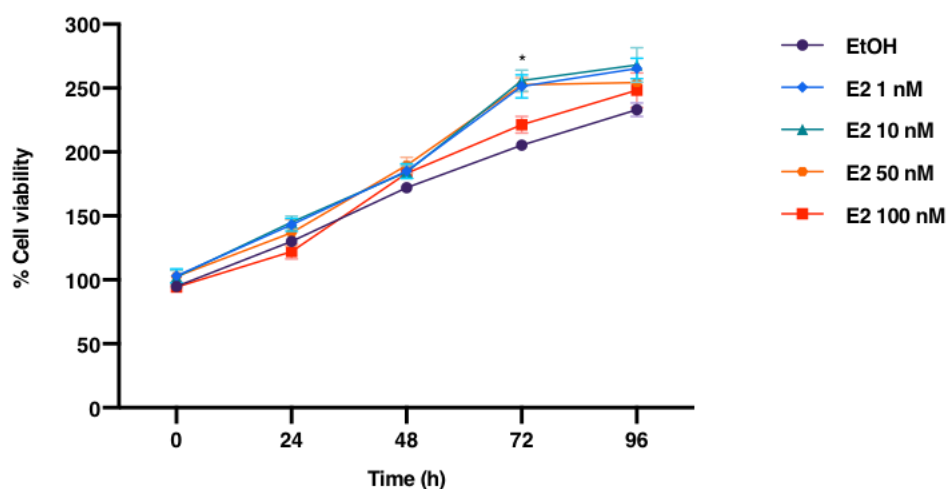


**Figure 39** Estradiol-induced MCF-7 breast cancer cell proliferation.

MCF-7 3,000 cells were cultured in 96 well plate in 5%DCC-DMEM. After 72 h, cells were treated with increasing concentration of  $17\beta$ -Estradiol (0-100 nM) in 5%DCC-DMEM. Cell viability assays were performed at 0 to 96 h after treatment compared to vehicle (ethanol). Values are shown as means  $\pm$  SEM in triplicate experiments (n=3) and \*denotes  $p \leq 0.05$ .

#### 4.6.2 BR2 peptide containing LXXLL motif mediate the inhibitory effect of Estradiol-induced cancer cell proliferation

The liganded-ER can induce cell proliferation by the recruitment of steroid receptor coactivators (SRCs). These coactivators contain the LXXLL motifs at the central region domain which directly bind to ER lead to transcription activation of estrogen-regulated genes (107). Previous studies have been reported that the LXXLL motif of steroid receptor coactivator 1 or SRC1 effectively bind to ER $\alpha$  (97, 108). Therefore, blockage of ER signaling by interfering with the NRx2-LXXLL peptide may reduce E2-induced breast cancer cell growth. To investigate the effect of BR2-LXXLL peptide on E2-induced growth, MCF-7 cells were treated with 10 nM E2 with or without the increasing concentration of BR2-LXXLL or BR2-LXXLL(Scramble) peptides for 72 h. Cell viability was measured by MTT. BR2-LXXLL dose-dependently decreased MCF-7 cell proliferation in about  $90 \pm 2$  %inhibition at the maximum dose tested (4

$\mu\text{M}$ ) while BR2-LXXLL (scramble) peptide did not affected to growth inhibition (Figure 40).

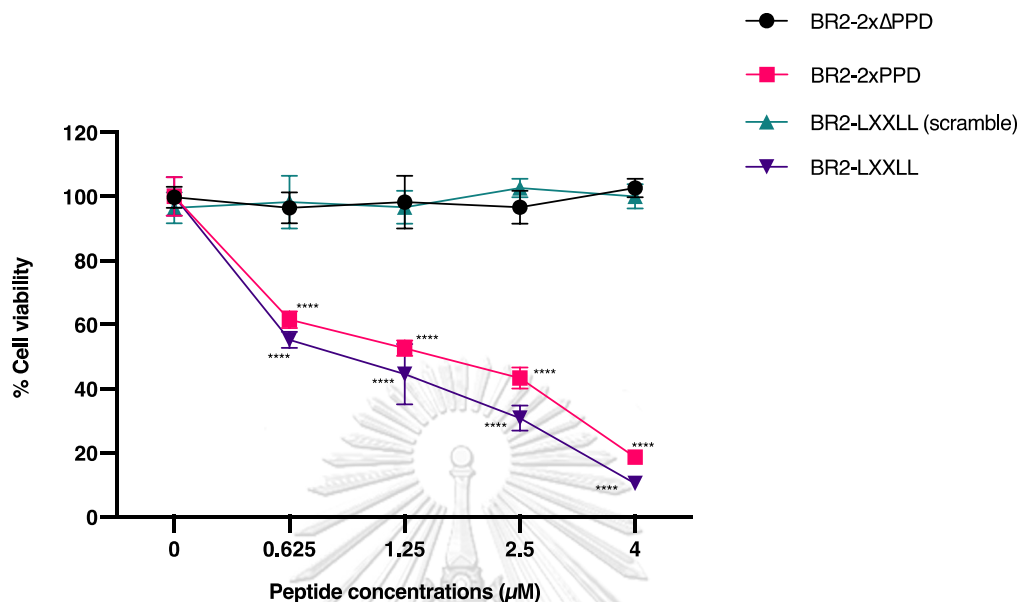


Figure 40 Effect of BR2 coupled with PR-PPD or LXXLL motifs on E2-stimulated breast cancer cell proliferation.

MCF-7 cells were treated with E2 10 nM alone or combined with increasing dose of BR2-PR-PPD peptide or LXXLL peptides (0-4  $\mu\text{M}$ ) for 24 h and analyzed for cell viability. Graphs represent percent cell viability of MCF-7 cells after indicated treatments normalized to untreated cells. Values are shown as means  $\pm$  SEM in triplicate experiments (n=3) and \*\*\*\* denotes  $p \leq 0.0001$ .

#### 4.6.3 BR2-2xPPD peptide could inhibit E2-induced proliferation of breast cancer cell

In addition to the classical mechanism, steroid hormones can regulate gene expression without binding to steroid response element (SREs). ER has been found to localize at the extranuclear compartment (109). E2 treatment can rapidly promote the extranuclear signaling which result from protein-protein interaction between membrane-associated receptors and cytoplasmic signaling molecules (110). Forming of ER and growth factor receptor complexes can induce signal transduction of MAPK pathways which required the Grb2-SOS interaction (40). As previous results

shown in NSCLC cell models, BR2 containing PR-PPD peptide effectively inhibited EGF-induced MAPK activation. We next examined the effect of BR2-2xPPD peptide on E2-stimulated cell growth in breast cancer cell line. ER-positive MCF-7 cells were plated with culture medium containing BR2-2xPPD or BR2-2x $\Delta$ PPD in the presence of 10 nM E2 and measured cell viability by MTT assays. As shown in **Figure 40**, BR2-2xPPD dose-dependently decreased MCF-7 cell proliferation in about  $81 \pm 2\%$  inhibition at the maximum dose tested (4  $\mu$ M) while BR2-2x $\Delta$ PPD peptide had a little to no effect on growth inhibition.

#### 4.6.4 BR2-LXXLL peptide effectively reduced the transcriptional activation of progesterone receptor in breast cancer cells

We next examined whether LXXLL peptide can disrupt the interaction between nuclear receptor and coactivator. In this study, T47DC42 cells which defined as ER and PR-negative breast cancer cell lines were used as a cell model. T47DC42 cells were expressed the PR-B isoform which previously described as a stronger transcriptional activity than PR-A isoform (111, 112). To investigate the effect of BR2-LXXLL peptide on PR-dependent transcription, T47DC42-PRB cells were next transfected with PRE-TK-Luciferase vector to mimic the endogenous progesterone response element (PRE) in target cells. Doxycycline at 1,000 ng/ $\mu$ l was used to induced PR-B expression. Cells were next treated with 10 nM R5020 (Progesterin) either 10 nM R5020 with increasing dose of BR2-LXXLL or BR2-LXXLL (scramble) peptides compared to untreated cells. Treatment of Doxycycline and R5020 could induce PR transcription as 6.2 folds compared to Doxycycline or R5020 alone. BR2-LXXLL peptide dose-dependently decreased the transcriptional activity of PR-B in approximately  $50 \pm 2\%$  inhibition after cells were treated with 7.5  $\mu$ M of peptide in the presence of Doxycycline and R5020. While the inhibition effect was no observed in the scramble peptide treatment at all concentration tested. These results suggested that BR2 containing LXXLL motifs peptide could disrupt the transcription activation possessed by PR and coactivator interaction (**Figure 41**).

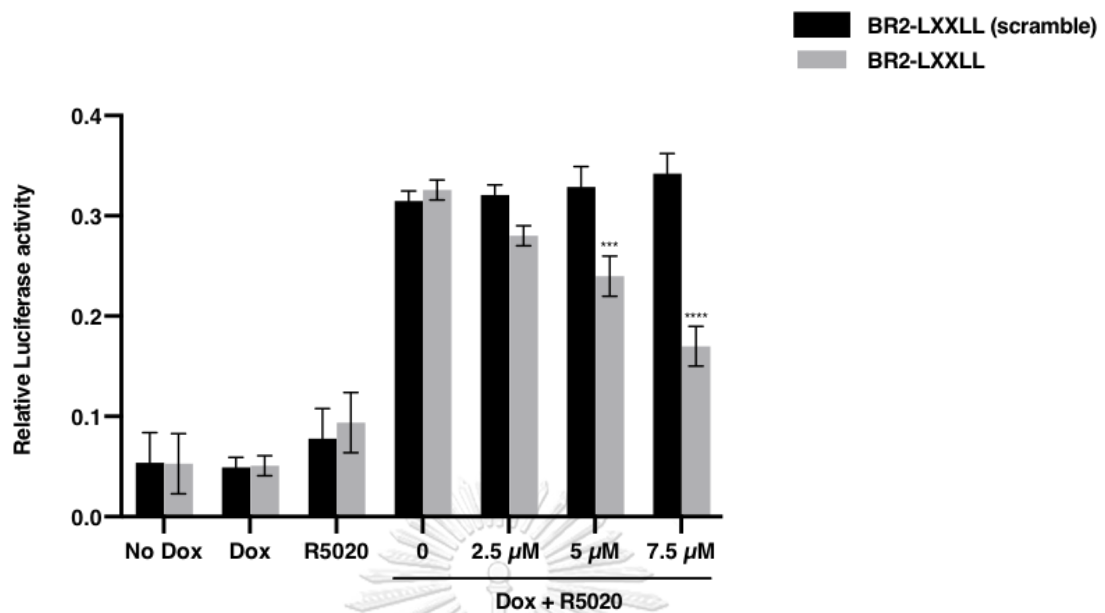


**Figure 41 Effect of LXXLL peptide on PR-dependent transcription.**

Bar graphs represent the relative luciferase activity of Doxycycline and R5020 treatment or in combination with BR2-LXXLL or scramble peptide in T47DC42-PRB cells normalized to Renilla luciferase levels. Values are shown as means  $\pm$  SEM in triplicate experiments (n=3) (\*\*p  $\leq$  0.01) and (\*\*\*p  $\leq$  0.001) and (\*\*\*\*p  $\leq$  0.0001).

#### 4.7 Effect of BR2 containing PR-PPD and LXXLL peptides on Triple-negative breast cancer cell proliferation.

Triple-negative breast cancer or TNBC is one of breast cancer subtype which lack of ER, PR and HER2 expression. Approximately 15-20% of breast cancer cases are TNBC (113). The patients with TNBC has the worst clinical outcome and poor prognosis compare with the other two major classifications: ER+ PR+; HER2+. The patients are more likely to undergo metastasize and relapse (114). There is an urgent need for more targeted therapy development of TNBC. Despite lacking in steroid hormone receptor, there are several transcription factors which contain the LXXLL motifs (115). Moreover, the amplification or overexpression of EGFR have been found in TNBC in about 30-35% (116). Therefore, we next evaluated the effect of PR-PPD and LXXLL peptides on TNBC cell proliferation. MDA-MB-231 TNBC cells were

incubated with increasing concentration of BR2-2xPPD, BR2-2x $\Delta$ PPD, BR2-LXXLL or BR2-LXXLL scramble peptides for 24 h. Then, cell viability assays were tested by MTT. As shown in **Figure 42**, BR2-2xPPD and BR2-LXXLL peptide dose-dependently inhibited TNBC cell proliferation in approximately  $82\pm 1\%$  and  $56\pm 1\%$  inhibition, respectively, at the maximum dose 7.5  $\mu$ M. While the mutant PR-PPD peptide and the scramble peptide had a little to no effect on growth inhibition.

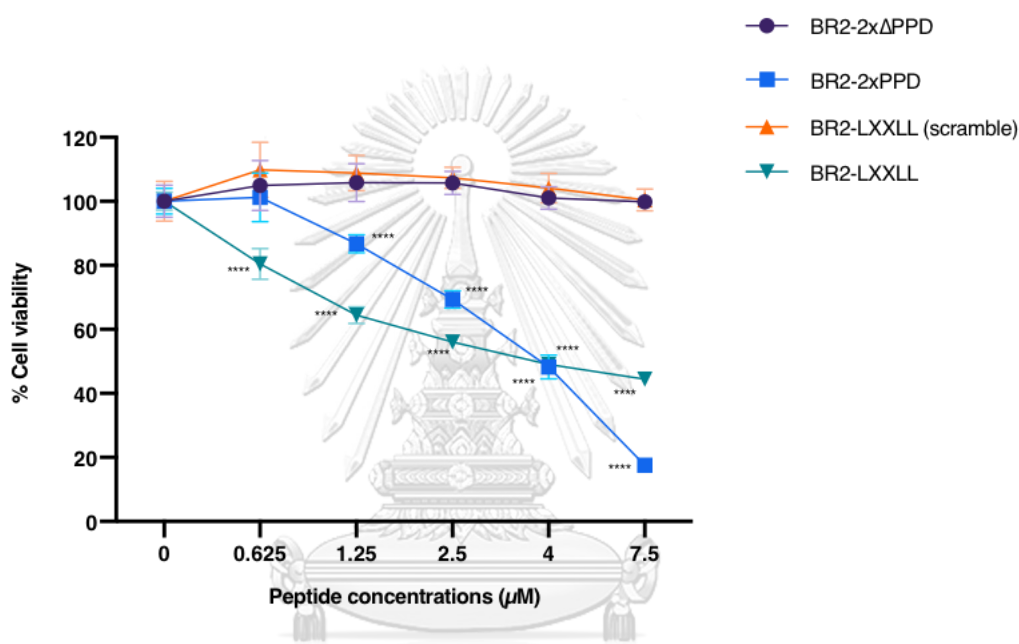


**Figure 42** Effect of BR2 containing PR-PPD and LXXLL peptides on Triple-negative breast cancer cell proliferation.

MDA-MB-231 cells were treated with increasing dose of BR2-PR-PPD peptide or LXXLL peptides (0-7.5  $\mu$ M) for 24 h and analyzed for cell viability. Graphs represent percent cell viability of MDA-MB-231 cells after indicated treatments normalized to untreated cells (control) treated cells. Values are shown as means  $\pm$  SEM in triplicate experiments (n=3) and \*\*\*\* denotes  $p \leq 0.0001$ .

## CHAPTER V

### DISCUSSION AND CONCLUSION

Cancer constitutes a major cause of mortality in both men and women worldwide. Current treatments are available for cancers such as surgery, radiotherapy and chemotherapy. For NSCLC, the predominant type of lung cancer, surgical resection is the most effective in the early stages of the disease; however, the recurrence rates after the surgical resection remain high (117). Chemotherapy and radiotherapy are commonly used to improve survival outcomes in recurrent patients. These combination approaches are often used to treat patients with advanced and metastatic NSCLC (118). Despite being able to reduce the mortality rates of patients with advanced NSCLC, most patients frequently suffer from adverse side effects due to non-specific targeting of chemotherapy drugs. These agents not only affect the rapidly dividing cancer cells but also affect the fast-growing normal or healthy cells. Therefore, new therapeutics options focusing on novel strategies to selectively target cancer cells without affecting noncancerous cells are urgently needed.

It is well established that PR signaling plays essential roles in endocrine-related cancers such as breast, endometrium and ovary (119). PR is expressed as two isoforms from a single gene, PR-A and PR-B. Proteomics profiling has been demonstrated the difference in biological actions of each isoform in breast cancer (120). In addition to progestin-activated transcriptional effects, liganded-PR can rapidly activate others transduction signaling molecules through SH3-specific polyproline domain (PR-PPD) (8). Although both PR isoforms shared the identical PPD sequence, only PR-B can mediate c-Src/ Ras/ MAPK signaling in cytoplasm (10). Increasing data suggests that PR also has a potential role in non-endocrine tumors including NSCLC (67, 121). Clinical data show that high level of PR is correlated with better clinical outcome in NSCLC patients (122-125). Treatment of progesterone promoted the inhibition of NSCLC growth in *vitro* and in *vivo*, and PR could potentially be used as a prognostic marker in NSCLC patients. However, a previous

study failed to demonstrate a correlation between PR expression and clinical outcomes in NSCLC clinical tissues (126).

To better understand the role of PR in NSCLC, we constructed NSCLC cell models for PR functional analysis. We demonstrated that PR-B expression in A549 NSCLC significantly inhibited EGF-induced-NSCLC cell growth (12). In this study, we extended our investigation by expressing the PR-PPD peptides fused with a cell-penetrating peptide domain, BR2. Consistent with our previous study, both BR2-PPD and BR2-2xPPD peptides inhibited EGF-induced A549 cell proliferation, while the mutant PR-PPD peptide did not affect A549 cell proliferation. These data implicated the crucial role of a short PR-PPD motif for suppressing NSCLC cell growth (12), suggesting that PR expression can directly affect cell proliferation.

Additionally, our results suggested a crosstalk between PR extranuclear signaling and growth factor receptors could play a role in NSCLC progression. A549 cells pretreated with BR2-2xPPD before treating with EGF in the absence of progesterin to exclude PR transcriptional activity showed significant attenuation of Erk1/2 activation. Little to no inhibition was observed in cells pretreated with the mutant peptide, BR2- $\Delta$ PPD. Together, these data suggested that BR2-PRPPD peptides inhibited EGF-mediated MAPK activation, leading to a decrease in A549 cell proliferation.

Upon growth factor receptor activation, Grb2 and Sos interaction stimulates a variety of downstream signaling. Sos-derived peptides was previously designed to disrupt Grb2-Sos interaction (127, 128). Peptidimer peptide containing two-repeats of the proline-rich sequence were more effective in inhibiting Grb2-Sos interaction and more potent in reducing MAP kinase activation than monomer peptide with one copy of the PRPPD. Furthermore, treatment of peptidimer served as Grb2-SH3 ligand and eventually reduced the growth of HER2-positive breast cancer cells (129). This data is consistent with our results, in which the BR2-2xPPD peptide was more effective in reducing A549 than BR2-PPD. These results suggested that the PPD in these peptides shared a similar polyproline type II (PPII) helices structure and can

efficiently block Grb2-Sos complex through dual interactions of PR-PPD with both SH3 domains of Grb2.

The PR-PPD mediating rapid progestin-mediated c-Src kinase activation through directly binds to c-Src-SH3 domain (8). This PPD is a unique sequence presence in PR and absence in all others nuclear hormone receptors, including estrogen receptor (ER), androgen receptor (AR), glucocorticoid receptor (GR) and thyroid hormone receptor (TR) (8). These proline-rich peptides are particularly useful in obstructing the PPD of Grb2 from binding to the SH3 domains. However, the inability of these protein sequences to enter cells and bind to cytoplasmic signaling molecules limited its use of the peptides. In this study, we added a cell-penetrating peptide domain to the PR-PPD to promote peptide internalization, allowing the PR-PPD to enter cells block PPD-SH3 mediated signal transductions.

In recent years, a new class of drug delivery such as cell-penetrating peptides or CPPs have been introduced. The truncated HIV-1 Tat peptide has been described as the first CPP that could mediate the cellular uptake of target molecules (130, 131). However, several CPPs exhibit non-specific penetration or cytotoxic effects at high concentrations. Recently, the tumor-specific cell-penetrating BR2 peptide has been successfully developed and was used as a drug transporter and tested in an vivo model of colorectal carcinoma and hepatocellular cancer (89, 132). In this study, we designed and expressed the anticancer BR2 containing PR-PPD peptide from *P. pastoris* to target growth factor signaling pathways that required PPD-SH3 interactions in NSCLC. Our results demonstrated the ability of BR2 peptide to be internalized into NSCLC cancer cells, with little to no effect on normal cells. Because of the high positively charge peptide, BR2 preferentially bind to negatively charge on cancer cell membrane and consequently internalize into the cytoplasm by macropinocytosis (133). In contrast, the cell membrane of most normal cells is neutral, resulting in low electrostatic interaction and inefficiently passing through the cell membrane (89, 134). Thus, the PR-PPD present in the BR2-2XPPD may compete with the PPD in SOS to bind to the Grb2-SH3 domains, leading to a suppression of Grb2-SOS signal transduction, a significant reduction Erk1/2 activation and a decrease NSCLC cell proliferation.

Tyrosine Kinase Inhibitors (TKIs), such as Gefitinib or Erlotinib, are used as targeted therapy for patients with NSCLC whose tumors overexpress EGFR. TKIs compete with ATP to bind to the ATP binding pocket of tyrosine kinases, resulting in a reduction in tyrosine kinase phosphorylation and a decrease in cell proliferation (135). Meta-analysis studies suggested that EGFR-TKIs improved progression-free survival (PFS) in patients with advanced NSCLC expressing mutant EGFR but had no significant impact in NSCLC patients with NSCLC expressing wild-type EGFR (136-140). The mechanism mediating resistance to EGFR-TKIs in wild-type EGFR is well understood. A previous study suggested that lower TKI binding affinity of the wild-type EGFR could attribute to TKIs insensitivity (141). Therefore, there is a need to identify novel compounds that could block or suppress wild-type EGFR signaling. In this study, we demonstrated that the addition of BR2-2xPPD peptide to the currently available EGFR-TKIs could significantly improve TKI-mediated inhibition of NSLC cell proliferation. Furthermore, our results showed that a decrease in NSCLC by BR2-2xPPD was mediated, in part, through cell cycle arrest G<sub>0</sub>/G<sub>1</sub> and a reduction in cyclin D1 and CDK2 expression in A549 NSCLC expressing wild-type EGFR (**Figure 31-33**). Cyclin D1 is known as a critical regulator in cell cycle progression from G<sub>1</sub> to S phase and has previously been described as a target in progestin-mediated Src kinase signaling pathways, while CDK2 can help promote DNA replication prior to cell cycle progression into G<sub>2</sub>/S phase (10, 11, 142). It is well known that the activation of PI3K/Akt and c-Src/Erk/MAPK signaling pathways are involved in cytoskeleton remodeling and migration in cancer cells (143). From our results, BR2-2xPPD also exhibited the antimetastatic activity in NSCLC which may result from Erk activation inhibition effect of BR2-2xPPD peptide (**Figure 35**). In addition, there are others transcription factors such as CREB, NF- $\kappa$ B,  $\beta$ -catenin and the extracellular matrix metalloproteinase which can be mediated by Erk signaling and play a key role in cancer metastasis (144-146). Therefore, the effect of Br2-2xPPD peptide on these factor expressions are needed to determine.

BR2-2xPPD peptide treatment of NSCLC with wild-type EGFR effectively induced cell cycle arrest and decreased numbers of proliferative cells, while EGFR-TKIs including Gefitinib and Erlotinib failed to inhibit cell proliferation of NSCLC with

EGFR wild-type. These results suggested that BR2-2xPPD peptide could be an attractive molecule that should be further developed as a targeted therapeutic agent to help treat NSCLC harboring wild-type EGFR in the future.

Constitutive hyperactivation of MAPK cascade is frequently found in cells expressing activated EGFR mutants in which the kinase domain is constitutively activated independent of ligand. Exon 19 deletion and L858R point mutation are the most common activating mutation and are often associated with sensitivity to TKIs, including Gefitinib and Erlotinib (55, 105). Although NSCLC patients whose tumors bear EGFR mutation often showed better clinical outcomes and are more preferable to be treated EGFR-TKIs, a large proportions of these patients (50-60%) eventually developed acquired resistance to TKIs caused by a secondary mutation, such as T790M mutation (57, 147, 148). The EGFR-T790M gatekeeper mutation is a substitution mutation inside the ATP binding cleft leading to the low-affinity binding of TKIs to EGFR. Administration of TKIs at high concentrations can cause adverse side effects in NSCLC patients, such as skin rash and diarrhea. Therefore, patients may benefit from an alternative therapeutic strategy for NSCLC treatment. In this study, we demonstrated that BR2-2xPPD peptide treatment increased the sensitivity to EGFR-TKIs in both TKI-sensitive PC9-6M cells and Gefitinib-resistant PC9-GR cells. Both PC9-6M and PC9-GR cells were previously shown to express a typical EGFR mutation in exon 19 (**Figure 37**). However, we found that BR2-2xPPD peptide could also suppressed cell proliferation in Erlotinib-resistant PC9-ER cells, which harbor exon 19 deletion, L858R mutation and a secondary T790M mutation (**Figure 38**). However, % inhibition of NSCLC cell proliferation in cells treated BR2-2XPPD was not significantly different from those of cells treated with BR2-2XPPD in combination with Erlotinib, suggesting that differences in EGFR mutation could be involved in TKI sensitivity (94). In TKIs-sensitive cells, TKI can effectively reduce Erk1/2 and Akt phosphorylation, leading to NSCLC growth inhibition (149). While in TKI-resistant cells, the other growth factor receptors or other gene abnormalities are often activated and serve as alternative pathways promoting cancer cell survival (150). Thus, it is possible that PC9-ER cells bear an activated EGFR mutant along with activation of other signaling pathways that are dependent on PPD-SH3 interactions for signal transduction, making

PC9-ER to be insensitive to Erlotinib treatment but sensitive to BR2-2XPPD. Therefore, the combination of EGFR-TKIs and drugs targeting others signaling pathways such as BR2-2XPPD could be an effective strategy to overcome TKI resistance (151, 152).

Several studies have shown that the interaction between nuclear receptors and coactivators is a crucial protein-protein interaction and act as a significant target for cancer treatment (153). In this study, we produced the peptide containing LXXLL motifs which designed from GRIP-1 and F6 peptide to specifically interrupt NR-coactivator binding. LXXLL motifs were recombined with BR2 and SV40 peptide to enter the nucleus (**Figure 23**). Our results demonstrated that PR transcriptional activity was significantly decreased in the presence of BR2-LXXLL peptide (**Figure 41**). These data were consistent with previous study that LXXLL motifs could inhibit NR-coactivator interaction and also supported by nuclear localization of BR2-LXXLL (154). Moreover, we determined that LXXLL and PR-PPD peptides affected the growth of ER-positive and triple-negative breast cancer cell lines (**Figure 40 and 42**). These results exhibited the efficacy of LXXLL motifs and PR-PPD to inhibit nuclear and extra-nuclear signaling, respectively. Therefore, the combination treatment between BR2-LXXLL and BR2-2xPPD peptides may concurrent inhibit cancer cell proliferation by disturbing both nuclear and extra-nuclear cascades. However, the underlying mechanism mediated growth inhibitory effect is needed to investigate in future study.

Our results demonstrated the potential of BR2 which can be used as a small peptides carrier and specifically targeted the cancer cells without causing damage to normal cells. Intracellular delivery of PR-PPD and LXXLL motifs by BR2 achieved to suppress cancer cell proliferation in both NSCLC and breast cancer cells. However, further studies are needed to investigate the antitumor activity of BR2-2XPPD and BR2-LXXLL *in vivo*. Altogether, our data established a proof of concept that a cancer cell-specific CPP in combination with the PR-PPD or LXXLL motifs could serve as a novel therapeutic strategy to inhibit cancer growth.

## APPENDIX A

Cell type	Treatments	Peptides		
		BR2-PPD	BR2-2xPPD	BR2-2x $\Delta$ PPD
A549	EGF 50 ng/ml	100 $\pm$ 8.0	100 $\pm$ 7	100 $\pm$ 2.0
	EGF + 0.625 $\mu$ M peptide	84 $\pm$ 7.0	80 $\pm$ 2.0	99 $\pm$ 3.0
	EGF + 1.25 $\mu$ M peptide	75.77 $\pm$ 5.0	63.66 $\pm$ 2.0	99 $\pm$ 2.0
	EGF + 2.5 $\mu$ M peptide	63.66 $\pm$ 8.0	51.72 $\pm$ 5.0	100 $\pm$ 3.0
HaCaT	EGF 50 ng/ml	100 $\pm$ 0.8	100 $\pm$ 2.0	100 $\pm$ 1.3
	EGF + 0.625 $\mu$ M peptide	111 $\pm$ 2.4	103.598 $\pm$ 2.5	105.496 $\pm$ 2.4
	EGF + 1.25 $\mu$ M peptide	113.282 $\pm$ 1.3	105.252 $\pm$ 1.9	108.351 $\pm$ 1.7
	EGF + 2.5 $\mu$ M peptide	107.862 $\pm$ 2.6	106.151 $\pm$ 1.1	106.151 $\pm$ 3.2

Table 1 Cell viability of EGF and peptide treatments

Time (mins)	Treatments			
	EGF	EGF plus BR2-2xPPD	EGF	EGF plus BR2-2x $\Delta$ PPD
Control	0.042 $\pm$ 0.005	0.042 $\pm$ 0.005	0.1 $\pm$ 0.005	0.1 $\pm$ 0.005
5	0.774 $\pm$ 0.023	0.379 $\pm$ 0.042	0.409 $\pm$ 0.052	0.382 $\pm$ 0.033
10	1.343 $\pm$ 0.015	0.595 $\pm$ 0.058	1.209 $\pm$ 0.048	1.229 $\pm$ 0.016
30	1.254 $\pm$ 0.041	0.944 $\pm$ 0.039	0.854 $\pm$ 0.040	0.806 $\pm$ 0.042

Table 2 pMAPK and total MAPK activation

Cell type	Concentrations ( $\mu\text{M}$ )	EGFR-TKIs Treatments (72 h)	
		Gefitinib ( $\mu\text{M}$ )	Erlotinib ( $\mu\text{M}$ )
PC9	DMSO	100 $\pm$ 2.4	100 $\pm$ 5.1
	0.01	87.016 $\pm$ 4.8	86.064 $\pm$ 4.8
	0.1	50.855 $\pm$ 2.0	51.443 $\pm$ 3.0
	1	45.862 $\pm$ 2.1	46.909 $\pm$ 4.0
	5	36.098 $\pm$ 3.6	33.179 $\pm$ 2.4
	10	12.637 $\pm$ 1.7	23.483 $\pm$ 4.5
A549	DMSO	100 $\pm$ 1.8	100 $\pm$ 2.2
	0.01	91.767 $\pm$ 8.3	87.137 $\pm$ 2.0
	0.1	88.900 $\pm$ 6	81.752 $\pm$ 1.4
	1	79.486 $\pm$ 4.5	74.275 $\pm$ 2.4
	5	64.667 $\pm$ 2.3	65.946 $\pm$ 0.3
	10	47.426 $\pm$ 3.6	50.660 $\pm$ 1.2

Table 3 Cell viability of EGFR-TKIs treatments

Cell phase	Treatment (24 h)		
	Control	BR2-2x $\Delta$ PPD	BR2-2xPPD
G0/G1	108.53 $\pm$ 2.6	109.27 $\pm$ 3.3	125.1 $\pm$ 1.3
S+G2M	86.74 $\pm$ 1.3	83.33 $\pm$ 0.9	67.5 $\pm$ 2.7

Table 4 Cell cycle distributions

EGFR-TKIs Treatment for 72 h			
EGFR-TKIs	Concentrations	Cell type	
		PC9-6M	PC9-GR
Gefitinib	DMSO	100 ± 2.4	100 ± 2.4
	0.01	87.016 ± 4.9	85.594 ± 3.4
	0.1	58.855 ± 2.0	77.770 ± 2.3
	1	52.862 ± 2.1	77.424 ± 1.5
	5	36.098 ± 3.6	67.379 ± 2.5
	10	12.637 ± 1.8	47.045 ± 5.0
EGFR-TKIs	Concentrations	Cell type	
		PC9-6M	PC9-ER
Erlotinib	DMSO	100 ± 10.1	100 ± 3.0
	0.01	86.064 ± 4.8	88.776 ± 3.2
	0.1	57.443 ± 3.0	86.396 ± 3.4
	1	50.909 ± 4.0	80.861 ± 3.4
	5	33.179 ± 2.4	57.872 ± 4.6
	10	23.483 ± 4.5	44.191 ± 2.4

Table 5 Cell viability of EGFR-TKIs treatment in EGFR mutant cells

Treatments	Time of treatment (h)				
	0	12	24	48	72
Control	4.55 ± 0.01	5.24 ± 0.01	4.78 ± 0.11	5.35 ± 0.13	4.35 ± 0.08
BR2-2x $\Delta$ PPD	4.56 ± 0.01	5.25 ± 0.01	4.63 ± 0.11	5.16 ± 0.13	4.46 ± 0.08
BR2-2xPPD	4.57 ± 0.01	5.905 ± 0.19	5.35 ± 0.06	5.085 ± 0.04	5.435 ± 0.15

Table 6 Percent apoptotic cells

Treatments	Time (h)		
	0	24	48
Control	100.034 ± 0.05	65.614 ± 1.32	31.480 ± 1.78
BR2-2x $\Delta$ PPD	102.254 ± 0.51	72.845 ± 1.08	26.703 ± 0.74
BR2-2xPPD	100 ± 0.71	81.082 ± 4.27	63.299 ± 3.42

Table 7 Percent wound area

Treatment	BR2-LXXLL	BR2-LXXLL(scramble)
No Dox	0.052 ± 0.03	0.054 ± 0.03
Dox	0.0507 ± 0.01	0.049 ± 0.01
R5020	0.093 ± 0.03	0.078 ± 0.03
Dox + R5020	0	0.326 ± 0.01
	2.5	0.280 ± 0.01
	5	0.240 ± 0.02
	7.5	0.170 ± 0.02
		0.315 ± 0.01
		0.321 ± 0.01
		0.329 ± 0.02
		0.342 ± 0.02

Table 8 Relative luciferase assay

## APPENDIX B

### 1. *E. coli* media recipes

#### Luria-Bertani (LB) medium with ampicillin (1L)

Tryptone	10	g
NaCl	1	g
Yeast Extract	5	g
Agar	20	g

Dissolved these recipes in 950 ml deionized water, adjusted the pH of solution to 7.5 with 1 M NaOH and brought the volume up to 1 liter. Sterilized by autoclave for 20 mins of liquid cycle. Cooled the medium to ~55°C and then added ampicillin to 100 µg/ml final concentration. Stored at 4°C.

#### Low salt LB medium with zeocin (1L)

Tryptone	10	g
NaCl	5	g
Yeast Extract	5	g
Agar	15	g

Dissolved these recipes in 950 ml deionized water, adjusted the pH of solution to 7.5 with 1 M NaOH and brought the volume up to 1 liter. Sterilized by autoclaving for 20 mins on liquid cycle. Cool the medium to ~55°C and then add zeocin to 25 µg/ml final concentration. Store at 4°C in the dark.

## 2. *Pichia pastoris* Media Recipes

### 1 M HEPES buffer pH 8.0 (10 ml)

Dissolved HEPES free acid 2.383 g in deionized water and adjusted pH to 8 with 5 M NaOH. Added deionized water to a final volume of 10 ml and sterilized by filtration.

### 1 M DTT (1.5 ml)

Dissolved DTT 231.4 mg in deionized water and adjusted volume to 1.5 ml. Then, sterilized by filtration.

### 1 M D-sorbitol (100 ml)

Dissolved D-sorbitol 18.2 g in deionized water and adjusted volume to 100 ml. Sterilized by filtration. Stored at 4°C in the dark.

### Stock Solutions

- **10xDextrose (20% Dextrose)**

Dissolved 200 g of D-glucose in 1000 ml deionized water and sterilized by autoclaving.

- **10xYNB (13.4% Yeast Nitrogen Base w/o Amino acids w/o Ammonium sulfate)**

Dissolved 134 g of YNB in 1000 ml deionized water and sterilized by filtration.

- **500xBiotin (0.02% Biotin)**

Dissolved 10 mg of biotin in 50 ml deionized water and sterilized by filtration.

- **10xMethanol (5% Methanol)**

Mixed 50 ml of methanol with 950 ml deionized water and sterilized by filtration.

- **10xGlycerol (10% Glycerol)**

Mixed 100 ml of methanol with 900 ml deionized water and sterilized by autoclaving.

- **1 M Potassium Phosphate Buffer pH 6.0**

Mixed 132 ml of 1 M  $K_2HPO_4$  to 868 ml of 1 M  $KH_2PO_4$  and adjusted the pH to 6.0 by KOH. Sterilized by autoclaving.

**Yeast Extract Peptone Dextrose (YPD) medium (1L)**

Yeast Extract	10	g
Peptone	20	g
Agar	20	g

Dissolve these recipes in 900 ml deionized water and sterile by autoclave. Cool the medium to  $\sim 60^\circ\text{C}$  and then add 100 ml of 10XDextrose and zeocin to 100ug/ml final concentration. Store at  $4^\circ\text{C}$  in the dark.

**Buffered Glycerol-complex (BMGY) Medium**

Yeast Extract	10	g
Peptone	20	g

Dissolved in 700 ml deionized water and sterilized by autoclaving.

Cooled the medium to room temperature and then mixed with the following solution.

- 100 ml 1 M Potassium Phosphate Buffer pH 6.0
- 100 ml 10xYNB
- 100 ml 10xGlycerol

**Buffered Methanol-complex (BMMY) Medium**

Yeast Extract	10	g
Peptone	20	g

Dissolved in 700 ml deionized water and sterilized by autoclaving.

Cooled the medium to room temperature and then mixed with the following solution.

- 100 ml 1M Potassium Phosphate Buffer pH 6.0
- 100 ml 10xYNB
- 100 ml 10xMethanol

### 3. HisTrap column and AKTA start buffers

#### Stock solutions

- **5 M NaCl (1L)**

Dissolved NaCl 292.2 g in deionized and mixed by stirring. Adjusted the final volume to 1 L and sterilized by autoclaving or filtration. Stored at room temperature.

- **5 M Imidazole (500 ml)**

Dissolved imidazole 170.2 g in deionized water. Swirled the bottle until completely dissolved and adjusted the total volume to 1 L. Sterilized by filtration and stored at 4°C.

- **1 M NaH<sub>2</sub>PO<sub>4</sub> (monobasic)**

Dissolved NaH<sub>2</sub>PO<sub>4</sub> 119.98 g in deionized water and adjusted total volume to 1 L.

- **1 M Na<sub>2</sub>HPO<sub>4</sub> (dibasic)**

Dissolved Na<sub>2</sub>HPO<sub>4</sub> 141.96 g in deionized water and adjusted total volume to 1 L.

- **1 M Sodium phosphate buffer pH 7.4 (1L)**

Mixed 226 ml of 1 M NaH<sub>2</sub>PO<sub>4</sub> with 774 ml of 1 M Na<sub>2</sub>HPO<sub>4</sub> and sterilized by autoclaving. Stored at 4°C.

CHULALONGKORN UNIVERSITY

#### Binding buffer (1L)

5 M NaCl	100	ml
1 M Sodium phosphate buffer pH 7.4	20	ml
5 M Imidazole	4	ml
Deionized water	876	ml

Sterilized by filtration followed by autoclaving and stored at 4°C.

**Elution buffer (1L)**

5 M NaCl	100	ml
1 M Sodium phosphate buffer pH 7.4	20	ml
5 M Imidazole	100	ml
Deionized water	780	ml

Sterilized by filtration followed by autoclaving and stored at 4°C.

**20% Ethanol (1L)**

Filtered 800 ml of deionized water in sterile bottle and cooled at room temperature. Then, added 200 ml of absolute Ethanol.

**Stripping buffer (500 ml)**

20 mM Sodium phosphate	3.8	g
0.5 M NaCl	14.61	g
50 mM EDTA	10.11	g

Dissolved the recipes and adjusted to the final volume at 500 ml. The solution was sterilized by filtration and autoclaving.

**Recharging buffer (50 ml)**

Prepared 0.1 M  $\text{NiSO}_4$  by dissolving  $\text{NiSO}_4$  1.314 g in deionized water and made the final volume to 50 ml. Sterilized by filtration and stored at 4°C.

#### 4. Cell culture reagents

##### Roswell Park Memorial Institute (RPMI) 1640 Medium

RPMI 1640 powder with L-glutamine, phenol red and without HEPES, sodium bicarbonate	10.4	g
Sodium Bicarbonate	2	g

Dissolved the recipes in 950 ml Milli Q water and adjusted the pH to 7.2-7.4 by acetic acid or HCl. Added Milli Q water to the final volume 1 liter and sterilized by filtration (0.2  $\mu$ M PVDF membrane) and stored at 4°C.

##### Dulbecco's Modified Eagle Medium

DMEM powder with L-glutamine, phenol red or red free and without HEPES, sodium bicarbonate	10.4	g
Sodium Bicarbonate	3.7	g

Dissolved the recipes in 950 ml Milli Q water and adjusted the pH to 7.2-7.4 by acetic acid or HCl. Added Milli Q water to the final volume 1 liter and sterilized by filtration (0.2  $\mu$ M PVDF membrane) and stored at 4°C.

##### Epidermal Growth Factor (EGF)

To prepare a stock solution at concentration 1 mg/ml, the lyophilized EGF was reconstituted in 1 ml of 10 mM acetic acid. Gently swirled to dissolve. Sterilized by 0.2  $\mu$ M filter and stored at -20°C.

##### MTT reagent

To prepare a 5 mg/ml MTT solution, MTT powder 0.1 g was dissolved in 1xPBS 200 ml. Mixed by vortexing and then sterilized by filtration. Stored at -20°C in the dark.

## REFERENCES

1. Jorissen RN, Walker F, Pouliot N, Garrett TP, Ward CW, Burgess AW. Epidermal growth factor receptor: mechanisms of activation and signalling. *Exp Cell Res.* 2003;284(1):31-53.
2. Hirsch FR, Varella-Garcia M, Bunn PA, Jr., Di Maria MV, Veve R, Bremmes RM, et al. Epidermal growth factor receptor in non-small-cell lung carcinomas: correlation between gene copy number and protein expression and impact on prognosis. *J Clin Oncol.* 2003;21(20):3798-807.
3. Onn A, Correa AM, Gilcrease M, Isobe T, Massarelli E, Bucana CD, et al. Synchronous overexpression of epidermal growth factor receptor and HER2-neu protein is a predictor of poor outcome in patients with stage I non-small cell lung cancer. *Clin Cancer Res.* 2004;10(1 Pt 1):136-43.
4. Schlessinger J. Cell signaling by receptor tyrosine kinases. *Cell.* 2000;103(2):211-25.
5. Dawson JP, Berger MB, Lin CC, Schlessinger J, Lemmon MA, Ferguson KM. Epidermal growth factor receptor dimerization and activation require ligand-induced conformational changes in the dimer interface. *Mol Cell Biol.* 2005;25(17):7734-42.
6. Pawson T, Schlessinger J. SH2 and SH3 domains. *Curr Biol.* 1993;3(7):434-42.
7. Rozakis-Adcock M, Fernley R, Wade J, Pawson T, Bowtell D. The SH2 and SH3 domains of mammalian Grb2 couple the EGF receptor to the Ras activator mSos1. *Nature.* 1993;363(6424):83-5.
8. Boonyaratanakornkit V, Scott MP, Ribon V, Sherman L, Anderson SM, Maller JL, et al. Progesterone receptor contains a proline-rich motif that directly interacts with SH3 domains and activates c-Src family tyrosine kinases. *Mol Cell.* 2001;8(2):269-80.
9. Edwards DP, Wardell SE, Boonyaratanakornkit V. Progesterone receptor interacting coregulatory proteins and cross talk with cell signaling pathways. *J Steroid Biochem Mol Biol.* 2002;83(1-5):173-86.
10. Boonyaratanakornkit V, McGowan E, Sherman L, Mancini MA, Cheskis BJ, Edwards DP. The role of extranuclear signaling actions of progesterone receptor in

mediating progesterone regulation of gene expression and the cell cycle. *Mol Endocrinol.* 2007;21(2):359-75.

11. Boonyaratanakornkit V, Bi Y, Rudd M, Edwards DP. The role and mechanism of progesterone receptor activation of extra-nuclear signaling pathways in regulating gene transcription and cell cycle progression. *Steroids.* 2008;73(9-10):922-8.

12. Kawprasertsri S, Pietras RJ, Marquez-Garban DC, Boonyaratanakornkit V. Progesterone receptor (PR) polyproline domain (PPD) mediates inhibition of epidermal growth factor receptor (EGFR) signaling in non-small cell lung cancer cells. *Cancer Lett.* 2016;374(2):279-91.

13. Skotland T, Iversen TG, Torgersen ML, Sandvig K. Cell-Penetrating Peptides: Possibilities and Challenges for Drug Delivery in Vitro and in Vivo. *Molecules.* 2015;20(7):13313-23.

14. Lee HS, Park CB, Kim JM, Jang SA, Park IY, Kim MS, et al. Mechanism of anticancer activity of buforin IIb, a histone H2A-derived peptide. *Cancer Lett.* 2008;271(1):47-55.

15. Xu J, Wu RC, O'Malley BW. Normal and cancer-related functions of the p160 steroid receptor co-activator (SRC) family. *Nat Rev Cancer.* 2009;9(9):615-30.

16. Mangelsdorf DJ, Thummel C, Beato M, Herrlich P, Schütz G, Umesono K, et al. The nuclear receptor superfamily: The second decade. *Cell.* 1995;83(6):835-9.

17. Onate SA, Boonyaratanakornkit V, Spencer TE, Tsai SY, Tsai M-J, Edwards DP, et al. The Steroid Receptor Coactivator-1 Contains Multiple Receptor Interacting and Activation Domains That Cooperatively Enhance the Activation Function 1 (AF1) and AF2 Domains of Steroid Receptors. *Journal of Biological Chemistry.* 1998;273(20):12101-8.

18. Grimaldi M, Boulahtouf A, Delfosse V, Thouennon E, Bourguet W, Balaguer P. Reporter cell lines for the characterization of the interactions between human nuclear receptors and endocrine disruptors. *Front Endocrinol.* 2015;6.

19. Nunez AM, Jakowlev S, Briand JP, Gaire M, Krust A, Rio MC, et al. Characterization of the estrogen-induced ps2 protein secreted by the human breast cancer cell line mcf-7. *Endocrinology.* 1987;121(5):1759-65.

20. Brown AMC, Jeltsch JM, Roberts M, Chambon P. Activation of pS2 gene

transcription is a primary response to estrogen in the human breast cancer cell line MCF-7. Proceedings of the National Academy of Sciences of the United States of America. 1984;81(20):6344-8.

21. Meyer M-E, Gronemeyer H, Turcotte B, Bocquel M-T, Tasset D, Chambon P. Steroid hormone receptors compete for factors that mediate their enhancer function. Cell. 1989;57(3):433-42.

22. Oñate SA, Tsai SY, Tsai M-J, O'Malley BW. Sequence and Characterization of a Coactivator for the Steroid Hormone Receptor Superfamily. Science. 1995;270(5240):1354-7.

23. Johnson AB, O'Malley BW. Steroid Receptor Coactivators 1, 2, and 3: Critical Regulators of Nuclear Receptor Activity and Steroid Receptor Modulator (SRM)-based Cancer Therapy. Molecular and cellular endocrinology. 2012;348(2):430-9.

24. Belandia B, Orford RL, Hurst HC, Parker MG. Targeting of SWI/SNF chromatin remodelling complexes to estrogen-responsive genes. The EMBO Journal. 2002;21(15):4094-103.

25. Kraus WL, Manning ET, Kadonaga JT. Biochemical Analysis of Distinct Activation Functions in p300 That Enhance Transcription Initiation with Chromatin Templates. Molecular and Cellular Biology. 1999;19(12):8123-35.

26. Koh SS, Chen D, Lee Y-H, Stallcup MR. Synergistic Enhancement of Nuclear Receptor Function by p160 Coactivators and Two Coactivators with Protein Methyltransferase Activities. Journal of Biological Chemistry. 2001;276(2):1089-98.

27. Chang C-y, Norris JD, Grøn H, Paige LA, Hamilton PT, Kenan DJ, et al. Dissection of the LXXLL Nuclear Receptor-Coactivator Interaction Motif Using Combinatorial Peptide Libraries: Discovery of Peptide Antagonists of Estrogen Receptors  $\alpha$  and  $\beta$ . Molecular and Cellular Biology. 1999;19(12):8226-39.

28. Heery DM, Kalkhoven E, Hoare S, Parker MG. A signature motif in transcriptional co-activators mediates binding to nuclear receptors. Nature. 1997;387(6634):733-6.

29. Coulthard VH, Matsuda S, Heery DM. An Extended LXXLL Motif Sequence Determines the Nuclear Receptor Binding Specificity of TRAP220. Journal of Biological Chemistry. 2003;278(13):10942-51.

30. Shiau AK, Barstad D, Loria PM, Cheng L, Kushner PJ, Agard DA, et al. The Structural Basis of Estrogen Receptor/Coactivator Recognition and the Antagonism of This Interaction by Tamoxifen. *Cell*. 1998;95(7):927-37.
31. Nilsson S, Mäkelä S, Treuter E, Tujague M, Thomsen J, Andersson G, et al. Mechanisms of Estrogen Action. *Physiological Reviews*. 2001;81(4):1535-65.
32. Levin ER. Rapid signaling by steroid receptors. *American Journal of Physiology - Regulatory, Integrative and Comparative Physiology*. 2008;295(5):R1425-R30.
33. Improta-Brears T, Whorton AR, Codazzi F, York JD, Meyer T, McDonnell DP. Estrogen-induced activation of mitogen-activated protein kinase requires mobilization of intracellular calcium. *Proceedings of the National Academy of Sciences of the United States of America*. 1999;96(8):4686-91.
34. Zhang W, Liu HT. MAPK signal pathways in the regulation of cell proliferation in mammalian cells. *Cell Res*. 2002;12(1):9-18.
35. Pattarozzi A, Gatti M, Barbieri F, Würth R, Porcile C, Lunardi G, et al. 17 $\beta$ -Estradiol Promotes Breast Cancer Cell Proliferation-Inducing Stromal Cell-Derived Factor-1-Mediated Epidermal Growth Factor Receptor Transactivation: Reversal by Gefitinib Pretreatment. *Molecular Pharmacology*. 2008;73(1):191-202.
36. Chardin P, Camonis J, Gale N, van Aelst L, Schlessinger J, Wigler M, et al. Human Sos1: a guanine nucleotide exchange factor for Ras that binds to GRB2. *Science*. 1993;260(5112):1338-43.
37. Simon JA, Schreiber SL. Grb2 SH3 binding to peptides from Sos: evaluation of a general model for SH3-ligand interactions. *Chemistry & Biology*. 1995;2(1):53-60.
38. Rozakis-Adcock M, Fernley R, Wade J, Pawson T, Bowtell D. The SH2 and SH3 domains of mammalian Grb2 couple the EGF receptor to the Ras activator mSos1. *Nature*. 1993;363(6424):83-5.
39. Yue W, Wang J-P, Conaway M, Masamura S, Li Y, Santen RJ. Activation of the MAPK Pathway Enhances Sensitivity of MCF-7 Breast Cancer Cells to the Mitogenic Effect of Estradiol. *Endocrinology*. 2002;143(9):3221-9.
40. Pietras RJ, Marquez-Garban DC. Membrane-associated estrogen receptor signaling pathways in human cancers. *Clin Cancer Res*. 2007;13(16):4672-6.

41. Siegel RL, Miller KD, Jemal A. Cancer statistics, 2019. *Ca-Cancer J Clin.* 2019;69(1):7-34.
42. Molina JR, Yang P, Cassivi SD, Schild SE, Adjei AA. Non-small cell lung cancer: epidemiology, risk factors, treatment, and survivorship. *Mayo Clin Proc.* 2008;83(5):584-94.
43. Piao YS, Iwakura Y, Takei N, Nawa H. Differential distributions of peptides in the epidermal growth factor family and phosphorylation of ErbB1 receptor in adult rat brain. *Neuroscience Letters.* 2005;390(1):21-4.
44. Normanno N, De Luca A, Bianco C, Strizzi L, Mancino M, Maiello MR, et al. Epidermal growth factor receptor (EGFR) signaling in cancer. *Gene.* 2006;366(1):2-16.
45. Kumar A, Petri ET, Halmos B, Boggon TJ. Structure and clinical relevance of the epidermal growth factor receptor in human cancer. *J Clin Oncol.* 2008;26(10):1742-51.
46. Ciardiello F, Tortora G. EGFR antagonists in cancer treatment. *N Engl J Med.* 2008;358(11):1160-74.
47. Sharma SV, Bell DW, Settleman J, Haber DA. Epidermal growth factor receptor mutations in lung cancer. *Nat Rev Cancer.* 2007;7(3):169-81.
48. Perez-Soler R, Chachoua A, Hammond LA, Rowinsky EK, Huberman M, Karp D, et al. Determinants of tumor response and survival with erlotinib in patients with non-small-cell lung cancer. *J Clin Oncol.* 2004;22(16):3238-47.
49. Thatcher N, Chang A, Parikh P, Pereira JR, Ciuleanu T, von Pawel J, et al. Gefitinib plus best supportive care in previously treated patients with refractory advanced non-small-cell lung cancer: results from a randomised, placebo-controlled, multicentre study (Iressa Survival Evaluation in Lung Cancer). *Lancet.* 2005;366(9496):1527-37.
50. Riely GJ, Pao W, Pham DK, Li AR, Rizvi N, Venkatraman ES, et al. Clinical course of patients with non-small cell lung cancer and epidermal growth factor receptor exon 19 and exon 21 mutations treated with gefitinib or erlotinib. *Clinical Cancer Research.* 2006;12(3):839-44.
51. Gow CH, Shih JY, Chang YL, Yu CJ. Acquired gefitinib-resistant mutation of EGFR in a chemonaive lung adenocarcinoma harboring gefitinib-sensitive mutation L858R. *PLoS Med.* 2005;2(9):e269.

52. Bell DW, Gore I, Okimoto RA, Godin-Heymann N, Sordella R, Mulloy R, et al. Inherited susceptibility to lung cancer may be associated with the T790M drug resistance mutation in EGFR. *Nat Genet.* 2005;37(12):1315-6.
53. Pao W, Miller VA, Politi KA, Riely GJ, Somwar R, Zakowski MF, et al. Acquired resistance of lung adenocarcinomas to gefitinib or erlotinib is associated with a second mutation in the EGFR kinase domain. *Plos Medicine.* 2005;2(3):225-35.
54. Kumar A, Petri ET, Halmos B, Boggon TJ. Structure and clinical relevance of the epidermal growth factor receptor in human cancer. *Journal of Clinical Oncology.* 2008;26(10):1742-51.
55. Lynch TJ, Bell DW, Sordella R, Gurubhagavatula S, Okimoto RA, Brannigan BW, et al. Activating mutations in the epidermal growth factor receptor underlying responsiveness of non-small-cell lung cancer to gefitinib. *N Engl J Med.* 2004;350(21):2129-39.
56. Arcila ME, Nafa K, Chaft JE, Rekhtman N, Lau C, Reva BA, et al. EGFR exon 20 insertion mutations in lung adenocarcinomas: prevalence, molecular heterogeneity, and clinicopathologic characteristics. *Mol Cancer Ther.* 2013;12(2):220-9.
57. Kosaka T, Yatabe Y, Endoh H, Yoshida K, Hida T, Tsuboi M, et al. Analysis of epidermal growth factor receptor gene mutation in patients with non-small cell lung cancer and acquired resistance to gefitinib. *Clin Cancer Res.* 2006;12(19):5764-9.
58. Remon J, Steuer CE, Ramalingam SS, Felip E. Osimertinib and other third-generation EGFR TKI in EGFR-mutant NSCLC patients. *Annals of Oncology.* 2018;29:120-17.
59. Mehlman C, Cadranel J, Rousseau-Bussac G, Lacave R, Pujals A, Girard N, et al. Resistance mechanisms to osimertinib in EGFR-mutated advanced non-small-cell lung cancer: A multicentric retrospective French study. *Lung Cancer.* 2019;137:149-56.
60. Engelman JA, Zejnullahu K, Mitsudomi T, Song YC, Hyland C, Park JO, et al. MET amplification leads to gefitinib resistance in lung cancer by activating ERBB3 signaling. *Science.* 2007;316(5827):1039-43.
61. Cortot AB, Repellin CE, Shimamura T, Capelletti M, Zejnullahu K, Ercan D, et al. Resistance to Irreversible EGF Receptor Tyrosine Kinase Inhibitors through a Multistep Mechanism Involving the IGF1R Pathway. *Cancer Res.* 2013;73(2):834-43.
62. Ohashi K, Sequist LV, Arcila ME, Moran T, Chmielecki J, Lin YL, et al. Lung

cancers with acquired resistance to EGFR inhibitors occasionally harbor BRAF gene mutations but lack mutations in KRAS, NRAS, or MEK1. *P Natl Acad Sci USA*. 2012;109(31):E2127-E33.

63. Costa DB, Halmos B, Kumar A, Schumer ST, Huberman MS, Boggon TJ, et al. BIM mediates EGFR tyrosine kinase inhibitor-induced apoptosis in lung cancers with oncogenic EGFR mutations. *Plos Medicine*. 2007;4(10):1669-80.

64. Cheong HT, Xu F, Choy CT, Hui CWC, Mok TSK, Wong CH. Upregulation of Bcl2 in NSCLC with acquired resistance to EGFR-TKI. *Oncology Letters*. 2018;15(1):901-7.

65. Kwon Y, Kim M, Jung HS, Kim Y, Jeoung D. Targeting Autophagy for Overcoming Resistance to Anti-EGFR Treatments. *Cancers*. 2019;11(9).

66. Kuiper GGJM, Enmark E, Peltola-Huikko M, Nilsson S, Gustafsson JA. Cloning of a novel estrogen receptor expressed in rat prostate and ovary. *P Natl Acad Sci USA*. 1996;93(12):5925-30.

67. Skjefstad K, Richardsen E, Donnem T, Andersen S, Kiselev Y, Grindstad T, et al. The prognostic role of progesterone receptor expression in non-small cell lung cancer patients: Gender-related impacts and correlation with disease-specific survival. *Steroids*. 2015;98:29-36.

68. Lim CS, Baumann CT, Htun H, Xian WJ, Irie M, Smith CL, et al. Differential localization and activity of the A- and B-forms of the human progesterone receptor using green fluorescent protein chimeras. *Mol Endocrinol*. 1999;13(3):366-75.

69. Ishibashi H, Suzuki T, Suzuki S, Niikawa H, Lu LY, Miki Y, et al. Progesterone receptor in non-small cell lung cancer - A potent prognostic factor and possible target for endocrine therapy. *Cancer Res*. 2005;65(14):6450-8.

70. Marquez-Garban DC, Mah V, Alavi M, Maresh EL, Chen HW, Bagryanova L, et al. Progesterone and estrogen receptor expression and activity in human non-small cell lung cancer. *Steroids*. 2011;76(9):910-20.

71. Kawprasertsri S, Pietras RJ, Marquez-Garban DC, Boonyaratanakornkit V. Progesterone receptor (PR) polyproline domain (PPD) mediates inhibition of epidermal growth factor receptor (EGFR) signaling in non-small cell lung cancer cells. *Cancer Letters*. 2016;374(2):279-91.

72. Wang J-C, Stafford JM, Granner DK. SRC-1 and GRIP1 Coactivate Transcription

with Hepatocyte Nuclear Factor 4. The Journal of biological chemistry. 1998;273(47):30847-50.

73. Xu J, Qiu Y, DeMayo FJ, Tsai SY, Tsai M-J, Malley BW. Partial Hormone Resistance in Mice with Disruption of the Steroid Receptor Coactivator-1 (SRC-1) Gene. Science. 1998;279(5358):1922.

74. Sadow PM, Koo E, Chassande O, Gauthier K, Samarut J, Xu J, et al. Thyroid Hormone Receptor-Specific Interactions with Steroid Receptor Coactivator-1 in the Pituitary. Molecular Endocrinology. 2003;17(5):882-94.

75. Tai H, Kubota N, Kato S. Involvement of Nuclear Receptor Coactivator SRC-1 in Estrogen-Dependent Cell Growth of MCF-7 Cells. Biochemical and Biophysical Research Communications. 2000;267(1):311-6.

76. Weldon CB, Elliott S, Zhu Y, Clayton JL, Curiel TJ, Jaffe BM, et al. Regulation of estrogen-mediated cell survival and proliferation by p160 coactivators. Surgery. 2004;136(2):346-54.

77. Cavarretta ITR, Mukopadhyay R, Lonard DM, Cowser LM, Bennett CF, O'Malley BW, et al. Reduction of Coactivator Expression by Antisense Oligodeoxynucleotides Inhibits ER $\alpha$  Transcriptional Activity and MCF-7 Proliferation. Molecular Endocrinology. 2002;16(2):253-70.

78. Wang S, Yuan Y, Liao L, Kuang S-Q, Tien JC-Y, O'Malley BW, et al. Disruption of the SRC-1 gene in mice suppresses breast cancer metastasis without affecting primary tumor formation. Proceedings of the National Academy of Sciences of the United States of America. 2009;106(1):151-6.

79. Redmond AM, Bane FT, Stafford AT, McLlroy M, Dillon MF, Crotty TB, et al. Coassociation of estrogen receptor and p160 proteins predicts resistance to endocrine treatment; SRC-1 is an independent predictor of breast cancer recurrence. Clinical Cancer Research. 2009;15(6):2098-106.

80. Xu JM, Wu RC, O'Malley BW. Normal and cancer-related functions of the p160 steroid receptor co-activator (SRC) family. Nat Rev Cancer. 2009;9(9):615-30.

81. Ramsey JD, Flynn NH. Cell-penetrating peptides transport therapeutics into cells. Pharmacology & Therapeutics. 2015;154:78-86.

82. Trabulo S, Cardoso AL, Mano M, De Lima MCP. Cell-Penetrating Peptides—Mechanisms of Cellular Uptake and Generation of Delivery Systems. *Pharmaceuticals*. 2010;3(4).
83. Bechara C, Sagan S. Cell-penetrating peptides: 20 years later, where do we stand? *FEBS Letters*. 2013;587(12):1693-702.
84. Vivès E, Brodin P, Lebleu B. A truncated HIV-1 Tat protein basic domain rapidly translocates through the plasma membrane and accumulates in the cell nucleus. *Journal of Biological Chemistry*. 1997;272(25):16010-7.
85. Derossi D, Joliot AH, Chassaing G, Prochiantz A. The third helix of the Antennapedia homeodomain translocates through biological membranes. *Journal of Biological Chemistry*. 1994;269(14):10444-50.
86. Raucher D, Ryu JS. Cell-penetrating peptides: strategies for anticancer treatment. *Trends in Molecular Medicine*. 21(9):560-70.
87. Lee HS, Park CB, Kim JM, Jang SA, Park IY, Kim MS, et al. Mechanism of anticancer activity of buforin IIb, a histone H2A-derived peptide. *Cancer Letters*. 2008;271(1):47-55.
88. Cho JH, Sung BH, Kim SC. Buforins: Histone H2A-derived antimicrobial peptides from toad stomach. *Biochimica et Biophysica Acta (BBA) - Biomembranes*. 2009;1788(8):1564-9.
89. Lim KJ, Sung BH, Shin JR, Lee YW, Kim DJ, Yang KS, et al. A Cancer Specific Cell-Penetrating Peptide, BR2, for the Efficient Delivery of an scFv into Cancer Cells. *PLoS ONE*. 2013;8(6):e66084.
90. Daly R, Hearn MTW. Expression of heterologous proteins in *Pichia pastoris*: a useful experimental tool in protein engineering and production. *Journal of Molecular Recognition*. 2005;18(2):119-38.
91. Ahmad M, Hirz M, Pichler H, Schwab H. Protein expression in *Pichia pastoris*: recent achievements and perspectives for heterologous protein production. *Applied Microbiology and Biotechnology*. 2014;98(12):5301-17.
92. Lueking A, Holz C, Gotthold C, Lehrach H, Cahill D. A System for Dual Protein Expression in *Pichia pastoris* and *Escherichia coli*. *Protein Expression and Purification*. 2000;20(3):372-8.

93. Cereghino GPL, Cereghino JL, Ilgen C, Cregg JM. Production of recombinant proteins in fermenter cultures of the yeast *Pichia pastoris*. *Current Opinion in Biotechnology*. 2002;13(4):329-32.
94. Nihira K, Miki Y, Iida S, Narumi S, Ono K, Iwabuchi E, et al. An activation of LC3A-mediated autophagy contributes to de novo and acquired resistance to EGFR tyrosine kinase inhibitors in lung adenocarcinoma. *Journal of Pathology*. 2014;234(2):277-88.
95. Li SS. Specificity and versatility of SH3 and other proline-recognition domains: structural basis and implications for cellular signal transduction. *Biochem J*. 2005;390(Pt 3):641-53.
96. Walsh CA, Qin L, Tien JCY, Young LS, Xu JM. The Function of Steroid Receptor Coactivator-1 in Normal Tissues and Cancer. *Int J Biol Sci*. 2012;8(4):470-85.
97. Chang CY, Norris JD, Gron H, Paige LA, Hamilton PT, Kenan DJ, et al. Dissection of the LXXLL nuclear receptor-coactivator interaction motif using combinatorial peptide libraries: Discovery of peptide antagonists of estrogen receptors alpha and beta. *Mol Cell Biol*. 1999;19(12):8226-39.
98. Jang JH, Kim MY, Lee JW, Kim SC, Cho JH. Enhancement of the cancer targeting specificity of buforin IIb by fusion with an anionic peptide via a matrix metalloproteinases-cleavable linker. *Peptides*. 2011;32(5):895-9.
99. Dhillon AS, Hagan S, Rath O, Kolch W. MAP kinase signalling pathways in cancer. *Oncogene*. 2007;26(22):3279-90.
100. Vicent S, Lopez-Picazo JM, Toledo G, Lozano MD, Torre W, Garcia-Corchon C, et al. ERK1/2 is activated in non-small-cell lung cancer and associated with advanced tumours. *Brit J Cancer*. 2004;90(5):1047-52.
101. <EGFR TKI as first-line treatment for patients with advanced EGFR mutation-positive non-small-cell lung cancer .pdf>.
102. Gautschi O, Ratschiller D, Gugger M, Betticher DC, Heighway J. Cyclin D1 in non-small cell lung cancer: a key driver of malignant transformation. *Lung Cancer*. 2007;55(1):1-14.
103. Wang X, Lu Y, Feng W, Chen Q, Guo H, Sun X, et al. A two kinase-gene signature model using CDK2 and PAK4 expression predicts poor outcome in non-small cell lung cancers. *Neoplasma*. 2016;63(2):322-9.

104. Gazdar AF. Activating and resistance mutations of EGFR in non-small-cell lung cancer: role in clinical response to EGFR tyrosine kinase inhibitors. *Oncogene*. 2009;28 Suppl 1:S24-31.
105. Paez JG, Janne PA, Lee JC, Tracy S, Greulich H, Gabriel S, et al. EGFR mutations in lung cancer: correlation with clinical response to gefitinib therapy. *Science*. 2004;304(5676):1497-500.
106. Coser KR, Chesnes J, Hur J, Ray S, Isselbacher KJ, Shioda T. Global analysis of ligand sensitivity of estrogen inducible and suppressible genes in MCF7/BUS breast cancer cells by DNA microarray. *Proc Natl Acad Sci U S A*. 2003;100(24):13994-9.
107. Onate SA, Tsai SY, Tsai MJ, O'Malley BW. Sequence and characterization of a coactivator for the steroid hormone receptor superfamily. *Science*. 1995;270(5240):1354-7.
108. Heery DM, Kalkhoven E, Hoare S, Parker MG. A signature motif in transcriptional co-activators mediates binding to nuclear receptors. *Nature*. 1997;387(6634):733-6.
109. Boonyaratanakornkit V. Scaffolding proteins mediating membrane-initiated extra-nuclear actions of estrogen receptor. *Steroids*. 2011;76(9):877-84.
110. Bjornstrom L, Sjoberg M. Mechanisms of estrogen receptor signaling: convergence of genomic and nongenomic actions on target genes. *Mol Endocrinol*. 2005;19(4):833-42.
111. Richer JK, Jacobsen BM, Manning NG, Abel MG, Wolf DM, Horwitz KB. Differential gene regulation by the two progesterone receptor isoforms in human breast cancer cells. *J Biol Chem*. 2002;277(7):5209-18.
112. Jacobsen BM, Schittone SA, Richer JK, Horwitz KB. Progesterone-independent effects of human progesterone receptors (PRs) in estrogen receptor-positive breast cancer: PR isoform-specific gene regulation and tumor biology. *Mol Endocrinol*. 2005;19(3):574-87.
113. Thike AA, Cheok PY, Jara-Lazaro AR, Tan B, Tan P, Tan PH. Triple-negative breast cancer: clinicopathological characteristics and relationship with basal-like breast cancer. *Mod Pathol*. 2010;23(1):123-33.
114. Bosch A, Eroles P, Zaragoza R, Vina JR, Lluch A. Triple-negative breast cancer: molecular features, pathogenesis, treatment and current lines of research. *Cancer Treat*

Rev. 2010;36(3):206-15.

115. Plevin MJ, Mills MM, Ikura M. The LxxLL motif: a multifunctional binding sequence in transcriptional regulation. *Trends Biochem Sci.* 2005;30(2):66-9.

116. Reis-Filho JS, Tutt AN. Triple negative tumours: a critical review. *Histopathology.* 2008;52(1):108-18.

117. Sugimura H, Nichols FC, Yang P, Allen MS, Cassivi SD, Deschamps C, et al. Survival after recurrent nonsmall-cell lung cancer after complete pulmonary resection. *Ann Thorac Surg.* 2007;83(2):409-17; discussion 17-8.

118. Ho C, Ramsden K, Zhai YL, Murray N, Sun S, Melosky B, et al. Less Toxic Chemotherapy Improves Uptake of All Lines of Chemotherapy in Advanced Non-Small-Cell Lung Cancer A 10-Year Retrospective Population-Based Review. *Journal of Thoracic Oncology.* 2014;9(8):1180-6.

119. Henderson BE, Feigelson HS. Hormonal carcinogenesis. *Carcinogenesis.* 2000;21(3):427-33.

120. Pateetin P, Pisitkun T, McGowan E, Boonyaratanakornkit V. Differential quantitative proteomics reveals key proteins related to phenotypic changes of breast cancer cells expressing progesterone receptor A. *J Steroid Biochem Mol Biol.* 2020;198:105560.

121. Jeong Y, Xie Y, Xiao G, Behrens C, Girard L, Wistuba II, et al. Nuclear receptor expression defines a set of prognostic biomarkers for lung cancer. *PLoS Med.* 2010;7(12):e1000378.

122. Ishibashi H, Suzuki T, Suzuki S, Niikawa H, Lu L, Miki Y, et al. Progesterone receptor in non-small cell lung cancer--a potent prognostic factor and possible target for endocrine therapy. *Cancer Res.* 2005;65(14):6450-8.

123. Marquez-Garban DC, Mah V, Alavi M, Maresh EL, Chen HW, Bagryanova L, et al. Progesterone and estrogen receptor expression and activity in human non-small cell lung cancer. *Steroids.* 2011;76(9):910-20.

124. Stabile LP, Dacic S, Land SR, Lenzner DE, Dhir R, Acquafondata M, et al. Combined analysis of estrogen receptor beta-1 and progesterone receptor expression identifies lung cancer patients with poor outcome. *Clin Cancer Res.* 2011;17(1):154-64.

125. Raso MG, Behrens C, Herynk MH, Liu S, Prudkin L, Ozburn NC, et al.

Immunohistochemical expression of estrogen and progesterone receptors identifies a subset of NSCLCs and correlates with EGFR mutation. *Clin Cancer Res.* 2009;15(17):5359-68.

126. Toh CK, Ahmad B, Soong R, Chuah KL, Tan SH, Hee SW, et al. Correlation between Epidermal Growth Factor Receptor Mutations and Expression of Female Hormone Receptors in East-Asian Lung Adenocarcinomas. *Journal of Thoracic Oncology.* 2010;5(1):17-22.

127. Cussac D, Vidal M, Leprince C, Liu WQ, Tiraboschi G, Roques BP, et al. A Sos-derived peptidimer blocks the Ras signaling pathway by binding both Grb2 SH3 domains and displays antiproliferative activity. *Faseb Journal.* 1999;13(1):31-9.

128. Simon JA, Schreiber SL. Grb2 Sh3 Binding to Peptides from Sos - Evaluation of a General-Model for Sh3-Ligand Interactions. *Chem Biol.* 1995;2(1):53-60.

129. Gril B, Vidal M, Assayag F, Poupon MF, Liu WQ, Garbay C. Grb2-SH3 ligand inhibits the growth of HER2(+) cancer cells and has antitumor effects in human cancer xenografts alone and in combination with docetaxel. *International Journal of Cancer.* 2007;121(2):407-15.

130. Kamada H, Okamoto T, Kawamura M, Shibata H, Abe Y, Ohkawa A, et al. Creation of novel cell-penetrating peptides for intracellular drug delivery using systematic phage display technology originated from tat transduction domain. *Biol Pharm Bull.* 2007;30(2):218-23.

131. Ferrari A, Pellegrini V, Arcangeli C, Fittipaldi A, Giacca M, Beltram F. Caveolae-mediated internalization of extracellular HIV-1 tat fusion proteins visualized in real time. *Mol Ther.* 2003;8(2):284-94.

132. Zhang X, Lin C, Lu A, Lin G, Chen H, Liu Q, et al. Liposomes equipped with cell penetrating peptide BR2 enhances chemotherapeutic effects of cantharidin against hepatocellular carcinoma. *Drug Deliv.* 2017;24(1):986-98.

133. Lim KJ, Sung BH, Shin JR, Lee YW, Kim DJ, Yang KS, et al. A Cancer Specific Cell-Penetrating Peptide, BR2, for the Efficient Delivery of an scFv into Cancer Cells. *Plos One.* 2013;8(6).

134. Hayashi N, Chiba H, Kuronuma K, Go S, Hasegawa Y, Takahashi M, et al. Detection of N-glycosylated gangliosides in non-small-cell lung cancer using GMR8

monoclonal antibody. *Cancer Science*. 2013;104(1):43-7.

135. Sierra JR, Cepero V, Giordano S. Molecular mechanisms of acquired resistance to tyrosine kinase targeted therapy. *Mol Cancer*. 2010;9:75.

136. Mitsudomi T, Morita S, Yatabe Y, Negoro S, Okamoto I, Tsurutani J, et al. Gefitinib versus cisplatin plus docetaxel in patients with non-small-cell lung cancer harbouring mutations of the epidermal growth factor receptor (WJTOG3405): an open label, randomised phase 3 trial. *Lancet Oncol*. 2010;11(2):121-8.

137. Maemondo M, Inoue A, Kobayashi K, Sugawara S, Oizumi S, Isobe H, et al. Gefitinib or chemotherapy for non-small-cell lung cancer with mutated EGFR. *N Engl J Med*. 2010;362(25):2380-8.

138. Li GF, Gao SJ, Sheng ZX, Li B. The Efficacy of Single-Agent Epidermal Growth Factor Receptor Tyrosine Kinase Inhibitor Therapy in Biologically Selected Patients with Non-Small-Cell Lung Cancer: A Meta-Analysis of 19 Randomized Controlled Trials. *Chemotherapy*. 2015;61(4):179-89.

139. Lee CK, Brown C, Gralla RJ, Hirsh V, Thongprasert S, Tsai CM, et al. Impact of EGFR Inhibitor in Non-Small Cell Lung Cancer on Progression-Free and Overall Survival: A Meta-Analysis. *Jnci-J Natl Cancer I*. 2013;105(9):595-605.

140. Zhao N, Zhang XC, Yan HH, Yang JJ, Wu YL. Efficacy of epidermal growth factor receptor inhibitors versus chemotherapy as second-line treatment in advanced non-small-cell lung cancer with wild-type EGFR: A meta-analysis of randomized controlled clinical trials. *Lung Cancer*. 2014;85(1):66-73.

141. Yun CH, Boggon TJ, Li Y, Woo MS, Greulich H, Meyerson M, et al. Structures of lung cancer-derived EGFR mutants and inhibitor complexes: mechanism of activation and insights into differential inhibitor sensitivity. *Cancer Cell*. 2007;11(3):217-27.

142. Qin A, Reddy HG, Weinberg FD, Kalemkerian GP. Cyclin-dependent kinase inhibitors for the treatment of lung cancer. *Expert Opin Pharmacother*. 2020;21(8):941-52.

143. Huang C, Jacobson K, Schaller MD. MAP kinases and cell migration. *Journal of Cell Science*. 2004;117(20):4619-28.

144. Ryu BJ, Lee H, Kim SH, Heo JN, Choi SW, Yeon JT, et al. PF-3758309, p21-activated kinase 4 inhibitor, suppresses migration and invasion of A549 human lung

cancer cells via regulation of CREB, NF-kappaB, and beta-catenin signalings. *Mol Cell Biochem.* 2014;389(1-2):69-77.

145. Dong QZ, Wang Y, Tang ZP, Fu L, Li QC, Wang ED, et al. Derlin-1 Is Overexpressed in Non-Small Cell Lung Cancer and Promotes Cancer Cell Invasion via EGFR-ERK-Mediated Up-Regulation of MMP-2 and MMP-9. *Am J Pathol.* 2013;182(3):954-64.

146. Wu ZG, Wang T, Fang M, Huang WD, Sun ZW, Xiao JR, et al. MFAP5 promotes tumor progression and bone metastasis by regulating ERK/MMP signaling pathways in breast cancer. *Biochem Bioph Res Co.* 2018;498(3):495-501.

147. Balak MN, Gong Y, Riely GJ, Somwar R, Li AR, Zakowski MF, et al. Novel D761Y and common secondary T790M mutations in epidermal growth factor receptor-mutant lung adenocarcinomas with acquired resistance to kinase inhibitors. *Clin Cancer Res.* 2006;12(21):6494-501.

148. Kobayashi S, Boggon TJ, Dayaram T, Janne PA, Kocher O, Meyerson M, et al. EGFR mutation and resistance of non-small-cell lung cancer to gefitinib. *N Engl J Med.* 2005;352(8):786-92.

149. Ono M, Hirata A, Kometani T, Miyagawa M, Ueda S, Kinoshita H, et al. Sensitivity to gefitinib (Iressa, ZD1839) in non-small cell lung cancer cell lines correlates with dependence on the epidermal growth factor (EGF) receptor/extracellular signal-regulated kinase 1/2 and EGF receptor/Akt pathway for proliferation. *Mol Cancer Ther.* 2004;3(4):465-72.

150. Kuwano M, Sonoda K, Murakami Y, Watari K, Ono M. Overcoming drug resistance to receptor tyrosine kinase inhibitors: Learning from lung cancer. *Pharmacol Ther.* 2016;161:97-110.

151. Song YA, Ma T, Zhang XY, Cheng XS, Olajuyin AM, Sun ZF, et al. Apatinib preferentially inhibits PC9 gefitinib-resistant cancer cells by inducing cell cycle arrest and inhibiting VEGFR signaling pathway. *Cancer Cell Int.* 2019;19:117.

152. Huang MH, Lee JH, Chang YJ, Tsai HH, Lin YL, Lin AM, et al. MEK inhibitors reverse resistance in epidermal growth factor receptor mutation lung cancer cells with acquired resistance to gefitinib. *Mol Oncol.* 2013;7(1):112-20.

153. Geistlinger TR, Guy RK. Novel selective inhibitors of the interaction of individual

nuclear hormone receptors with a mutually shared steroid receptor coactivator 2. *J Am Chem Soc.* 2003;125(23):6852-3.

154. Tints K, Prink M, Neuman T, Palm K. LXXLL peptide converts transportan 10 to a potent inducer of apoptosis in breast cancer cells. *Int J Mol Sci.* 2014;15(4):5680-98.





จุฬาลงกรณ์มหาวิทยาลัย  
**CHULALONGKORN UNIVERSITY**

## VITA

**NAME** Panthita Kaewjanthong

**DATE OF BIRTH** 26 November 1990

**PLACE OF BIRTH** Yala

**INSTITUTIONS ATTENDED** Bachelor Degree in Medical Technology, Faculty of Allied Health Sciences, Chulalongkorn University

**HOME ADDRESS** 88/4 Moo.7 Satangnork Sub district Muang Yala, 95000

